

INVESTIGATION OF PHYSICO-CHEMICAL CHARACTERISTICS OF SIZE-  
SEGREGATED PARTICULATE MATTER IN A METROPOLITAN  
ENVIRONMENT AND THEIR IMPACT ON AIR QUALITY IN SOUTHERN  
CALIFORNIA

by

Payam Pakbin

---

A Dissertation Presented to the  
FACULTY OF THE USC GRADUATE SCHOOL  
UNIVERSITY OF SOUTHERN CALIFORNIA  
In Partial Fulfillment of the  
Requirements for the Degree  
DOCTOR OF PHILOSOPHY  
(ENVIRONMENTAL ENGINEERING)

December 2011

Copyright 2011

Payam Pakbin

## **Dedication**

To my parents for their love; they are the reason I am here.

## **Acknowledgments**

This thesis was done under the guidance of my graduate advisor, Professor Costantinos Sioutas. I express my sincere gratitude and appreciation to him for giving me the opportunity to work in his research group and his expert advice and encouragement during the whole course of this thesis work. His enthusiasm and energetic approach, along with his professional and scientific intuition has inspired and motivated me greatly throughout these years, helping me to develop my intellectual maturity and teaching me how to appreciate the good scientific work that helps other researchers to build on it.

I would also like to express my deep sense of gratitude to the members of my guidance committee, Prof. Ronald C Henry and Prof. James Moffett.

My sincere thanks are due to my previous and current labmates and friends in the USC Aerosol Lab. I would like to thank the previous post doctors in the group: Dr. Katharine Moore, Dr. Mike Geller, Dr. Andrea Polidori, Dr. Shaohua Hu, Dr. Markus Sillanpaa and Dr. Arantza Eiguren-Fernandez from UCLA who have contributed greatly to the development of my research expertise, with special thanks to my great friend and colleague Dr. Zhi Ning for his friendship and invaluable help throughout my graduate study at USC.

It was a pleasure to share doctoral studies and life with wonderful people in the USC Aerosol Group: Dr. Ehsan Arhami, Dr. Subhasis Biswas, Dr. Harish Phuleria, Dr. Vishal Verma, Neelakshi Hudda, Kalam Cheung, Winnie Kam, Nancy Daher, Jimmy Liacos, Ali Attar and Xu Zhen. This thesis would not have been possible without their involvement and support.

I want to express my warmest gratitude to my parents for their endless support and encouragement throughout my whole life. Last but not least, my relatives and friends are thanked for their pleasant company and unconditioned love.

## Table of Contents

Dedication.....	ii
Acknowledgments .....	iii
List of Tables .....	viii
List of Figures.....	ix
Abstract.....	xii
Chapter 1 - Introduction.....	1
1.1 Introduction.....	1
1.1.1 Characteristics of Ambient Particulate Matter.....	1
1.1.2 Health Effects of the Exposure to Particulate Matters in the Atmosphere .....	3
1.2 Rationale of the Proposed Research .....	5
1.3 Thesis overview .....	9
Chapter 2 - Characterization of Particle Bound Organic Carbon from Diesel Vehicles Equipped with Advanced Emission Control Technologies .....	12
2.1 Abstract.....	12
2.2 Introduction.....	14
2.3 Experimental Methodology .....	16
2.3.1. Vehicles and control devices .....	17
2.3.2. Sampling methodology and chemical analysis.....	17
2.3. Results and Discussion .....	18
2.4 Acknowledgments .....	31

Chapter 3 - Modification of the Versatile Aerosol Concentration Enrichment System (VACES) for Conducting Inhalation Exposures to Semi-volatile Vapor Phase	
Pollutants .....	32
3.1 Abstract.....	32
3.2 Introduction.....	33
3.3 Experimental Methodology .....	35
3.3.1 Design of the VACES-heater-filter (VHF) system.....	35
3.3.2 Experiment set up .....	37
3.4 Results and Discussion .....	42
3.4.1 Laboratory evaluation of the system.....	42
3.4.2 Field test of the system for optimization of operational temperature .....	49
3.4.3 Time Integrated Measurements of particle and vapor phases Polycyclic Aromatic Hydrocarbons (PAHs) .....	52
3.4 Summary and conclusions .....	59
3.5 Acknowledgments .....	60
 Chapter 4 - Spatial and Temporal Variability of Coarse (PM <sub>10-2.5</sub> ) Particulate Matter Concentrations in the Los Angeles Area .....	 61
4.1 Abstract.....	61
4.2 Introduction.....	62
4.2. Methodology.....	64
4.2.1 Site Selection and Meteorology .....	64
4.2.2 Sampling Period and Frequency .....	69
4.2.3 Sampling Equipment and Sample Screening.....	69
4.3. Results and Discussion .....	71
4.3.1 Temporal and Spatial variations .....	71
4.3.2 Comparison of PM <sub>2.5</sub> and CPM concentrations and relationships .....	76
4.3.3 Coefficients of Divergence (COD) calculations for CPM mass concentrations .....	81
4.4. Conclusions and Summary .....	84
4.5 Acknowledgements.....	85

Chapter 5 - Seasonal and Spatial Coarse Particle Elemental Concentrations in the Los Angeles Area .....	86
5.1 Abstract.....	86
5.2 Introduction.....	87
5.3 Methodology.....	89
5.3.1 Sample collection.....	89
5.3.2 Site selection.....	89
5.4 Analytical methods .....	90
5.5 Results and Discussion .....	92
5.5.1 Temporal and spatial variations in CPM mass concentrations .....	92
5.5.2 Principal Component Analysis (PCA).....	95
5.5.3 Crustal material.....	99
5.5.4 Abrasive vehicular emissions .....	102
5.5.5 Other sources of CPM-bound metals and trace elements .....	105
5.6 Summary and Conclusions .....	109
5.7 Acknowledgements.....	111
Chapter 6 - Future Research .....	112
6.1 Conclusions.....	112
6.2 Discussion and Future Recommendations.....	117
Bibliography .....	120

## List of Tables

Table 3.1 - PAH codes, molecular weights, subcooled liquid vapor pressure at 293K and HPLC-FL instrument detection limits.	53
Table 4.1 - Site information including sampling area, the designation code, description, geographic co-ordinates, site elevation, sampling period and data recovery.	68
Table 4.2 - Summary of statistics for the coarse particles mass concentrations ( $\mu\text{g}/\text{m}^3$ ) at each sampling site.	72
Table 5.1 - Principal component loadings (VARIMAX normalized) of selected trace element and metal species in airborne coarse particulate matter.	97



## List of Figures

Figure 1.1 – Typical size distribution of urban atmospheric particles.	2
Figure 2.1 – (a) Emission factors of PAHs, hopanes and steranes of baseline and control device-equipped vehicles in UDDS cycle. (b) Emission factors of <i>n</i> -alkanes and acids of baseline and control device-equipped vehicles in UDDS cycle.	21
Figure 2.2 – (a) Emission factors of PAHs, hopanes and steranes of baseline and control device-equipped vehicles in cruise cycle. (b) Emission factors of <i>n</i> -alkanes and acids of baseline and control device-equipped vehicles in cruise cycle.	23
Figure 2.3 – (a) Ratios of PAHs to organic carbon (OC) emission factors in $\mu\text{g/g}$ from baseline vehicle and their comparison with PAH composition of diesel fuel and lubricating oil taken from Zielinska et. al. (Zielinska et al. 2004). (b) Ratios of hopanes and steranes to organic carbon (OC) emission factors in $\mu\text{g/g}$ from baseline vehicle and their comparison with PAH composition of diesel fuel and lubricating oil taken from Zielinska et. al. (Zielinska et al. 2004).	26
Figure 2.4 – (a) Comparison of the ratios of PAHs, hopanes and steranes to organic carbon emission factors in $\mu\text{g/g}$ from baseline and controlled vehicles running on UDDS cycle. (b) Comparison of the ratios of PAHs, hopanes and steranes to organic carbon emission factors in $\mu\text{g/g}$ from baseline and controlled vehicles running on cruise cycle. (c) Ratios of PAHs, hopanes and steranes to organic carbon emission factors in $\mu\text{g/g}$ as reported by Riddle et al. (Riddle et al. 2007).	28
Figure 3.1 – Schematic of laboratory test set up.	39
Figure 3.2 – Schematic of field test set up and the filter holder.	41
Figure 3.3 - Particle size distributions of ammonium sulfate at 150°C with no filter after the heater. Same figure presented in the inset in logarithmic scale.	45
Figure 3.4a - Particle size distributions of ammonium sulfate at 150°C. Same figure presented in the inset in logarithmic scale.	46
Figure 3.4b - Particle size distributions of ammonium sulfate at 170°C. Same figure presented in the inset in logarithmic scale.	47
Figure 3.5a - Particle size distributions of adipic acid at 100°C. Same figure presented in the inset in logarithmic scale.	48
Figure 3.5b - Particle size distributions of glutaric acid at 200°C. Same figure presented in the inset in logarithmic scale.	49

Figure 3.6 - Particle size distributions of concentrated ambient particulate matter at 150°C. Same figure presented in the inset in logarithmic scale.	51
Figure 3.7 - Particle size distributions of concentrated ambient particulate matter at 170°C. Same figure presented in the inset in logarithmic scale.	52
Figure 3.8 – Correlation between natural logarithm of the measured PAH concentrations upstream and natural logarithm of sum of the measured PAH concentrations downstream of the system and on the heater filter (non-volatile fraction).	55
Figure 3.9a – Comparison of PAH concentrations measured upstream of the system in particle and vapor phase, PAH concentrations on the heater filter (the non-volatile fraction), and the recovered vapor phase PAHs measured after the cooling section and downstream of the system.	56
Figure 3.9b – Comparison of the upstream particle phase PAH concentrations ( $\pm$ standard error, SE) and the recovered vapor phase PAH concentrations ( $\pm$ SE), calculated by subtracting the upstream vapor phase concentration from the downstream vapor phase concentration of PAH species.	58
Figure 4.1 - Map of 10 monitoring locations used in this study.	67
Figure 4.2 – Average monthly coarse PM concentrations in three site clusters and Long Beach and Lancaster sites.	73
Figure 4.3 - monthly $PM_{2.5}$ concentrations in three site clusters and Long Beach sites.	74
Figure 4.4 - Site-by-site correlation contour plot of CPM mass concentrations.	75
Figure 4.5 – Annual and seasonal correlations between $PM_{2.5}$ and CPM in Riverside County cluster GRA. Data shown are from April 2008 – March 2009.	78
Figure 4.6 - Annual and seasonal correlations between $PM_{2.5}$ and CPM in Los Angeles and West Los Angeles clusters (a) GRD, (b) CCL. Data from April 2008 – March 2009.	79
Figure 4.7 - Annual and seasonal correlations between $PM_{2.5}$ and CPM in East Los Angeles cluster HMS. Data from April 2008 – March 2009.	80
Figure 4.8 - Annual and seasonal correlations between $PM_{2.5}$ and CPM in Long Beach site.	80
Figure 4.9 - Coefficients of Divergence for Coarse PM concentrations calculated across all sites pairs (with the exception of the Lancaster site) by month for the entire study (April 2008 – March 2009). Whisker-box plot shows minimum, 1 <sup>st</sup> quartile, median, 3 <sup>rd</sup> quartile and maximum values.	83

Figure 4.10 - Coefficients of Divergence for coarse PM concentrations calculated across all urban site pairs (USC, CCL, FRE, HMS, GRD and LDS) by month for the entire study (April 2008 – March 2009). Whisker-box plot as described previously.	83
Figure 5.1 (a – b) - Pearson coefficient matrix for selected trace metals in each site cluster; a) Los Angeles cluster, b) Long Beach.	93
Figure 5.1 (c – d) - Pearson coefficient matrix for selected trace metals in each site cluster; c) Riverside cluster, and d) Lancaster.	94
Figure 5.2 - Annual variations of crustal material tracers across all sampling sites.	100
Figure 5.3 (a – d) - Temporal variation of selected mineral dust tracers in different Sampling site clusters; a) Los Angeles cluster, b) Long Beach, c) Riverside cluster, and d) Lancaster.	102
Figure 5.4 - Annual variation of abrasive vehicular tracers across all sampling sites.	104
Figure 5.5 – Annual variation of sodium, a sea salt tracer, across all sampling sites.	107
Figure 5.6 (a – d) - Annual variation of selected metal species from the identified sources using principal component analysis across all sampling sites.	109
Figure 5.7 - Annual variation of trace metals listed as air pollutants by US Environmental Protection Agency.	111

## **Abstract**

Numerous epidemiological studies have associated the adverse respiratory and cardiovascular effects to atmospheric particulate matter (PM) exposure. There is ample literature providing evidence of adverse effects for all inhalable particle size ranges, however the biological mechanisms responsible for the toxicity of PM are still uncertain. Due to the lack of data about how different PM components act in a complex mixture, it is not possible to precisely quantify the contributions from the main sources and components to the effects on human health. Thus, PM in health impact assessments is usually regarded as a uniform pollutant, regardless of the contribution from different sources, and assuming the same effect on mortality. This is probably not a correct assumption, but is a pragmatic compromise while waiting for sufficient knowledge that will allow the use of indicators other than particle mass. As a result linking the toxicity of PM with several of its chemical components has been the focus of considerable research over the past decade. The associations between health endpoints with the hundreds of potentially toxic chemical species and PM characteristics may be daunting and not cost efficient. Therefore it is desirable to focus on the casualty of the few critical chemical components that current science supports as potentially the most harmful to human health. Such information will allow for more effective regulatory control strategies, more targeted air quality standards, and as a result, reductions in population exposure to the most harmful types of airborne PM.

The current particulate matter emission standards are based on PM mass only. However, the prevailing scientific opinion contends that PM mass is a surrogate measure of other physical and chemical properties of PM that are the actual causes of the observed health effects. In this study we focus on the PM components that are not currently regulated, while there is ample evidence that they can cause hazardous health outcomes. The effect of the new after-

treatment technologies on the composition of the remaining organic compounds, including the semi-volatile organic carbon (SVOC) fraction, is studied. While the association of adverse health effects with SVOC compounds has been reasonably well documented, the exact mechanisms by which SVOC compounds inflict health effects remain largely unknown. Therefore a new technology is developed that makes it possible to conduct toxicity and inhalation exposure studies separately to PM and vapor phase SVOC to investigate the degree to which health effects attributable to these pollutants are affected by their phases. In addition, in regards of PM<sub>10</sub> standards, coarse PM emissions are usually from hard to control sources like windblown soil and dust, brake lining abrasion, tire wear and bioaerosols, therefore control of fine PM emissions is easier to achieve in order to meet PM<sub>10</sub> standards. Coarse and fine PM have substantially different sources and sinks, and as a result different chemical composition, which would lead to potentially different health outcomes. Moreover, the available CPM mass concentration data is much more limited compared to ambient PM<sub>2.5</sub> mass concentration data and hence significantly less is quantitatively known about the characteristics of CPM. In order to study the physical, chemical and toxicological characteristics of CPM in Los Angeles Basin, 10 distinct measurement sites were employed to sample the CPM for an entire year, in order to provide a much needed database of coarse PM characteristics in the Los Angeles basin, providing the seasonal and spatial variations over a variety of urban and semi-rural areas during one year of sampling period.

## Chapter 1 - Introduction

### 1.1 Introduction

#### 1.1.1 Characteristics of Ambient Particulate Matter

Ambient particulate matter or aerosols are solid and/or liquid droplets suspended in the atmosphere. The atmosphere, whether in urban or remote areas, contains significant concentrations of aerosol particles which constitutes a major class of pollution. There are number of properties of particles that are important for their role in atmospheric processes. These include their number concentration, mass, size, chemical composition, aerodynamic and optical properties. Of these, size is the most important; it is related not only to the source of the particles but also to their effects on health, visibility and climate. The airborne particles vary in diameter sizes from a few nanometers to tens of micrometers spanning over four orders of magnitude. The mass of a 10  $\mu\text{m}$  particle is equivalent to the mass of 10 billion 10 nm particles. Particles larger than 10 micron in *aerodynamic diameter*<sup>1</sup> have a very short residence time in the atmosphere and have near 100% deposition efficiency in the nose therefore particles smaller than 10 microns are the main focus in health and environmental studies (Hinds 1999). Particles are categorized in different groups based on their aerodynamic diameter: coarse mode (particles smaller than 10  $\mu\text{m}$  and larger than 2.5  $\mu\text{m}$ ,  $\text{PM}_{10-2.5}$ ), accumulation (Aitken) mode (0.1 – 2.5  $\mu\text{m}$ ) and the ultrafine mode (0.01 – 0.1  $\mu\text{m}$ ). These particles are conglomerates of various pollutant subclasses, comprising of both organic and inorganic species, most of which harmful to human health.

Particles may be either directly emitted into the atmosphere or formed there by chemical reactions; referred to as primary and secondary particles, respectively. Urban aerosols are mixtures of primary particulate emissions from industries, transportation, power generation

---

<sup>1</sup> *Aerodynamic diameter* is defined as the diameter of a sphere of unit density that has the same terminal falling speed in air as the particle under consideration.

and natural sources and secondary material formed by gas-to-particle conversion mechanisms. These secondary photochemical reactions in addition to the vehicular sources constitute the most prominent sources of ultrafine particles in an urban metropolis like Los Angeles Basin (Fine et al. 2004; Zhang et al. 2004).

Particle size is the most important parameter for characterizing the behavior of aerosols. All properties of aerosols depend on particle size; furthermore, the nature of the laws governing these properties may change with particle size. A typical size distribution of urban atmospheric particles is shown in figure 1.

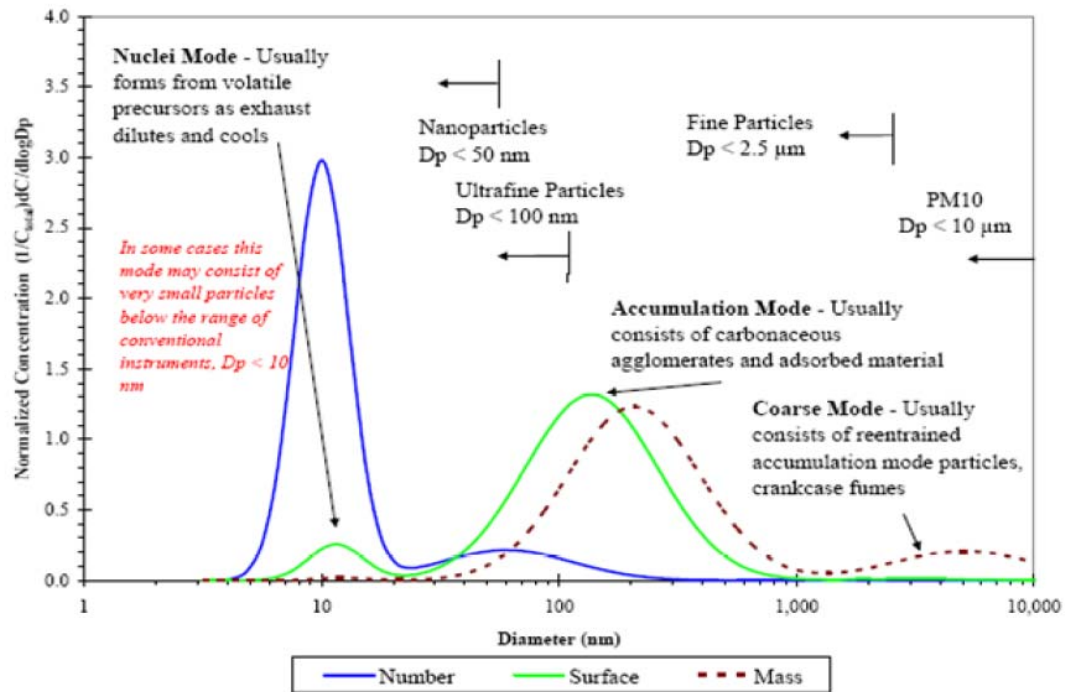


**Figure 1.1** – Typical size distribution of urban atmospheric particles.

In general the volume or mass distribution is dominated in most areas by two modes: the accumulation and coarse modes. Accumulation mode particles are the result of primary emissions or coagulation of smaller particles. Particles in the coarse mode however, are

usually produced by mechanical processes such as wind or erosion (dust, sea salt, pollens, etc.). While the particles larger than 0.1  $\mu\text{m}$  in diameter practically contribute all the aerosol mass, they are negligible in number compared to particles smaller than 0.1  $\mu\text{m}$ . These particles are mostly fresh aerosols created in situ from the gas phase by nucleation or through photochemistry and are often semi-volatile.

### 1.1.2 Health Effects of the Exposure to Particulate Matters in the Atmosphere

One of the prominent motivations in aerosol science is the impact of aerosols on human health. Polluted air has been associated with harmful health effects for decades. For example, well documented air pollution episodes occurred in the Meuse Valley of Belgium in December 1930 and in London in December 1952, leading to significant morbidity during the days of high pollution. After the London smog episode, the action taken to reduce emissions over the years, including the use of better combustion technologies, cleaner fuels, combustion after-treatment technologies as well as the construction of higher stacks in power plants, dramatically improved urban air quality. Particle related regulations in the US started in the 70s when the US Environmental Protection Agency (US EPA) incorporated total suspended particle (TSP) as one of the criteria pollutants as part of the Clean Air Act, which was passed in 1963 and required EPA to develop and enforce regulations to protect the general public from exposure to airborne contaminants that are known to be hazardous to human health. TSP standard was subsequently replaced by  $\text{PM}_{10}$  (particles smaller than 10  $\mu\text{m}$ ) standards in 1987. The growing evidence on fine particle toxicity led to new legislation for  $\text{PM}_{2.5}$  standards in 1997. Recent epidemiological studies have shown there is growing proof that elevated airborne PM mass concentration of size fractions ranging from ultrafine- to fine –to coarse is well associated with adverse human health outcomes including both respiratory and cardiac diseases (Becker et al. 2005; Hornberg et al. 1998; Kleinman et al.



2003; Li et al. 2003; Lipsett et al. 2006; Monn and Becker 1999; Oberdorster 2001; Pekkanen et al. 1997; Villeneuve et al. 2003; Xia et al. 2004; Yeatts et al. 2007). Urban air PM<sub>10</sub> is a highly complex mixture of different sized aerosols originating from a large variety of anthropogenic and natural sources. While epidemiological studies have most often given stronger exposure-response relationships for mortality and morbidity outcomes in association with fine particles than with PM<sub>10</sub>, some studies have shown stronger associations between urban air coarse particles with respiratory hospital admissions (Brunekreef and Forsberg 2005). While both ultrafine and fine PM size fractions fall into the PM<sub>2.5</sub> standards, the PM<sub>10</sub> standards encompass all three major size ranges (coarse, fine and ultrafine). These standards are mass based and although smaller particles (e.g. ultrafine PM) dominate the total number concentrations, mass concentrations are generally dictated by larger size fractions (e.g. coarse PM). In addition, in regards of PM<sub>10</sub> standards, coarse PM emissions are usually from hard to control sources like windblown soil and dust, brake lining abrasion, tire wear and bioaerosols, therefore control of fine PM emissions is easier to achieve in order to meet PM<sub>10</sub> standards. Coarse and fine PM have substantially different sources and sinks, and as a result different chemical composition, which would lead to potentially different health outcomes. Moreover, the available CPM mass concentration data is much more limited compared to ambient PM<sub>2.5</sub> mass concentration data and hence significantly less is quantitatively known about the characteristics of CPM.

There is increasing evidence that particle mass concentration may not be the most appropriate parameter for the assessment of health effects of particulate matter (Forsberg et al. 2005). Health studies and ambient air regulators need to consider various PM characteristics, such as size, mass and number concentration, and particle chemical speciation as alternative and/or supplementary exposure parameters for particle mass regulations and in health effect assessment. Current air quality standards all over the world

are based on PM<sub>10</sub> and PM<sub>2.5</sub> mass concentrations; however there is a shortage of legislation based on chemical constituent concentrations. Adverse health effects of exposure to urban particulate matter reported by epidemiological studies inform and motivate public perception which results in new regulations concerning ambient air quality and emission sources. Therefore, new toxicological studies focusing on identifying specific categories of ambient PM that need stricter control in order to protect public health are crucial.

## 1.2 Rationale of the Proposed Research

Epidemiological studies have shown an association between particulate matter (PM) exposure and human mortality. Further investigations showed a strong association between exposure to fine particles and human health. These findings have raised considerable concern over human exposure to PM<sub>2.5</sub> and its chemical characteristics. Vehicular emissions are known to be the major source of PM<sub>2.5</sub> in urban areas, particularly in Los Angeles Basin. In order to minimize the impact of human exposure to fine particles a better knowledge of vehicular emission factors is essential. Different approaches have been used to characterize vehicular emissions, including chassis dynamometer studies (Schauer et al. 1999; Schauer et al. 2002; Zielinska et al. 2004) and roadside pollutant concentration measurements (Kuhn et al. 2005; Ntziachristos et al. 2007b). Chassis dynamometer experiments have the ability to examine vehicle emissions under different driving and loading settings and effectively evaluate exhaust control technologies. The reduction in PM mass emission rates due to new advanced after-treatment technologies can also be investigated. However, a controlled laboratory environment may not necessarily be representative of real-world driving conditions (Zhang and Morawska 2002), and non-tailpipe emissions such as those from tire wear, the wear of brake linings and re-suspended road dust (Allen et al. 2001) are not accounted for by such approach. These emissions are often from hard to control sources and

mostly fall within coarse PM size range (2.5-10  $\mu\text{m}$ ). In order to capture these non-tailpipe emissions roadside measurements are required. Such measurements are of special interest in metropolitan areas where CPM mass concentrations are predominantly influenced by traffic volume and traffic speed.

Extensive number of studies have focused on effects of different after-treatment technologies on PM mass and number concentrations. These emission control devices significantly reduce PM mass emission rates. (Ayala et al. 2002) showed that PM mass emissions from diesel vehicles equipped with diesel particulate filter (DPF) have been reduced by 10 to 50-fold. However, the volatile and semi-volatile fraction of the exhaust can penetrate the DPF and subsequently undergo gas-to-particle conversion once exhaust is cooled and diluted in the atmosphere to form the semi-volatile particles (Kittelson et al. 2006; Matter et al. 1999a). In continuously regenerating technology (CRT<sup>®</sup>), diesel oxidation catalyst (DOC) is used in tandem with a DPF to effectively convert the total hydrocarbon (THC) and carbon monoxide (CO) to water and carbon dioxide. Moreover, in SCRT<sup>®</sup> systems NO<sub>x</sub> is converted to elemental nitrogen to further reduce the secondary formation of semi-volatile particles after emission. The effect of these high efficiency after-treatment devices on total PM mass and number concentrations is well investigated in several dynamometer studies (Ayala et al. 2002; Grose et al. 2006; Herner et al. 2007), however there is limited number of publications in the literature discussing the composition of the remaining organic compounds emitted from diesel truck equipped with after-treatment devices as the chemical PM composition may be altered (Biswas et al. 2008; CARB 1998). Moreover, the removal of solid, mostly carbonaceous non-volatile particles reduces the overall PM surface available for condensation of semi-volatile gases, which promotes nucleation and formation of nanoparticles (Maricq 2007). In order to better understand the origin of these organic species in the retrofitted vehicle exhaust and to evaluate the overall effectiveness of after-treatment

technologies in reducing harmful organic compounds the particle bound organic species from the vehicle exhaust is characterized in the present study. This study is part of the chassis dynamometer study done by the University of Southern California in collaboration with the California Air Resources Board (CARB) to investigate the physical, chemical and toxicological characteristics of diesel emissions of particulate matter (PM) from heavy-duty vehicles. Physical and chemical properties of PM emissions have been reported previously by Biswas et al. (Biswas et al. 2008) and Hu et al. (Hu et al. 2008).

While these after treatment technologies are very efficient in removing the particles from the exhaust the volatile and semi-volatile species, which are predominantly in vapor phase due to high exhaust temperatures, are not effectively removed. These vapors subsequently condense and bound to the particulate phase immediately following their release in the atmosphere as they are diluted and consequently cooled. After further dilution, the semi-volatile species partition back to the vapor phase. The low volatility vapors contribute to substantial formation of secondary organic aerosols (SOA) through photo-oxidation. As the recent studies focus more on the health effects of the individual particle chemical components, most notably to organic species, semi-volatile organic compounds (SVOC) are gaining more attention due to their toxic potency, including the capability to induce oxidative stress and consequently hazardous health effects. While the association of adverse health effects with SVOC compounds has been reasonably well documented, the exact mechanisms by which SVOC compounds inflict health effects remain largely unknown. For example, it is unclear whether the same SVOC species would elicit similar health effects if inhaled as a pure vapor as opposed to bound to ambient PM, therefore the importance of the specific phase of the SVOC on toxicity remains to be investigated. Traditionally, thermodenuders have been used to remove semi-volatile PM species from the particle phase and provide non-volatile PM for chemical and toxicological studies (Verma et al. 2011),

where the toxicity of the non-volatile fraction of PM is compared to the mixture of the non-volatile and semi-volatile fraction to assess the toxicity of the semi-volatile only fraction. In the present study, the thermodenuder (Dekati Ltd., Finland) is modified by replacing the adsorption section with a newly designed filter holder, and is used in tandem with the Versatile Aerosol Concentration Enrichment System (VACES), designed and engineered by University of Southern California, in order to separate semi-volatile species from the particle phase, and provide them in vapor phase for inhalation exposure studies. This technology makes it possible to conduct toxicity and inhalation exposure studies separately to PM and vapor phase SVOC to investigate the degree to which health effects attributable to these pollutants are affected by their phases.

As discussed before, the dynamometer studies only account for the exhaust emissions from combustion processes and roadside measurements are required to capture the resuspended coarse particulate matter. CPM consists of several mechanically generated species including resuspended road dust, industrial materials, brake lining abrasion, tire wear, trace metals, sea salt and bio-aerosols such as fungal spores and pollen (Almeida et al. 2005; Chow et al. 1994; Edgerton et al. 2009; Harrison et al. 1997; Hinds 1999). These species have substantially different sources and sinks compared to PM<sub>2.5</sub> fraction and can be composed of varying chemical species contributing to potentially different health outcomes. Coarse particles have substantially shorter residence time in the atmosphere compared to fine PM and therefore the CPM mass concentrations and more importantly its composition can vary widely in a metropolitan environment. While in urban areas the particles associated with motor vehicle operation are more important, the CPM mass concentration is dominated by mineral material from windblown dust and soil in rural areas. In order to study the physical, chemical and toxicological characteristics of CPM in Los Angeles Basin, 10 distinct measurement sites were employed to sample the CPM for 24 hours once a week for an entire

year. The sampling sites were selected to encompass rural-agricultural, urban and industrial environments within Los Angeles Basin; therefore an extensive dataset showing the temporal and spatial variations of 24-hour time-integrated daily mean coarse particle mass concentrations was obtained.

An increasing number of studies have reported associations between health effects and specific PM chemical species, rather than total PM mass (Claiborn et al. 2002; Tsai et al. 2000), with many studies linking trace element and metal species to various health outcomes (Gavett and Koren 2001; Luttinger and Wilson 2003; Smith and Aust 1997). US Environmental Protection Agency (EPA) listed several transition metals, As, Be, Cd, Co, Cr, Hg, Mn, Ni, Pb, Sb and Se, as air toxics. Trace elements and metals comprise a significant portion of the coarse PM mass. Wear of brake lining and tire wear in particular, contribute greatly to the high metal content of coarse mode PM. Analysis of PM elemental composition, in addition to evaluation of its impacts on human health, can be used in the identification of specific emission sources by introducing unique tracers. Concentrations of 49 trace elements were quantified by sector-field coupled plasma mass spectrometry (SF-ICP-MS) in order to provide a much needed database of trace element and metal content of coarse PM in the greater Los Angeles areas, providing the seasonal and spatial variations over a variety of urban and semi-rural areas during one year of sampling period.

### 1.3 Thesis overview

This thesis summarizes my research work during my doctoral study under supervision of Prof. Costantinos Sioutas with a goal to consolidate the current understanding of the characterization of the urban aerosols and their effect on Los Angeles air quality. Finally, the thesis discusses possible approaches and metrics for future PM emission and ambient air quality regulations and standards. The thesis includes the following chapters:

Chapter 1 provides a general overview on air pollution focusing on urban particulate matter, and discusses the characteristics of particles and their effect on air quality. Furthermore, the rationale of the thesis is also discussed, presenting a brief outline of the following chapters.

Chapter 2 discusses the characterization of the particle bound organic species from the vehicle exhaust of the heavy-duty diesel vehicles equipped with advanced emission control technologies. The contribution of diesel fuel and lubricating oil to the total organic carbon emitted from the retrofitted vehicles is also studied.

Chapter 3 introduces a new methodology to conduct toxicity and inhalation exposure studies separately to the PM and vapor phase semi-volatile pollutants to investigate the degree to which health effects attribute to these pollutants are effected by their physical phases. This technology makes it possible to better understand the mechanism by which semi-volatile compounds inflict health effects.

Chapter 4 focuses on ambient coarse PM mass concentrations and the relationships between CPM and PM<sub>2.5</sub> mass concentrations at 10 distinctly different locations in the greater Los Angeles area. The sources and behavior of coarse particles in a primarily urban and motor vehicle dominated environment are discussed.

Chapter 5 discusses the elemental content of the samples of CPM from the year-long measurement campaign at 10 sites in the greater Los Angeles area and is part of the CPM study focusing on physical, chemical and toxicological characteristics of the coarse particles. Using mathematical methods, elemental tracers and markers for some of the CPM sources are identified. The contribution of different sources to elemental content of CPM, such as mineral material, abrasive vehicular emissions, industrial emissions and sea salt spray are

reported. Moreover, a detailed description of temporal and spatial variations of the CPM metal content in the Los Angeles area is provided.

Chapter 6 summarizes the previous chapters and outlines the conclusions while discussing possible strategies, including additional metrics, to regulate PM emissions and establish air quality standards that are pertinent to public health.



## **Chapter 2 - Characterization of Particle Bound Organic Carbon from Diesel Vehicles Equipped with Advanced Emission Control Technologies**

### **2.1 Abstract**

A chassis dynamometer study was carried out by the University of Southern California in collaboration with the Air Resources Board (CARB) to investigate the physical, chemical and toxicological characteristics of diesel emissions of particulate matter (PM) from heavy-duty vehicles. These heavy-duty diesel vehicles (HDDV) were equipped with advanced emission control technologies, designed to meet CARB retrofit regulations. A HDDV without any emission control devices was used as the baseline vehicle. Three advanced emission control technologies; Continuously Regenerating Technology (CRT<sup>®</sup>), Zeolite- and Vanadium-based Selective Catalytic Reduction Technologies (Z-SCRT<sup>®</sup> and V-SCRT<sup>®</sup>), were tested under transient (UDDS) (Ayala et al. 2002) and cruise (80 kmph) driving cycles to simulate real-world driving conditions. This paper focuses on the characterization of the particle bound organic species from the vehicle exhaust. Physical and chemical properties of PM emissions have been reported by Biswas et al. (Biswas et al. 2008) and Hu et al. (Hu et al. 2008)

Significant reductions in the emission factors ( $\mu\text{g}/\text{mile}$ ) of particle bound organic compounds were observed in HDDV equipped with advanced emission control technologies. V-SCRT<sup>®</sup> and Z-SCRT<sup>®</sup> effectively reduced PAHs, hopanes and steranes, n-alkanes and acids by more than 99%, and often to levels below detection limits for both cruise and UDDS cycles. The CRT<sup>®</sup> technology also showed similar reductions with SCRT<sup>®</sup> for medium and high molecular weight PAHs, acids, but with slightly lower removal efficiencies for other organic compounds. Ratios of particle bound organics - to- OC mass ( $\mu\text{g}/\text{g}$ ) from the baseline exhaust were compared with their respective ratios in diesel fuel and lubricating oil, which

revealed that hopanes and steranes originate from lubricating oil, while PAHs can either form during the combustion process or originate from diesel fuel itself. With the introduction of emission control technologies, the particle bound organics-to-OC ratios ( $\mu\text{g/g}$ ) decreased considerably for PAHs, while the reduction was insignificant for hopanes and steranes, implying that fuel and lubricating oil have substantially different contributions to the total OC emitted by vehicles operating with after-treatment control devices compared to the baseline vehicle since these control technologies had a much larger impact on PAH OC than hopanes and steranes OC.

Keywords: diesel, CRT<sup>®</sup>, SCRT<sup>®</sup>, emission factor, speciated organics

## 2.2 Introduction

Diesel exhaust particles (DEP) have been classified as toxic by the California Air Resources Board (CARB 1998) and studies have linked them to various adverse health effects (Solomon and Balmes 2003). DEP contain a variety of chemical constituents, including element carbon (EC), organic carbon (OC), sulfate, trace metals etc, among which organic compounds, such as polycyclic aromatic hydrocarbons (PAH), hopanes and steranes, are of particular interests. PAHs are not specifically regulated, however they are considered to be among the most pervasive classes of potential environmental carcinogens (EPA 2002; Reed 1988). Moreover, particle phase PAHs can trigger oxidative stress in cells {Li, 2003 #46}. Schauer et al. (Schauer 2003) showed that hopanes and steranes could be used to distinguish diesel and gasoline engine emissions from other combustion sources. These non-labile species can serve as unique tracers in determining the contribution of diesel and gasoline vehicles to the total concentrations measured in ambient air (Rogge et al. 1993). It should be noted that these compounds are also emitted from the combustion of coal and fuel oil and cannot serve as unique traffic tracers in the proximity of such sources.

Various studies have focused on potential risks of diesel PM on human health, which has motivated policy makers to promulgate stricter emission control rules and regulations. The US EPA 2007 emission standard for PM reduced the diesel PM mass emission standard from 0.1 grams per brake horse power per hour of PM to  $0.01 \text{ g bhp}^{-1}\text{h}^{-1}$  (Merrion 2003). To meet this standard, efforts from the engine manufacturing community have been devoted to the development of advanced engine designs and emission control technologies for the newer fleet of heavy-duty trucks. These after-treatment devices significantly reduce PM mass emission rates (McGeehan et al. 2005), e.g. PM mass emissions from diesel vehicles equipped with diesel particulate filter (DPF) have been reduced by 10 to 50-fold (Ayala et al.

2002). Nonetheless, some potentially harmful and un-regulated volatile and semi-volatile PM species, such as PAHs, can penetrate the DPF and subsequently undergo gas-to-particle conversion, with the cooling of the exhaust, to form semi-volatile particles (Kittelson et al. 2006; Matter et al. 1999a). To address this issue, catalysts have been employed in various PM emission control technologies. Diesel oxidation catalysts (DOC) have been used in combination with a DPF in continuously regenerating technologies (CRT<sup>®</sup>). The DOC oxidizes total hydrocarbon (THC) and carbon monoxide (CO) to form carbon dioxide (CO<sub>2</sub>) and H<sub>2</sub>O. Selective catalytic reduction is used to oxidize nitrogen oxides (NO<sub>x</sub>) and reduce their emissions. These urea-SCRT<sup>®</sup> systems use ammonia (NH<sub>3</sub>) generated from urea solution to react selectively with NO<sub>x</sub> to form water (H<sub>2</sub>O) and elemental nitrogen (N<sub>2</sub>) (Liu et al. 2008). However, these after-treatment devices may alter the chemical PM composition or increase the PM number concentrations under certain conditions (Biswas et al. 2008; Kittelson et al. 2006). The removal of solid, mostly carbonaceous particles, reduces the overall PM surface available for condensation of semi-volatile compounds, which promotes nucleation and formation of nano-particles (Maricq 2007). SCRT<sup>®</sup> systems demonstrated high efficiencies in reducing NO<sub>x</sub> emissions, while reduction in PAH emissions were attributed to the downstream oxidation catalyst, and the ability of Zeolite-catalysts in particular to break heavy hydrocarbons into smaller molecules (Liu et al. 2008).

While an extensive number of studies have focused on effects of different after-treatment technologies on PM mass and number concentrations, there is limited number of papers in the literature discussing the composition of the remaining organic compounds emitted from diesel truck equipped with after-treatment devices. This information is vital in improving our understanding of the origin of these organic species in the retrofitted vehicle exhaust, and in evaluating the overall effectiveness of after-treatment technologies in reducing harmful organic compounds.

This paper is part of a collaborative study between the California Air Resources Board (CARB) and University of Southern California (USC) to investigate the physicochemical and toxicological properties of HDDV emissions equipped with advanced emission control devices aiming at the newest CARB retrofit regulations. In this paper, we will focus on the speciation of organic compounds of the PM emissions from vehicles equipped with various control devices under different driving cycles. Details of PM physical and chemical characteristics have been reported in companion studies from our group (Biswas et al. 2008; Hu et al. 2008).

### 2.3 Experimental Methodology

The chassis dynamometer experiments were carried out at California Air Resources Board's (CARB) Heavy-Duty Diesel Emission Testing Laboratory (HDETL) facility in downtown Los Angeles (Ayala et al. 2002). Two different driving cycles were tested to emulate real-world driving conditions, including steady state cruise (80 kmph) and transient EPA urban chassis dynamometer driving schedule (UDDS) which represents city driving conditions. The sampling train consists of a heavy duty chassis dynamometer, a constant volume sampling (CVS) (Ayala et al. 2002), and a dilution tunnel and a high volume sampler (Misra et al. 2002). A detailed schematic of the chassis dynamometer set-up can be found in the supporting information. The exhaust emissions were diluted with filtered air, using activated carbon and high-efficiency particulate air (HEPA) filters through the CVS. The USC high volume sampler (Misra et al. 2002) was placed approximately 18 diameter lengths downstream of the exhaust introduction in the CVS. CARB ultra-low sulfur diesel fuel (ULSD) with sulfur content <15 ppm was used in all vehicles. In addition to measuring tunnel blanks, all vehicles were warmed up and conditioned before the start of the official run. More detailed information about the experimental set up can be found in companion

studies (Biswas et al. 2008; Hu et al. 2008).

### 2.3.1. Vehicles and control devices

A 1998 Kenworth truck with an 11L engine without any after-treatment emission control devices was tested as the baseline vehicle. The same truck was also tested with three different emission control technologies: a continuously regenerating technology (CRT<sup>®</sup>) which consists of a diesel oxidation catalyst (DOC) followed by an un-catalyzed trap; CRT<sup>®</sup> systems in combination with selective catalytic reduction system (SCRT<sup>®</sup>) using Zeolite and Vanadium as catalysts. The test vehicles are referred to as baseline, CRT<sup>®</sup>, V-SCRT<sup>®</sup> and Z-SCRT<sup>®</sup> in this paper. The details of the tested emission control technologies are listed in Table S1 the supporting information.

The dilution factor affects the partitioning of semivolatile species such as the lighter PAH (it would have little effect on heavier PAH and hopanes - steranes); a lower dilution factor will drive this partitioning towards the particle phase, thereby leading to potential overestimation of it compared to an environment with lower dilution ratio. This is an important distinction between the sampling conditions in dynamometer studies compared to those encountered in the ambient atmosphere. The nominal dilution air flow rate in the CVS was 2600 cfm (74 m<sup>3</sup>min<sup>-1</sup>) for both cruise and UDDS driving cycles. As result, dilution ratios were 6-9 for cruise, 5-80 for UDDS (Biswas et al. 2008). The exhaust temperature at the sampling inlets of the CVS varied between 35 and 40 deg\_C, which was very consistent during the experiments.

### 2.3.2. Sampling methodology and chemical analysis

Particulate matter was collected on Teflon coated glass fiber filters (20 x 25 cm) (Pallflex Fiberfilm T60A20-8x10, Pall Corp., East Hills, NY) using a high volume sampler (Misra et

al. 2002) operating at 450 lpm. Teflon-coated glass fiber filters overcome some of the inherent inadequacies of glass fiber filters by being inert to catalyzing chemical transformations as well as by being less moisture-sensitive (Baron and Willeke 2001).

Numerous individual compounds were quantified by gas chromatography-mass spectrometry (GC/MS) including, polycyclic aromatic hydrocarbons (PAH), hopanes and steranes, *n*-alkanes and organic acids. Methods for the quantification of individual organic compounds were based on already established solvent extraction procedures reported earlier (Schauer et al. 1999). Samples were extracted in dichloromethane and methanol and were combined and reduced in volume to approximately 1 mL by rotary evaporation, followed by pure nitrogen evaporation. The underivatized samples were analyzed by auto injection into a GC/MSD system (GC model 5890, MSD model 5973, Agilent). A 30 m × 0.25 mm DB-5MS capillary column (Agilent) was used with a splitless injection. Along with the samples, a set of authentic quantification standard solutions were also injected and used to determine response factors for the compounds of interest. All the results were blank-corrected prior to data analysis and converted to mass of analyte per distance traveled.

### 2.3. Results and Discussion

Figures 1a and 1b present the PM organic compound mass emission factors (EF) for the UDDS driving cycle of the baseline vehicle as well as the same vehicle equipped with the different after-treatment technologies noted earlier (CRT<sup>®</sup>, V-SCRT<sup>®</sup> and Z-SCRT<sup>®</sup> respectively). The emission factors of PAHs, hopanes and steranes in UDDS range from 2.4 µg/km to 49.4 µg/km for the baseline vehicle, with an average of 14.5 µg/km and 7.6 µg/km for PAHs and hopanes and steranes, respectively. The emission factor of *n*-alkanes and organic acids range from 26.3 µg/km to 3287.2 µg/km with an average of 745.0 µg/km and 90.5 µg/km for *n*-alkanes and organic acids respectively. As shown in Figure 1a, low

molecular weight PAHs with three to four rings are the largest contributor to the total PAH emissions. These light PAHs account for 47.8% of the measured total PAHs mass while the contribution of medium and high molecular weight PAHs are 33.6% and 18.6% respectively. This is consistent with other studies, which showed that three- and four-ring PAHs are present in HDDV exhaust in very high levels (Liu et al. 2008; Marr et al. 1999; Riddle et al. 2008). These PAHs are semi-volatile and can be found in both gas phase and particle form. As shown in Figure 1a and 1b, both CRT<sup>®</sup> and S-CRT<sup>®</sup> technologies effectively reduced the particle bound PAH, hopanes and steranes emissions compared with the baseline configuration by more than 99%. For medium and high molecular weight PAHs, the emission levels were below the detection limit of the analytical method with the introduction of both CRT<sup>®</sup> and S-CRT<sup>®</sup> technologies. These higher molecular weight PAHs are often more carcinogenic according to the International Agency for Research on Cancer (IARC). In contrast to the non-detectable heavier PAHs, the presence of particle phase light PAHs (even in small amounts) in the exhaust of vehicles equipped with CRT<sup>®</sup> and S-CRT<sup>®</sup> is attributed to the high volatility of these organic species. Light PAHs have lower vapor pressure and are most likely in the vapor phase in the hot engine exhaust. After passing through the control devices, these semi-volatile species may nucleate to form fresh particles, or condense onto existing particles under favorable dilution and temperature conditions (Kittelson et al, 2006; Vaaraslahti et al, 2004). These compounds may also condense or absorb on organic particles that have already nucleated. The occurrence of this PM formation mechanism has also been reported by Wehner et al. (Wehner et al. 2002) and Yu (Yu et al. 2001). In our studies, this observation is further supported by the substantial increase in number concentrations of nucleation mode particles for the vehicles equipped with control devices compared to the baseline truck, as reported by Biswas et al. (Biswas et al. 2008). For *n*-alkanes, there was a higher than 99% reduction in the emission factors after the introduction of CRT<sup>®</sup> compared



to baseline, whereas both V-SCRT<sup>®</sup> and Z-SCRT<sup>®</sup> devices effectively reduced the *n*-alkanes emission actors to below the detection limits. All three devices reduced equally effectively the organic acid content of the exhaust effectively to under the detection limits.

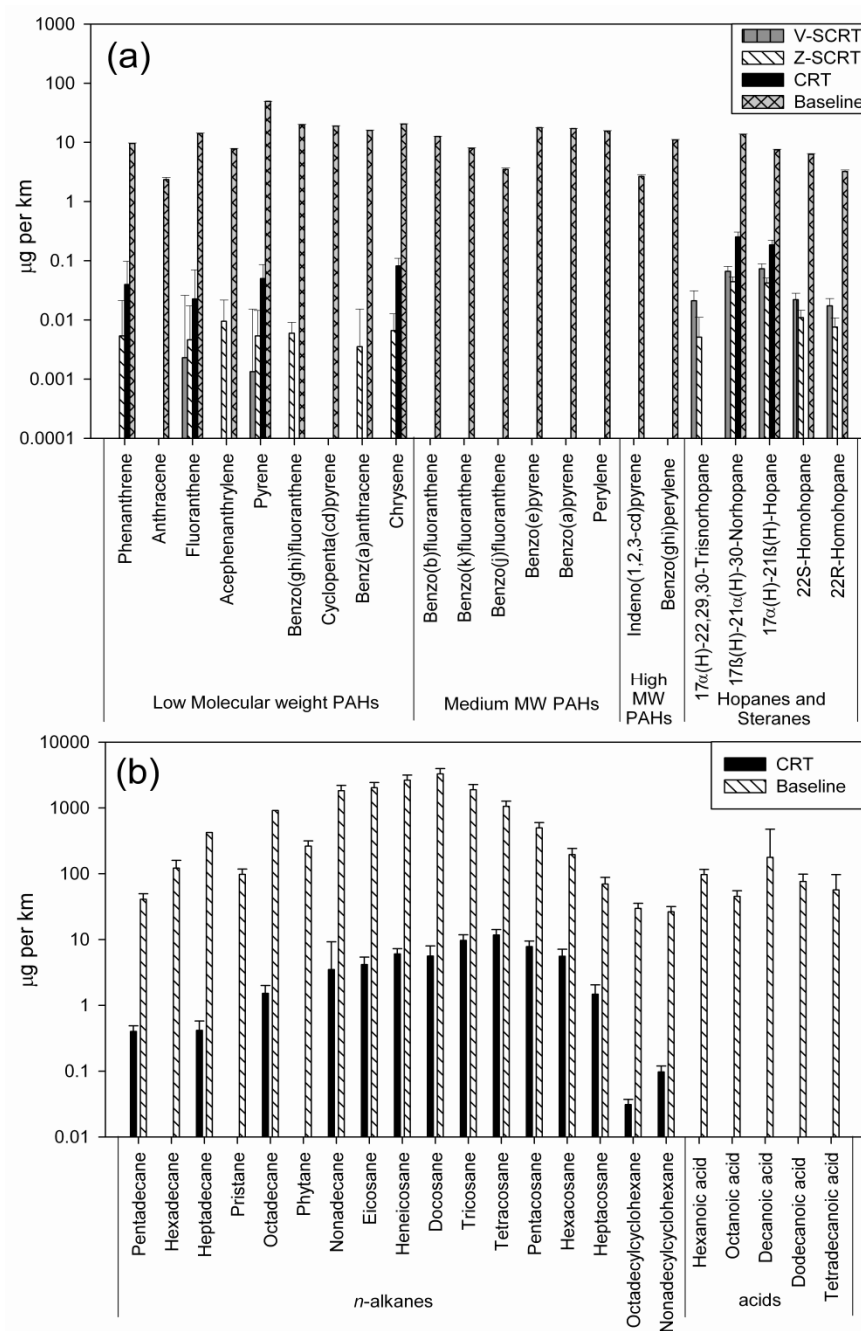


**Figure 2.1** – (a) Emission factors of PAHs, hopanes and steranes of baseline and control device-equipped vehicles in UDSS cycle. (b) Emission factors of *n*-alkanes and acids of baseline and control device-equipped vehicles in UDSS cycle.

Figure 2a and 2b present the emission factors (EF) of particle bound PAHs, hopanes and steranes, *n*-alkanes and organic acids for the cruise driving cycle. The EF of PAHs, hopanes and steranes range from 0.42 µg/km to 10.17 µg/km with an average of 2.66 µg/km and 2.92 µg/km respectively for the baseline vehicle. The average emission factors of PAHs, hopanes and steranes at UDDS are 5.5 and 2.6 times higher than those at cruise cycle, respectively. For *n*-alkanes and organic acids at the cruise cycle, the emission factors range from 1.74 µg/km to 122.78 µg/km with an average of 36.6 µg/km and 23.9 µg/km for *n*-alkanes and organic acids respectively. The emission factors are also significantly lower than their corresponding values at the UDDS cycle. The reduction of these organic compounds may be attributed to possible adsorption of these species on the large surface area of the catalyst, followed by oxidation (Heck and Farrauto 1995; Liu et al. 2008). PAH reduction by oxidation may be more efficient in the cruise compared to the UDDS cycle because the minimum activation temperature of the catalyst (for both V-SCRT<sup>®</sup> and Z-SCRT<sup>®</sup>) is reached much faster in the cruise cycle than the UDDS (Hu et al. 2008; Polidori et al. 2008). As the engine speed and load increase to a stable condition in cruise cycle, the exhaust temperature also increases to a level that enables full function of the catalyst.

All three control devices reduced the emissions of light molecular weight PAHs by more than 99%, while the emission factors of medium and high molecular weight PAHs after the devices were under the detection limits for the cruise cycle. The reduction of hopanes and steranes were equally high, i.e, 97.6%, 98.8% and 99.4% for CRT<sup>®</sup>, Z-SCRT<sup>®</sup> and V-SCRT<sup>®</sup>, respectively. The CRT<sup>®</sup> technology reduced *n*-alkanes and acids EF by 96% and 44% respectively, while both SCRT<sup>®</sup> technologies showed a better performance by reducing *n*-alkanes and acids to levels below detection limits. Similar results were also observed for UDDS cycles. The improved performance of the SCRT<sup>®</sup> catalyst may be due to their ability to break heavy hydrocarbons into smaller molecules {Ueno, 1998. #23}.

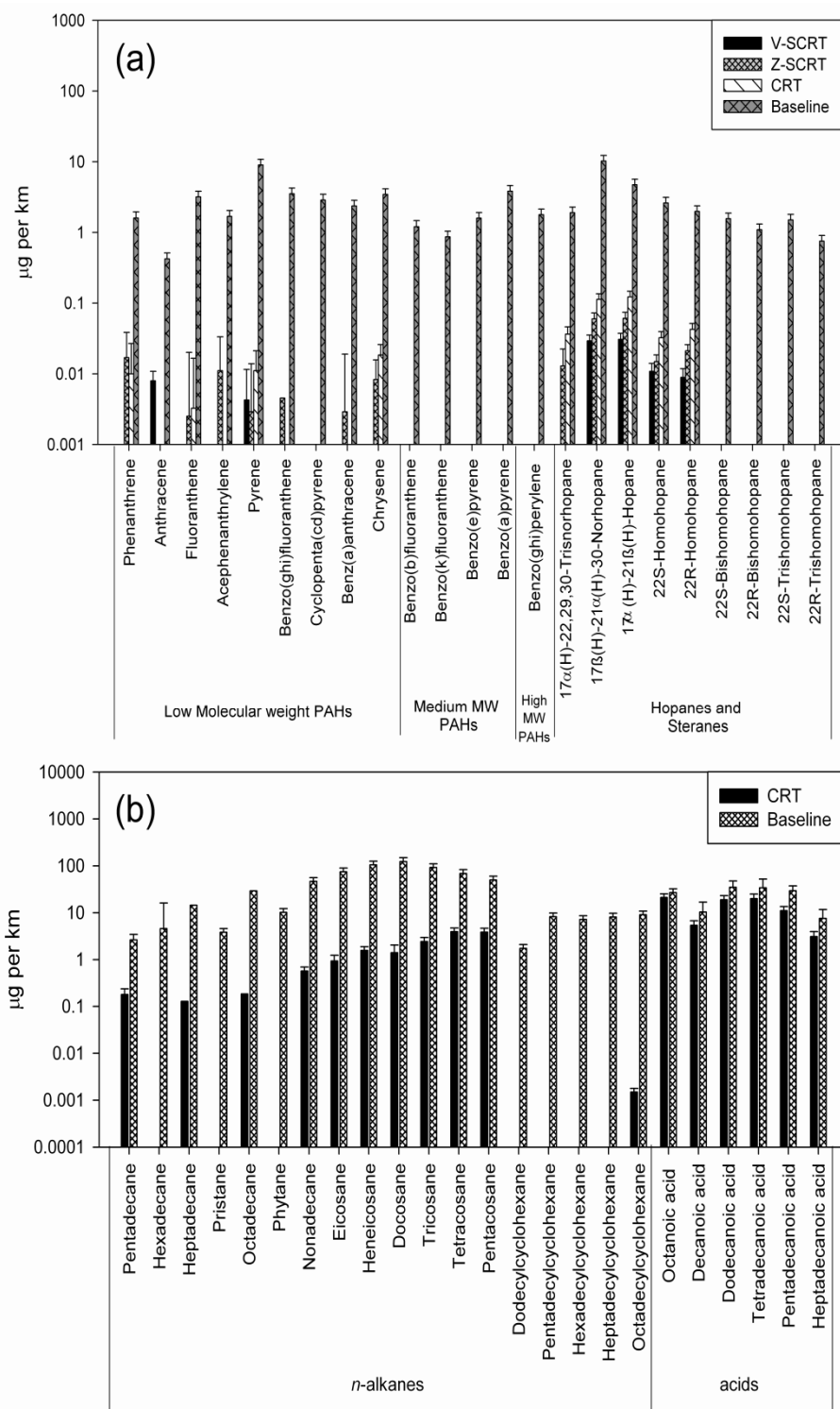


**Figure 2.2** – (a) Emission factors of PAHs, hopanes and steranes of baseline and control device-equipped vehicles in cruise cycle. (b) Emission factors of *n*-alkanes and acids of baseline and control device-equipped vehicles in cruise cycle.

Figure 3a and 3b show the concentrations of selected PAHs, hopanes and steranes in diesel fuel and used lubricating oil taken from Zielinska et al. (Zielinska et al. 2004) in  $\mu\text{g/g}$  of fuel and lubricating oil, along with their concentrations in  $\mu\text{g/g}$  of OC in both cruise and UDDS driving cycles from baseline vehicle in this study. The distribution of these PAHs, hopanes, and steranes can be used to investigate the mechanisms that lead to the formation of these PM species from diesel engines.

As shown in figure 3a, diesel fuel contains much higher levels of low molecular weight PAHs than lubrication oil ( $60.8 \mu\text{g/g}$  of diesel fuel versus to only  $3.7 \mu\text{g/g}$  of lube oil). The emission profiles of these light PAHs in both UDDS and cruise cycle vehicles showed very good agreement with those in diesel fuel, indicating that the origin of these low molecular weight PAHs is most likely from fuel or from combustion processes in engine. Similar results have been reported in many previous studies (Liu et al. 2008; Miguel et al. 1998; Riddle et al. 2008). Zielinska et al. (Zielinska et al. 2004) reported that medium and high molecular weight PAHs were both low in concentrations and have similar levels in diesel fuel and used lubricating oils. This is consistent with the measurements in this study which showed only  $0.32 \mu\text{g/g}$  of diesel fuel and  $0.94 \mu\text{g/g}$  of diesel oil on average for PAHs with medium and high molecular weights. However, some other studies have shown that concentrations of PAHs in new lubricating oil were actually very low, and their levels increase with driving distance of vehicle (Wang et al. 2000; Wong and Wang 2001). This is because these PAHs are most likely to accumulate in lubricating oil during combustion process in engine over time (Wang et al. 2000). In addition, the consumption of lubricating oil is negligible compared to diesel fuel combustion, suggesting that the dominant source of PAHs in engine exhaust is from diesel fuel. Diesel fuel is very rich in methyl-substituted PAHs, with significantly higher concentrations of methyl and di-methyl PAHs than normal PAHs. However, the PAH concentrations in the engine exhaust are higher or about the same

as the methyl and di-methyl PAHs. Schauer et al. (Schauer et al. 1999) found that these methyl and di-methyl compounds in diesel fuel are de-methylated to form PAHs during fuel combustion in the engine.

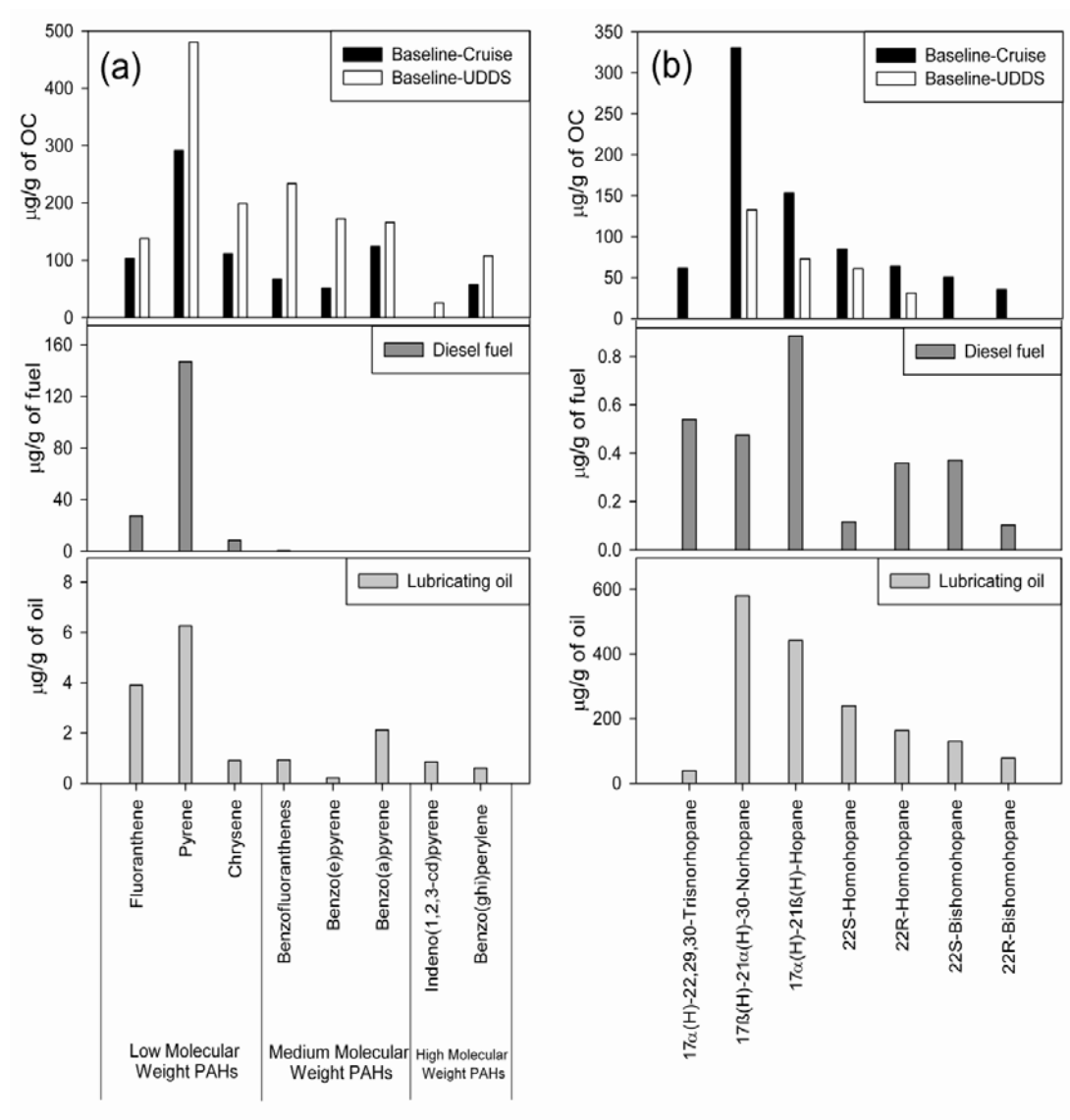


**Figure 2.3** – (a) Ratios of PAHs to organic carbon (OC) emission factors in  $\mu\text{g/g}$  from baseline vehicle and their comparison with PAH composition of diesel fuel and lubricating oil taken from Zielinska et. al. (Zielinska et al. 2004). (Benzofluoranthenes refer to Benzo(b)fluoranthene, Benzo(k)fluoranthene and Benzo(j)fluoranthene) (b) Ratios of hopanes and steranes to organic carbon (OC) emission factors in  $\mu\text{g/g}$  from baseline vehicle and their comparison with PAH composition of diesel fuel and lubricating oil taken from Zielinska et. al. (Zielinska et al. 2004).

Figure 3b compares the concentrations of selected hopanes and steranes in diesel fuel, used lubricating oil (Zielinska et al. 2004) and in the engine exhaust in the UDDS and cruise cycles. These organic compounds are thought to originate exclusively from lube oil and commonly used as tracers for diesel and gasoline emissions (Riddle et al. 2008). It can be seen in this figure that the hopanes and steranes concentration profiles in the vehicle exhaust (111.49  $\mu\text{g/g}$  of OC and 74.44  $\mu\text{g/g}$  of OC for cruise and UDDS cycles respectively) closely follow the hopanes and steranes composition in lubricating oil (238.37  $\mu\text{g/g}$  of oil), while their concentrations in fuel is negligible (0.41  $\mu\text{g/g}$  of fuel) compared to that in lubricating oil. The good agreement in the relative concentrations in the exhaust and lube oil composition observed in this study further corroborates the argument that the particle bound hopanes and steranes in vehicle emissions originate from lubricating oils. PAHs, hopanes and steranes have all been used as organic tracers for vehicle emissions. However, lubricating oil and diesel fuel make independent (and disparate) contributions to the levels of these species in the engine exhaust. A better understanding of the origins of these organic compounds can help investigations of PM formation mechanisms in the engine as well as in the exhaust (Kleeman et al. 2008).

Figures 4a, 4b and 4c show the concentration ratios of selected PAHs, hopanes and steranes to organic carbon of PM emissions from the baseline vehicle operating with and without control devices, running on UDDS (4a), and cruise (4b) cycles, and similar ratios of recently evaluated HDDV as reported recently by Riddle et al. (4c) (Riddle et al. 2007). As shown in these figures, the concentration ratios of the baseline vehicle displayed very similar profiles for these compounds between UDDS and cruise cycles, and in very similar magnitude as those observed by Riddle et al. (Riddle et al. 2007), which confirms the consistency in the sources of these PM organic tracers in both studies.



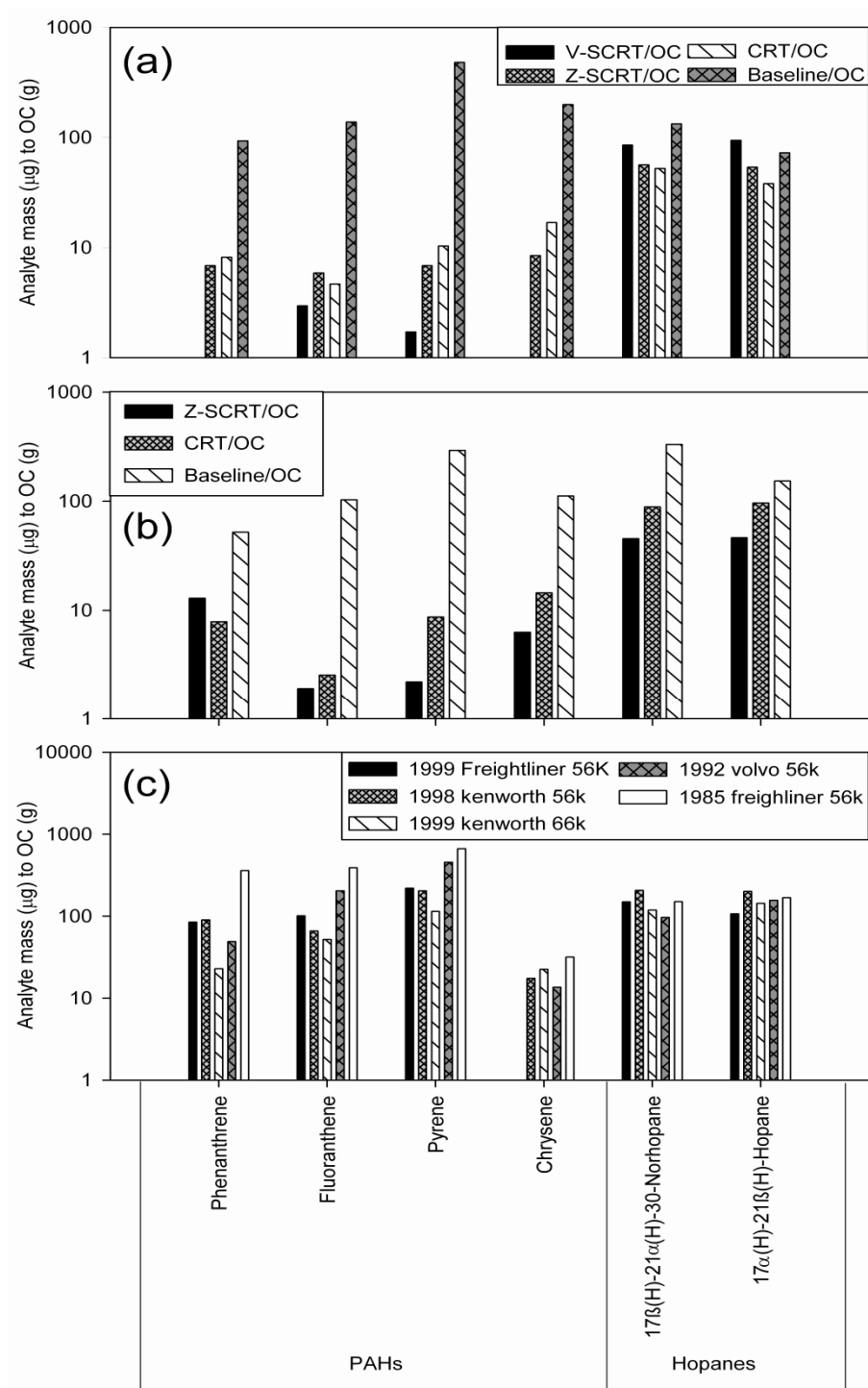


**Figure 2.4** – (a) Comparison of the ratios of PAHs, hopanes and steranes to organic carbon emission factors in  $\mu\text{g/g}$  from baseline and controlled vehicles running on UDDS cycle. (b) Comparison of the ratios of PAHs, hopanes and steranes to organic carbon emission factors in  $\mu\text{g/g}$  from baseline and controlled vehicles running on cruise cycle. (c) Ratios of PAHs, hopanes and steranes to organic carbon emission factors in  $\mu\text{g/g}$  as reported by Riddle et al. (Riddle et al. 2007).

As shown in figure 4a, PAHs-to-OC ratios are greatly reduced in vehicles equipped with control devices compared to baseline vehicle for the UDDS cycle. The average analyte mass ( $\mu\text{g}$ ) to OC mass (g) for the PAHs is 227.50 for baseline vehicle, and 10.0, 7.0, 2.3 for CRT<sup>®</sup>, Z-SCRT<sup>®</sup>, V-SCRT<sup>®</sup> respectively, thus indicating a significant reduction of PAHs contributions to OC in the emissions with the control devices. The reduction in PAHs is very important from the perspective of public exposure because of their carcinogenicity (Harvey 1985; Hewstone 1994). As discussed earlier, PAHs in the engine exhaust are considered to be predominantly products of incomplete combustion of diesel fuel. The significant reduction of the relative contribution of PAHs to OC suggests that these compounds are either not formed as readily in combustion, or they are reduced very effectively in after-treatment devices using oxidation catalysts (Liu et al. 2008).

In contrast to PAHs, the ratios of analyte mass ( $\mu\text{g}$ ) to OC mass (g) for the hopanes and steranes are in the same order of magnitude for baseline vehicle (102.7) and controlled vehicles (45.1, 54.9 and 89.6 for CRT<sup>®</sup>, Z-SCRT<sup>®</sup> and V-SCRT<sup>®</sup> respectively). Hopanes and steranes are exclusively found in lubricating oil. The similar ratios between retrofitted and baseline vehicles imply that even with the after-treatment devices, the relative contribution of the oil on the hopanes and steranes emissions are about the same order of magnitude as the baseline vehicle emissions. It should be noted that the ratio of hopanes and steranes to OC for the controlled vehicles is lower only by a factor of 2 or less (13%, 53% and 56% for CRT<sup>®</sup>, Z-SCRT<sup>®</sup> and V-SCRT<sup>®</sup>, respectively) compared to the baseline vehicle. This suggests that the relative contribution of lubricating oil to the OC emissions in the controlled vehicles is more than half of those in baseline vehicles, even with the reduction in OC emissions by almost two orders of magnitude (95.0%, 99.2%, 99.2% for CRT<sup>®</sup>, V-SCRT<sup>®</sup>, Z-SCRT<sup>®</sup>, respectively). It is possible that hopanes and steranes are oxidized at a slightly

higher rate than the rest of the lubricating oil. However, a reduction by a factor of  $<2$  is quite small in the context of the overall OC reduction.

Similar results were also observed in the cruise driving cycle, as shown in figure 4b. The average analyte mass ( $\mu\text{g}$ ) to OC mass (g) for the PAHs is 139.6 for baseline vehicle, 8.4 and 5.8 for CRT<sup>®</sup>, Z-SCRT<sup>®</sup>, respectively. The same ratio for the hopanes and steranes is 242, 92.4 and 45.9 for baseline, CRT<sup>®</sup> and Z-SCRT<sup>®</sup>, respectively. In general, the reduction efficiencies for high molecular weight PAHs, hopanes and steranes are consistently higher for the cruise cycle than the UDDS cycle. This is consistent with the fact that oxidation catalysts are more effectively activated to convert these organics by catalytic combustion in the cruise than the UDDS cycle, since the activation temperature is reached faster when the vehicles operate in the cruise cycle (Polidori et al. 2008). By comparison, low molecular weight PAHs, such as phenanthrene and fluoranthene, are largely in the gas-phase in the hot engine exhaust due to their high vapor pressure (Zielinska et al. 2004). Thus, their presence in the particle phase suggests that they are formed by nucleation or (more likely) by condensation onto pre-existing solid particles with the lowering of temperature as tailpipe emissions reach ambient conditions. Apparently, the effect of atmospheric dilution, which would favor the partitioning of these species in the gas phase, is outweighed by the drastic reduction in the exhaust temperature during cooling of the tailpipe exhaust (Hu et al, 2008; Kittelson et al, 2006; Vaaraslahti et al, 2004).

Comparisons in the emission factors of baseline and retrofitted vehicles for organic compounds showed that V-SCRT<sup>®</sup> and Z-SCRT<sup>®</sup> effectively reduced the PAHs, hopanes and steranes, n-alkanes and organic acids by more than 99% or even to the levels below detection limits for both cruise and UDDS cycles. The CRT<sup>®</sup> technology also showed similar removal efficiencies with SCRT<sup>®</sup> for medium and high molecular weight PAHs,

organic acids, but lower efficiencies for other organic compounds, probably due to the additional effect of catalytic reduction of these compounds in SCRT<sup>®</sup>. The faster thermal equilibration during the cruise cycle leads to a quicker catalyst activation and helps maintain a more stable catalytic reduction than the UDDS cycle. Ratios of organic analyte to OC mass from the baseline exhaust suggest that PAHs can form in combustion processes or originate from diesel fuel, whereas hopanes and steranes come from lubricating oils. With the introduction of control devices, the analyte to OC ratios reduced significantly for PAHs, while the reduction was more modest for hopanes and steranes, implying that fuel and lubricating oil have substantially different contributions to the OC emitted by vehicles operating with control devices compared to the baseline vehicle.

## 2.4 Acknowledgments

This research is sponsored by the California Air Resources Board (CARB), California Energy Commission (CEC), and South Coast Air Quality Management District (SCAQMD) through Grant No. 05-308 to USC. The authors would like to thank Dr. Subhasis Biswas, Vishal Verma, Dr. Harish Phuleria, Dr. Michael Geller, Mohammad Arhami, Ralph Rodas and George Gatt for their valuable support during experimental phase. The authors would also like to thank Mike Olson, Jeff DeMinter and Brandon Sheldon (Wisconsin State Laboratory of Hygiene) for help with chemical analysis. This research has not been subjected to CARB's peer and policy review, and official endorsements should not be inferred.

### **Chapter 3 - Modification of the Versatile Aerosol Concentration Enrichment System (VACES) for Conducting Inhalation Exposures to Semi-volatile Vapor Phase Pollutants**

#### **3.1 Abstract**

A novel sampling system was developed to provide concentrated vapor phase only semi-volatile organic species for in-vivo exposure studies. The system consists of two units: particles (including their semi-volatile component) are first concentrated by means of the Versatile Aerosol Concentration Enrichment System (VACES), and subsequently drawn through a heating section, in which semi-volatile particle-bound components partition to the gas phase, while non-volatile particles are removed by a quartz filter placed after the heater. The vapors are then cooled to ambient temperatures, without producing nano-particles by nucleation, and can be readily used for exposure studies. Laboratory tests were carried out at various heater temperatures using ammonium sulfate, adipic acid and glutaric acid to investigate the occurrence of nucleation in the cooling section. Subsequently the system was tested in the field with concentrated particle and vapor samples taken upstream of the heater, immediately downstream of the filter, and after the cooling section. Chemical analysis of particle and vapor phases upstream and downstream of the system was conducted for selected polycyclic aromatic hydrocarbons (PAHs), and showed very good PAH recovery. These tests indicate that the modified VACES-heater-filter (VHF) system can provide concentrated PM (including their semi-volatile compounds) and PM-bound semi-volatile species purely in the vapor phase for inhalation exposure studies separately, a feature that makes this system an attractive approach for toxicity studies, particularly in light of the increasing interest in health effects of exposures to multi-pollutant atmospheres.

*Keywords:* Semi-volatile, polycyclic aromatic hydrocarbon, particle concentrator, in-vivo exposure, VACES

### 3.2 Introduction

In the last decades, a number of epidemiological and toxicological studies have demonstrated robust associations between exposure to ambient particulate matter (PM) and increased cardiopulmonary morbidity and mortality (Cassee et al. 2005; Dockery et al. 1993; Laden et al. 2000; Peters and Pope 2002; Schulz et al. 2005; Smith et al. 2003; Zelikoff et al. 2003). Ambient PM is a complex mixture of chemical constituents originating from a variety of primary sources as well as by atmospheric transformations of gas precursors. Major components that contribute to the multi-pollutant atmosphere include inorganic compounds, (i.e., sulfate, nitrate and ammonium ions), trace metals and elements, and elemental and organic carbon (EC, OC). The latter comprised of non-volatile as well as semi-volatile species that are in dynamic equilibrium with their vapor phase in the atmosphere (Ning and Sioutas 2010). The photo-oxidation of gas precursors in the atmosphere, such as volatile organic compounds (VOCs), promotes the formation of secondary organic aerosols (Robinson et al. 2007). Recent studies indicate that semi-volatile organic compounds (SVOC), initially bound to the particulate phase, partition to the vapor phase as a result of atmospheric dilution following their release in the atmosphere; subsequent photo-oxidation of these low volatility vapors may contribute to substantial formation of secondary organic aerosols (SOAs) (Robinson et al. 2007). These findings emphasize the complex and dynamic behavior of ambient PM, especially those produced from combustion processes in the atmosphere.

Recent studies have linked individual particle chemical components with different adverse health effects (Gerlofs-Nijland et al. 2009). Of particular note is the role of SVOC and VOCs due to their toxic potency, including the capability to induce cellular oxidative stress (Baltensperger et al. 2008; Delfino et al. 2009; Ntziachristos et al. 2007a) and consequently adverse health effects (Arif and Shah 2007; Boeglin et al. 2006; Rumchev et al. 2004). For example, polar organic compounds such as quinones are reported to act as catalysts to directly produce reactive oxygen species (ROS), resulting in oxidative stress (Kumagai et al. 1997; Squadrito et al. 2001); polycyclic aromatic hydrocarbons (PAHs) can induce oxidative stress indirectly, through their biotransformation to generate redox active quinones (Penning et al. 1999). VOCs concentration levels in the ambient air have been linked to the incidence of chronic respiratory symptoms (Ware et al. 1993) and the frequency of hospital admissions due to ischemic heart disease and myocardial infarctions (Gordon et al. 1998; Klemm et al. 2004; Tolbert et al. 2001). In a recent exposure study of freeway traffic emissions on the cardiovascular effects of rats, vapor-phase components, rather than PM, were associated with a decrease in heart rate variability (Elder et al. 2007).

Although the association of adverse health effects with semi-volatile and/or volatile organic compounds has been reasonably well documented, the importance of the specific phase of the SVOC on toxicity remains to be investigated. For example, it is unclear whether the same SVOC species would elicit similar health effects if inhaled as a pure vapor as opposed to bound to ambient PM. A recent study by (Eiguren-Fernandez et al. 2010) assessed the redox and electrophilic potential of particle- and vapor-phase components of ambient aerosols using different chemical assays, and found differential distribution of redox activity and electrophiles between the two phases, underscoring the significance of vapor phase components in exposure and the need for health and risk assessment studies that include both

particles and vapors when assessing the overall toxic potency of ambient aerosols. In recent studies by our group, we evaluated the redox properties of the semi-volatile component of PM in dynamometer, roadway tunnel and ambient settings (Biswas et al. 2009; Verma et al. 2011). (Verma et al. 2011) demonstrated that over 60-90% of the overall redox activity of the sampled PM was indeed associated with these semi-volatile components, thereby underscoring their intrinsic toxicity and overall importance in understanding the health effects of air pollution.

In previous investigations, the Versatile Aerosol Concentration Enrichment System (VACES), designed and engineered by University of Southern California (Kim et al. 2001), has been used in tandem with commercially available thermodenuder (Dekati Ltd., Finland) to remove semi-volatile PM species from the particle phase and provide non-volatile PM for chemical and toxicological studies (Verma et al. 2011). In the present study, the thermodenuder was modified by replacing the adsorption section with a newly designed filter holder, and tested in tandem with the VACES in order to separate semi-volatile species from the particle phase, and provide them in vapor phase for inhalation exposure studies. Laboratory tests were carried out with selected aerosols of diverse volatility to characterize the optimal operating temperatures and flow settings of the system. Time-integrated field tests in an urban environment were also conducted to evaluate its performance with atmospheric aerosols in ambient conditions.

### 3.3 Experimental Methodology

#### 3.3.1 Design of the VACES-heater-filter (VHF) system

The VACES-heater-filter (VHF) system is comprised of two modules: the Versatile Aerosol Concentration Enrichment System (VACES) and a heater equipped with a quartz filter,



modified from a commercially available thermodenuder. The two major components of the system are described below.

#### 3.3.1.1 Versatile Aerosol Concentration Enrichment System (VACES)

The VACES is a particle concentrator technology whose laboratory and field characterization are described in detail by (Khlystov et al. 2005; Kim et al. 2001). Briefly, the sampled aerosol is drawn inside a saturator and mixed with ultrapure deionized water vapor to achieve saturation, and then it passes through a cooling section that induces condensational growth of the particles to super-micrometer size via supersaturation. The grown particles are then concentrated by virtual impaction. The VACES employs three virtual impactors in parallel, concentrating particles from a total flow of 300 liters per minute ( $\text{L}\cdot\text{min}^{-1}$ ) to a flow of  $15 \text{ L}\cdot\text{min}^{-1}$  ( $5 \text{ L}\cdot\text{min}^{-1}$  through each of the virtual impactors); hence achieving the overall theoretical concentration enrichment factor of 20 times.

#### 3.3.1.2 Heating and Filtration Unit

In order to separate the non-volatile particles from the semi-volatile vapors, a commercially available thermodenuder (TD; Model ELA-230, Dekati Ltd., Finland) was modified as follows. The Dekati thermodenuder consists of a heater module, followed by a cooling/adsorption unit. In the original design, the volatile/semi-volatile fraction of the ambient aerosol stream is evaporated in the heating section, and then adsorbed on the activated carbon in the cooling/adsorption section, leaving the non-volatile fraction of PM to pass through the system. For the purposes of this study, the cooling/adsorption section was removed, and a newly designed filter holder was inserted and sealed within the heater. During heating, semi-volatile aerosols partition to the vapor phase. The non-volatile particles are collected onto a pre-baked ( $550^\circ\text{C}$ ) quartz filter (Quartz microfiber filters, Whatman

International Ltd., UK), placed inside a filter holder, while semi-volatile vapors pass through the filter with the air stream. The quartz filter is placed inside the heater to minimize the condensation of gaseous semi-volatile species on the filter. Subsequently, the particle-free semi-volatile vapor stream is drawn through a cooling section, in which the stream temperature is reduced to ambient temperatures ( $\sim 25^{\circ}\text{C}$ ).

### 3.3.2 Experiment set up

The VHF tandem system was tested in the laboratory using different types of aerosols and in the field experiments with ambient aerosols. The VACES configured in tandem with the commercially available Dekati thermodenuder has been already used by our group to separate non-volatile PM components from the total concentrated aerosol stream (Biswas et al. 2009; Verma et al. 2011). In the present study, the VACES was configured in tandem with the heating and filtration unit modified from the Dekati thermodenuder as described above. Continuous particle measurement instruments were deployed to measure particle size distributions and number concentrations before and after the modified VACES. Subsequently, the sampling system was deployed in the field to be tested with ambient urban PM, in conjunction with time-integrated and continuous monitors.

#### 3.3.2.1 Test particles and instrumentation

The goal of the VHF tandem system is to partition PM-bound semi-volatile species to the gas phase by heating concentrated ambient aerosols, and separate the non-volatile particles from the semi-volatile vapors while suppressing particle formation by nucleation of these vapors as they are cooled to ambient temperatures. The vapor phase of semi-volatile species can subsequently be used in in-vivo inhalation exposures. The most critical feature in the selection of operating parameters of this system is the choice of a temperature that

maximizes the partitioning of semi-volatile species to the gas phase, while avoiding nucleation of the particle-free semi-volatile vapors in the cooling section. Intuitively speaking, the higher temperature values will maximize the partitioning of SVOC to the vapor phase; however, higher temperatures will also cause volatilization of very low volatile PM compounds, which will readily nucleate during cooling.

Laboratory experiments were carried out at various temperature settings using three types of polydisperse aerosols: ammonium sulfate, adipic acid, and glutaric acid. The Dekati thermodenuder can operate in temperatures as high as 300°C. Laboratory experiments were conducted in the temperature range of 100°C to 250°C. Aerosols were generated by atomizing dilute aqueous analyte suspensions of these species in ultra pure deionized water, using a commercially available nebulizer (VORTRAN Medical Technology, Inc., Sacramento, CA) in a process described in detail by (Misra et al. 2001). Following atomization, the aerosol was diluted with a dry, particle-free air stream. Ammonium sulfate was selected because it represents one of the most predominant inorganic salts in ambient PM<sub>2.5</sub> (Malm et al. 2007; Sardar et al. 2005a) and it is among the most stable semi-volatile species in the atmosphere due to its relatively low volatility (Scott and Cattell 1979). Adipic acid and glutaric acid are dicarboxylic acids found in ambient organic aerosols, and were chosen to represent typical products of secondary aerosol formation by photo-oxidation of organic gaseous precursors (Cruz and Pandis 1999; Sempere and Kawamura 1994). Both of these organic aerosols are water soluble and more volatile than ammonium sulfate.

Figure 1 shows the schematic of the laboratory test set up. A Scanning Mobility Particle Sizer (SMPS Model 3096, TSI, Inc., Shoreview, MN, USA) with a Differential Mobility Analyzer (DMA, Model 3080L, TSI Inc., Shoreview, MN, USA) in combination with a TSI Condensation Particle Counter (CPC 3022, TSI, Inc., Shoreview, MN, USA) was used for

the measurement of particle size distributions upstream, downstream of the heater, and after the cooling section. A quartz filter was placed immediate downstream of the heater. The SMPS sample and sheath air flows were adjusted to measure the particle size distribution in the range of 5.9 to 224.7 nm in mobility diameter. For all the test aerosols, the volatility measurements were made at a flow rate of 10 L.min<sup>-1</sup> and the heater temperature was gradually increased in 10°C increments, covering the temperature range of 50°C – 250°C. The air stream temperature was reduced to ambient levels (~25°C) in the cooling section for all heater temperature settings.

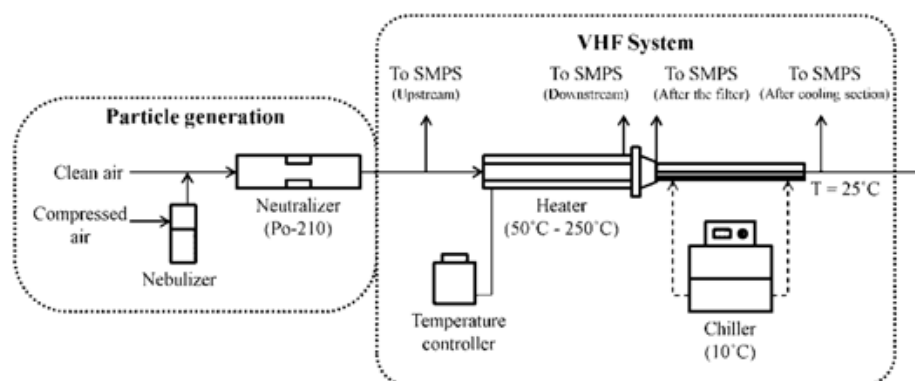


**Figure 3.1** – Schematic of laboratory test set up.

Particle losses in the system were evaluated first without heating the aerosols, by measuring the particle size distributions at the inlet and exit of the system. These tests showed minimal diffusion losses, with particle number loss of less than 5% for 20 nm particles at 10 L.min<sup>-1</sup>, and lower losses for larger particles (data not shown), consistent with theoretical predictions (Baron and Willeke 1992).

### 3.3.2.2 Field tests

Following the laboratory experiments, the VHF system was deployed in an urban area adjacent to main campus of the University of Southern California (USC), about 150 meters west and downwind of a major freeway (I-110), with high light and heavy duty traffic, and about 3 km south of downtown Los Angeles, CA. The proximity to I-110 freeway ensures the presence of high concentrations of freshly emitted semi-volatile organic species (e.g. polycyclic aromatic hydrocarbons, PAHs) (Eiguren-Fernandez et al. 2004). A detailed schematic of the experimental set up is presented in Figure 2. Time-integrated samples were collected upstream of the system, immediate after the filter-equipped heater and downstream of the cooling section. A sampling matrix comprising of a 47 mm quartz fiber filter (Pall Corp., NY) and 20 g of XAD-4 resin (Acros Organics, NJ) was used to collect particle- and vapor-phase PAHs, respectively. Previous studies have shown that this amount of XAD (Eiguren-Fernandez et al. 2003) yields a collection efficiency of ~99% for the target vapor phase PAHs. The XAD-4 resin was held in a glass cylinder between two 400-mesh stainless steel screens. The XAD-4 resin and the quartz filters were pre-cleaned prior to sampling, following procedures reported elsewhere (Eiguren-Fernandez et al. 2004). The matrices were kept at -20°C before and after sampling. The quartz filter after the heater was removed and stored in -20°C and a new filter was used at the beginning of each sampling day to minimize the possibility of volatilization of the collected semi-volatile species. Lab and field blanks were used during the study for quality control. All reported PAH concentrations are adjusted for laboratory and field blanks. A small flow of 0.3 LPM at the exit of the VHF and before the XAD sampler was drawn into a CPC (Model 3022A, TSI Inc., Shoreview, MN, USA) throughout the experiments to monitor on line particle concentration and confirm that no nucleation occurs during the field experiments.

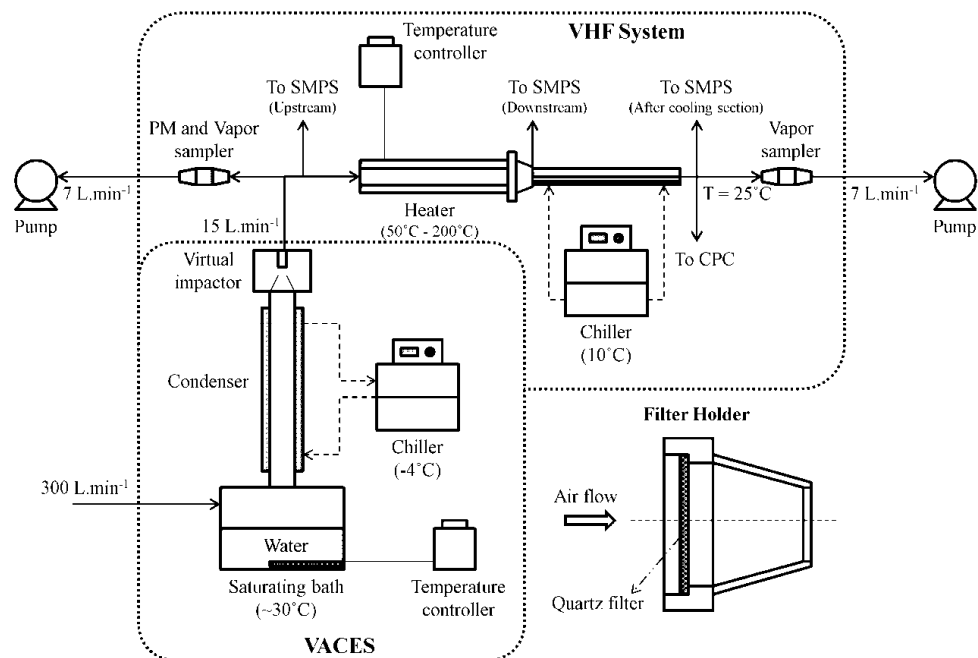


**Figure 3.2** – Schematic of field test set up and the filter holder.

### 3.3.2.3 Chemical analysis

The quartz filters and the XAD-4 resin were extracted by ultrasonication for two periods of 15 minutes each using 15 and 80 mL of a mixture of dichloromethane:acetonitrile (2:1 v/v) respectively. The extracts were filtered using a Millipore vacuum system (Millipore Corp., Bedford, MA) and 1 mL aliquots were taken from the vapor-phase extract for low molecular weight PAH analysis (naphthalene, acenaphthene and fluorene). The remaining extract of the vapor-phase sample and the particle-phase extract were volume reduced to ~100 uL for the quantification of rest of the PAHs. The entire extraction process was performed under yellow light condition using amber glass vials to avoid photodecomposition. Field blanks were extracted and analyzed for every ten samples. Details of extraction and PAH

quantification process using HPLC are described in (Eiguren-Fernandez et al. 2003). Results were only reported if the signal to noise ratios were higher than 3. SRM 1649a (NIST) was used to determine the analytical procedure precision (4.2%) and PAH extraction recovery efficiency (92-97%).

### 3.4 Results and Discussion

#### 3.4.1 Laboratory evaluation of the system

Figure 3 shows the particle size distributions of ammonium sulfate measured at upstream, downstream of heater without the filter, and after the cooling section at 150°C. Heating the aerosol to temperatures below 100°C had negligible effects on particle size distribution; however as the temperature increases to 100°C and beyond, ammonium sulfate particles start evaporating, with the mode diameter in the number distribution decreasing, as a result of particle shrinkage. As shown in Figure 3, heating the aerosols to 150°C causes substantial shrinkage, accompanied by a considerable increase in total number concentration (from  $4.7 \times 10^4$  particles per  $\text{cm}^3$  upstream of the heater to  $1.8 \times 10^6$  particles per  $\text{cm}^3$  to downstream of the heater and  $2.2 \times 10^7$  particles per  $\text{cm}^3$  after the cooling section, respectively), a clear indication of nucleation occurring after cooling. It should be noted that the volatility characteristics of any type of aerosols determined by thermodenuders or similar experimental approaches depend on the residence time of the particles in the heating section of the device. (Clarke 1991) and (Wu et al. 2009) reported lower temperatures for evaporation of ammonium sulfate particles, however both experiments were conducted at relatively lower flow rates, thus with longer residence times in their thermodenuders.

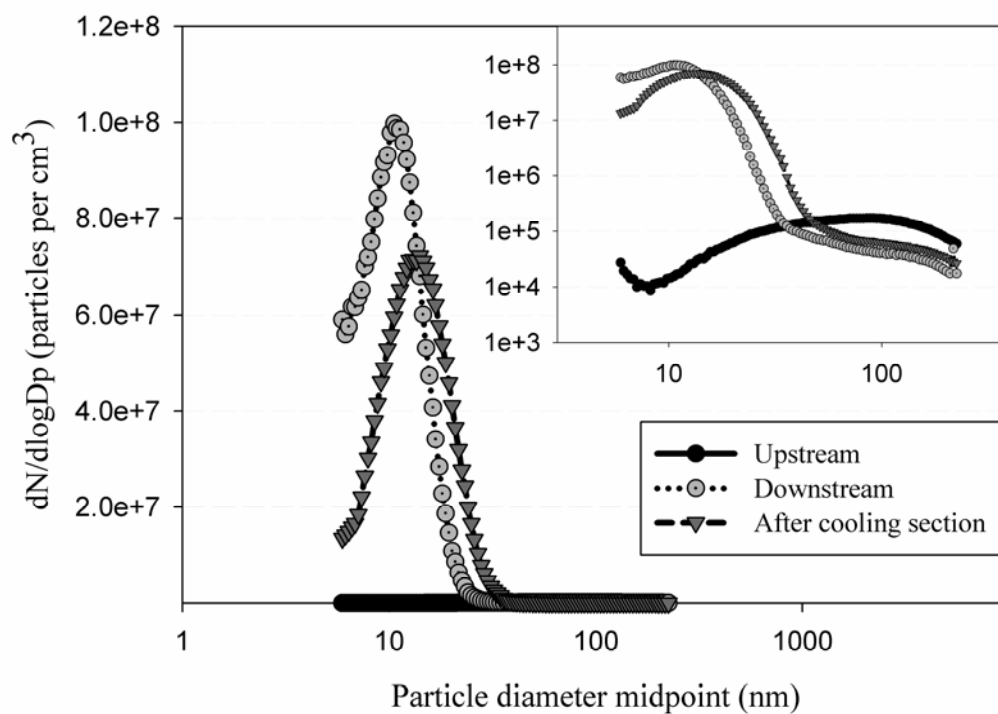
When the quartz filter was placed after the heating section, over 98% of particles by number were removed. In addition to these measurements, the particle size distribution and number concentration were also monitored downstream of the cooling section, since the accumulated

ammonium sulfate vapor after heating may pass through the filter and undergo nucleation during rapid cooling. To investigate the occurrence of nucleation, the heater temperature was increased stepwise, while the cooling section temperature was kept at 25°C in all experiments. No nucleation was observed with the heater temperatures set as high as 150°C; however nucleation became evident when the heater temperature reached 170°C ± 10°C in repeated experiments. Figures 4a and 4b show the size distribution of ammonium sulfate particles measured upstream and downstream of the heater, and after the cooling section at 150°C and 170°C, respectively. At 150°C, the particle number loss immediately after filter and after the cooling section was 96.3% and 97.0% respectively, indicating no nucleation (Figure 4a). However, at 170°C and above, nucleation is clearly evident after cooling, with the number concentration being significantly higher than the upstream concentration. The particle concentration immediately after the filter was 4.1e7 particles per cm<sup>3</sup> with a mode diameter of ~17nm at 170°C. The number concentration after the cooling section decreased to 3.2e7 particles per cm<sup>3</sup> with the mode diameter at ~21nm (Figure 4b), while the particle volume concentration increased from 2.09e11 nm<sup>3</sup>/cm<sup>3</sup> after the filter to 2.74e11 nm<sup>3</sup>/cm<sup>3</sup> downstream of the cooling section. Our observations are consistent with previous studies; (Burtcher et al. 2001) reported that ammonium sulfate starts evaporating at about 115°C, with a significant loss in particle volume at 160°C. (Clarke 1991) showed that ammonium sulfate starts evaporating slowly at about 150°C but remains unaffected at temperatures below 150°C. The slight differences in these observations may be due to different residence times in the heating sections of the particular experimental set ups, as we discussed earlier.

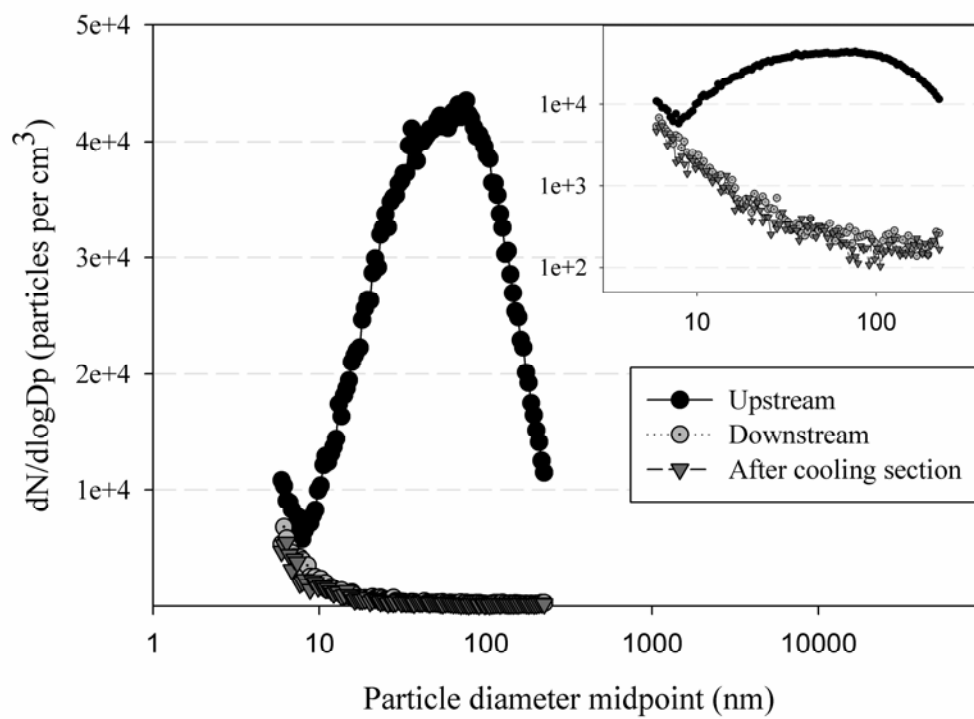
Similar tests were also carried out using adipic and glutaric acids, both of which are more volatile than ammonium sulfate, and higher heater temperatures would be required to induce their nucleation in the cooling section. With the step-wise increasing of heater temperature from 50 to 250°C, no sign of nucleation was observed in the VHF system for adipic acid.



Figure 5a shows the particle size distributions obtained for adipic acid at 100°C. The total number concentrations of aerosolized acids were set to approximately  $\sim 1\text{e}5$  particles per  $\text{cm}^3$  in the upstream, in the range of typical concentration-enriched ambient aerosols achieved by the VACES. Figure 5a presents the number size distribution of adipic acid aerosols measured at upstream, downstream of the heater, immediately after filter, and after the cooling section with the heater temperature set at 100°C. Substantial particle shrinkage by evaporation is evident after heating, with a particle number concentration reduction by 73.3%, from  $1.0\text{e}5$  particles per  $\text{cm}^3$  upstream to  $2.7\text{e}4$  particles per  $\text{cm}^3$  downstream of the heater, and before the filter. Particle evaporation is also accompanied by a change in the particle size distribution mode diameter from 60 nm upstream to 20 nm downstream of the heater. The particle number concentrations downstream of the filter and after the cooling section were negligible (632 and 36 particles per  $\text{cm}^3$ ) indicating more than 99% of particle were removed by the filter and the subsequent cooling did not induce any nucleation. Similar results were also observed for glutaric acid at a temperature range of 50-220°C. Figure 5b shows particle size distributions at the heater temperature of 200°C with significant reduction of the particle number concentrations after the heater as well as after the cooling section. During continued heating from 220 to 250°C, nucleation began after the cooling section. These data are not shown here, since these temperatures far exceed the range tested for the optimization experiments of the system.



**Figure 3.3** - Particle size distributions of ammonium sulfate at 150°C with no filter after the heater. Same figure presented in the inset in logarithmic scale.



**Figure 3.4a** - Particle size distributions of ammonium sulfate at 150°C. Same figure presented in the inset in logarithmic scale.

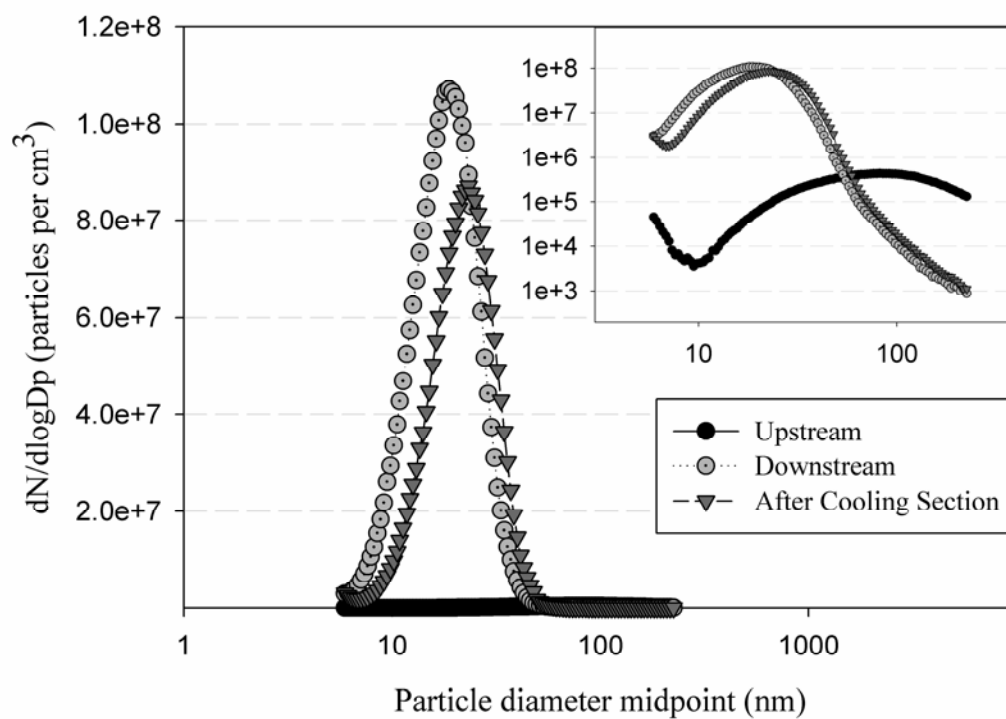


**Figure 3.4b** - Particle size distributions of ammonium sulfate at 170°C. Same figure presented in the inset in logarithmic scale.

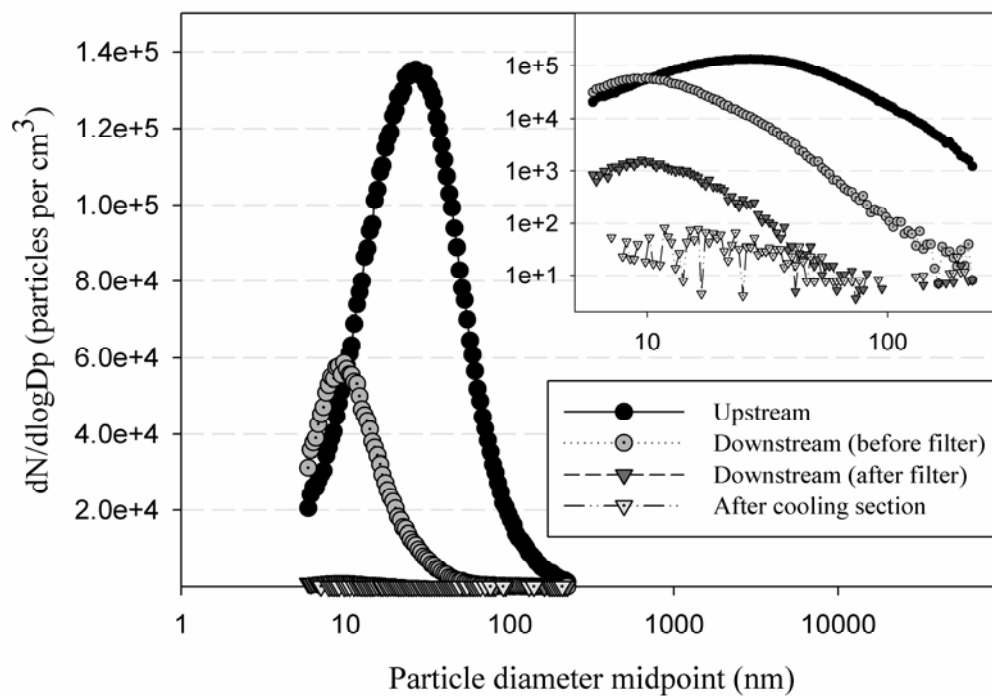


**Figure 3.5a** - Particle size distributions of adipic acid at 100°C. Same figure presented in the inset in logarithmic scale.

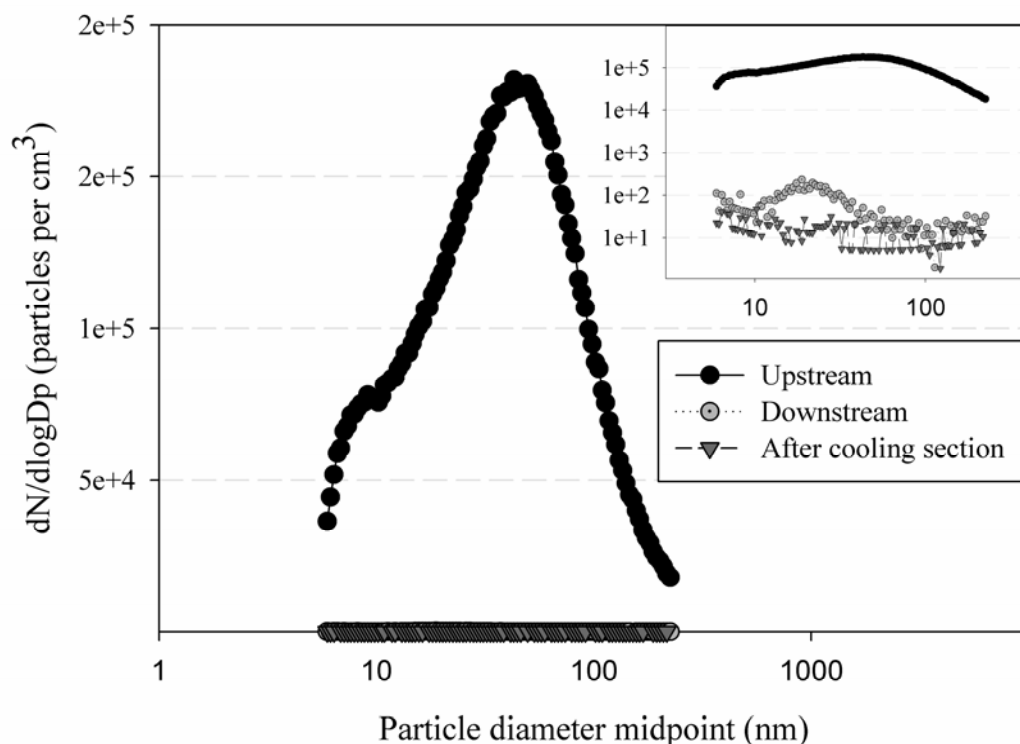


**Figure 3.5b** - Particle size distributions of glutaric acid at 200°C. Same figure presented in the inset in logarithmic scale.

### 3.4.2 Field test of the system for optimization of operational temperature

The particle size distribution and number concentrations of the urban aerosols at different sampling points of the VHF were measured by the SMPS during the field test of the system, as shown in Figure 2. The heater temperature was gradually increased from 50°C to 200°C similar to the approach for laboratory tests, and no nucleation was observed at heater temperatures up to 150°C. Figure 6 shows the number size distributions before and immediately after the heater, and also after the cooling section of the system at 150°C. The particle loss after the heater and after the cooling section was 99.8% and 99.9% respectively. As the heater temperature continued to increase, a slight increase of particle number

concentration was detected by the SMPS, while increasing the heater temperature to beyond 170°C induced a noticeable increase in particle number concentrations. Figure 7 shows the size distribution at 170°C at different measurement points of the system. While there are no signs of nucleation immediately after the quartz filter, nucleation is evident after the cooling section, producing particles smaller than 10 nm. The total number concentration after the VACES was  $1.72 \times 10^5$  particles per  $\text{cm}^3$ , while the number concentration dropped to  $1.75 \times 10^2$  particles per  $\text{cm}^3$  immediately after the filter and  $1.28 \times 10^4$  particles per  $\text{cm}^3$  after the cooling section, resulting in 99.9% and 92.6% particle loss, respectively. Similar results were observed in subsequent tests, with nucleation occurring in the temperature range of 160°C - 200°C. Based on the laboratory and field tests, 120°C was chosen as the optimal heater temperature, maximizing the partitioning of semi-volatile species to the vapor phase while preventing nucleation of less volatile and more stable atmospheric species (e.g. ammonium sulfate), in the cooling section of the system. This was the temperature at which the time integrated field tests were conducted, described in the following section.

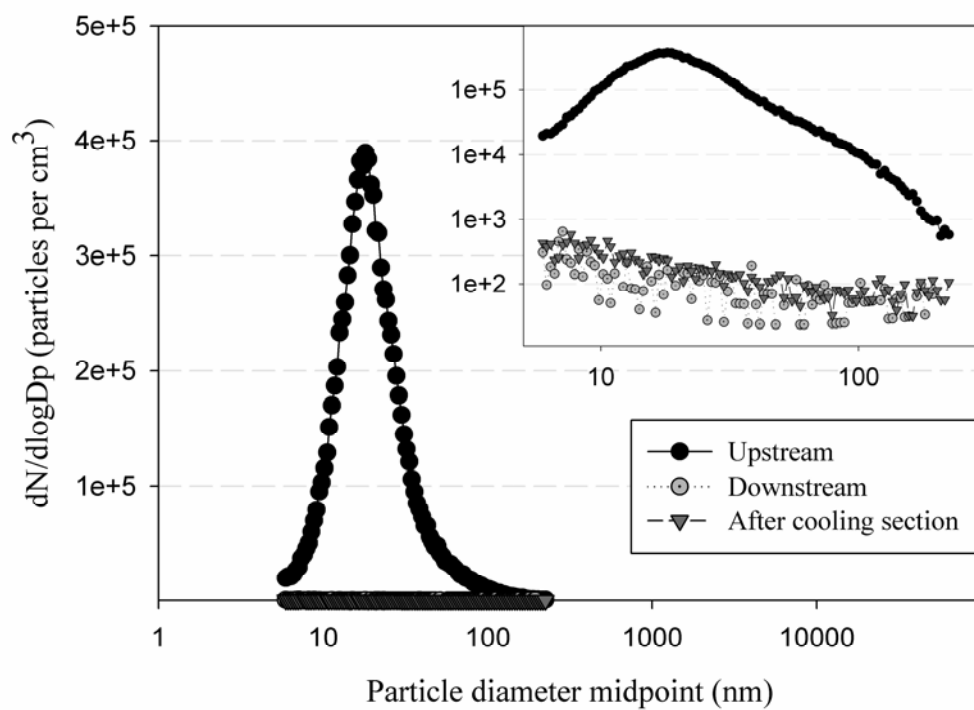


**Figure 3.6** - Particle size distributions of concentrated ambient particulate matter at 150°C. Same figure presented in the inset in logarithmic scale.



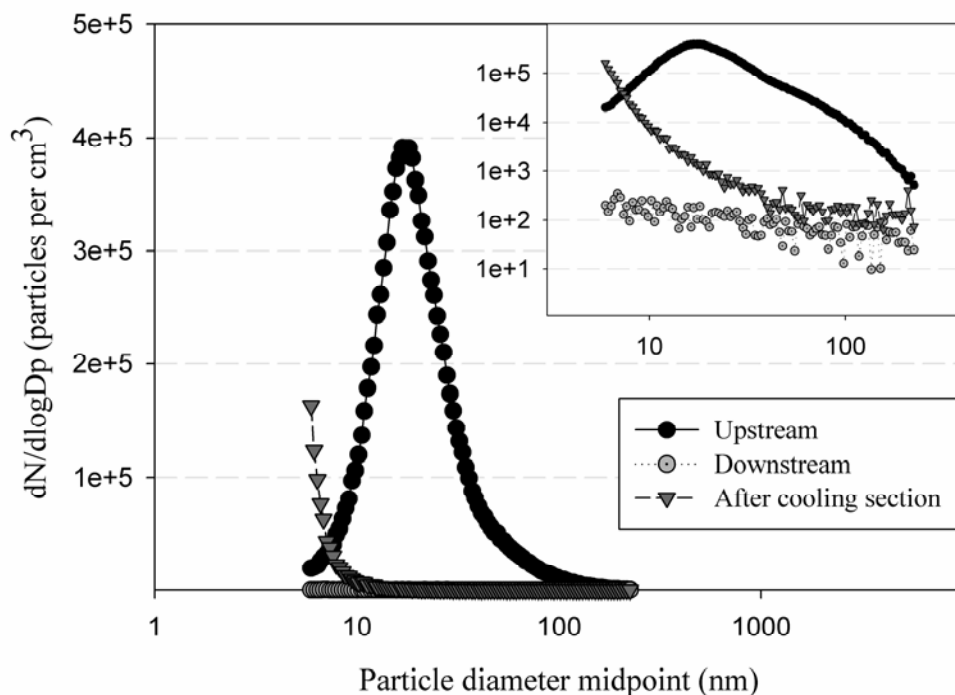


**Figure 3.7** - Particle size distributions of concentrated ambient particulate matter at 170°C. Same figure presented in the inset in logarithmic scale.

### 3.4.3 Time Integrated Measurements of particle and vapor phases Polycyclic Aromatic Hydrocarbons (PAHs)

In order to evaluate the effectiveness of the VHF system to partition semi-volatile PM-bound species from the particulate to the vapor phase without nucleation, time-integrated measurements of both particle and vapor phase PAHs at different parts of system were conducted. The sampling points upstream of the VHF, immediately after the heater, and downstream of the cooling section, using XAD samplers and/or filters, are shown in Figure 2. The collected samples were analyzed for 11 priority pollutant polycyclic aromatic hydrocarbons (PAHs – Table 1), as discussed earlier. During the time-integrated sampling period, particle number concentration after the cooling section was monitored continuously;

the measured concentrations were generally below 10 particles per cm<sup>3</sup> throughout the course of sampling, indicating that no nucleation occurred.

**Table 3.1** - PAH codes, molecular weights, subcooled liquied vapor pressure at 293K and HPLC-FL instrument detection limits

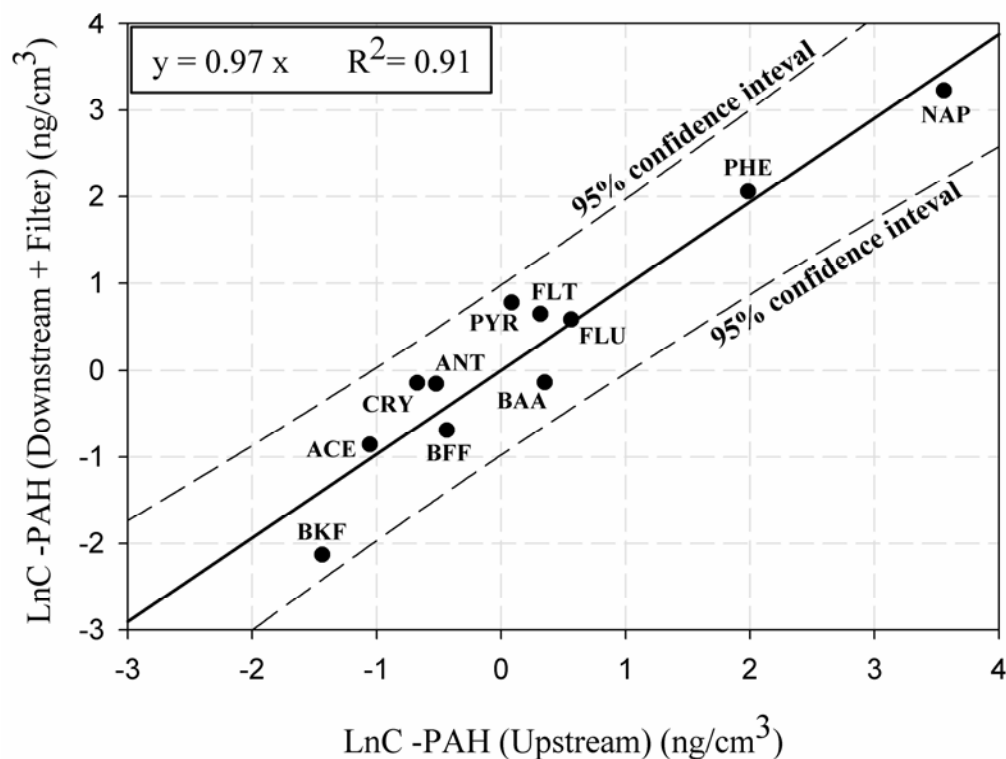
PAH	Code	MW	(log $p^*L$ ) <sup>a</sup>	IDL <sup>b</sup> (pg)
Naphthalene	NAP	128	1.59	0.52
Acenaphthene	ACE	154	0.18	0.16
Fluorene	FLU	166	-0.15	1.18
Phenanthrene	PHE	178	-0.95	0.72
Anthracene	ANT	178	-1.11	0.31
Fluoranthene	FLT	202	-2.06	1.29
Pyrene	PYR	202	-1.92	0.47
Benz[ <i>a</i> ]anthracene	BAA	228	-3.22	1.04
Chrysene	CRY	228	-3.97	0.37
Benzo[ <i>b</i> ]fluoranthene	BBF	252	-4.99	1.09
Benzo[ <i>k</i> ]fluoranthene	BKF	252	-5.39	0.32

<sup>a</sup> Data from (Peters et al., 2000).

<sup>b</sup> Instrument Detection Limits, from (Eiguren-Fernandez et al., 2003)

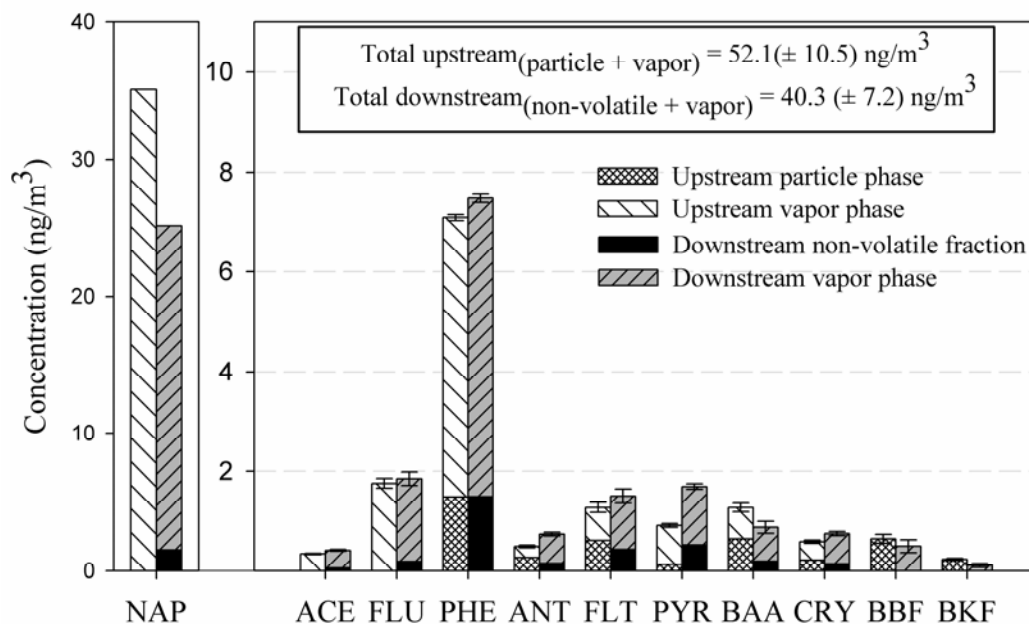
Samples collected upstream of the VHF include both particle and vapor phase of the PAHs, captured on the filter and XAD sampler, respectively. Upon heating at 120°C, the particle phase semi-volatile PAHs evaporate and partition to their vapor phase. The samples collected on the quartz filter immediately after the heater represent ideally non-volatile, particle phase PAHs, while those collected after the cooling section by the XAD sampler represent the sum of PAHs originally in the vapor phase plus the semi-volatile PAHs that evaporated from the particle phase during heating. The mass balance of PAHs was determined by comparing their total (i.e, PM plus vapor) concentrations measured upstream of the heater to the sum of the particle phase PAHs measured by the quartz filter placed immediately after the heater plus the vapor PAH concentrations measured by the XAD downstream of the cooling section.

Figure 8 shows the linear regression plot between the total PAHs concentrations upstream and downstream of the VHF, including the 95% confidence intervals based on the standard deviations of our measurements. Natural logarithms were used to cover the wide range of measured concentrations, spanning roughly over 3 orders of magnitude (a linear regression plot would have been almost entirely driven by naphthalene concentrations, accounting for about 70% of the total measured PAH). The regression results demonstrated very good agreement in the PAH mass balance between the upstream and downstream total concentrations, with a slope of  $0.97 (\pm 0.22)$  and a regression coefficient ( $R^2$ ) value of 0.91, indicating limited overall diffusional loss of vapor phase PAHs to the walls of the cooling section, and efficient semi-volatile PAH recovery in the system, after heating and cooling sections.



**Figure 3.8** – Correlation between natural logarithm of the measured PAH concentrations upstream and natural logarithm of sum of the measured PAH concentrations downstream of the system and on the heater filter (non-volatile fraction).

The upstream and downstream PAH concentrations are also presented in Figure 9a, with upstream concentrations segregated to PM-bound and vapor phase, whereas downstream concentrations are split into the non-volatile fraction, collected on the quartz filter immediately after the heater, and vapor phase PAH collected by the XAD sampler. The latter corresponds ideally to the upstream vapor phase PAHs plus the semi-volatile fraction of PAHs that evaporated from their particle phase after heating. The total (particle and vapor phase) PAHs concentration entering the VHF was  $52.1 (\pm 10.5) \text{ ng/m}^3$ , whereas the total concentrations measured on the quartz filter and XAD sampler downstream the VHF were  $4.5 (\pm 0.6) \text{ ng/m}^3$  and  $40.3 (\pm 7.2) \text{ ng/m}^3$ , respectively.



**Figure 3.9a** – Comparison of PAH concentrations measured upstream of the system in particle and vapor phase, PAH concentrations on the heater filter (the non-volatile fraction), and the recovered vapor phase PAHs measured after the cooling section and downstream of the system. The total (particle and vapor phase) PAHs concentrations entering the VHF were 52.1 (± 10.5) ng/m<sup>3</sup>, whereas the total concentrations measured on the quartz filter and XAD sampler downstream the VHF were 4.5 (± 0.6) ng/m<sup>3</sup> and 40.3 (± 7.2) ng/m<sup>3</sup>, respectively.

The measured PM concentrations of the two- and three -ring PAHs (naphthalene, acenaphthene and fluorene) were below detection limit, as these low molecular weight PAHs are predominantly in vapor phase under atmospheric conditions, and were entirely adsorbed on XAD resins, with some small fraction (on average 6-7%) detected on the heater filter, likely due to adsorption. These low molecular weight PAHs accounted for about 73% (± 5%) of the total measured PAH, and were fully recovered downstream of the system, with some potential losses for NAP (Figure 9a) possibly due to diffusion of NAP molecules on the walls of the system. The medium molecular weight PAHs (phenanthrene - chrysene) are

present in both gas and particle phases in atmospheric conditions, with an average mass ratio of 29% in the particle phase, as measured upstream of VHF system. Following gas-particle repartitioning in the heater at 120°C, the particle fraction decreased to 18% as measured downstream of heater, with the rest in vapor phase collected after cooling section. We defined the ratio of the downstream minus the upstream vapor phases PAH to the upstream particle phase concentration as the % recovery. Based on that definition, the total average recovery for medium molecular weight PAHs was 127.9% ( $\pm 31.8\%$ ). The higher molecular weight PAHs (i.e. benzo[b]fluoranthene and benzo[k]fluoranthene) are predominantly in particle phase and their gas phase concentrations upstream of the system were negligible. Similar to the medium molecular weight PAHs, their concentrations downstream of the system are entirely in the vapor phase, collected by the XAD sampler after they pass through the heating and cooling sections. The average recovery ratio of the high molecular weight PAHs was 138.9% ( $\pm 2.4\%$ ). The somewhat higher than 100% recovery for certain species may be due to some underestimation of the particulate phase PAH upstream of the VHF due to volatilization losses from the upstream filter during sampling, which would lead to an overestimation of the ambient vapor phase of these PAH measured by the XAD sampler. The sum of particle phase concentrations of medium and high molecular weight PAHs entering the system was  $4.6 \pm 0.4 \text{ ng/m}^3$ , whereas their downstream minus upstream vapor concentrations were  $4.5 \pm 0.3 \text{ ng/m}^3$  after heating and cooling, with an overall recovery ratio of 99%.

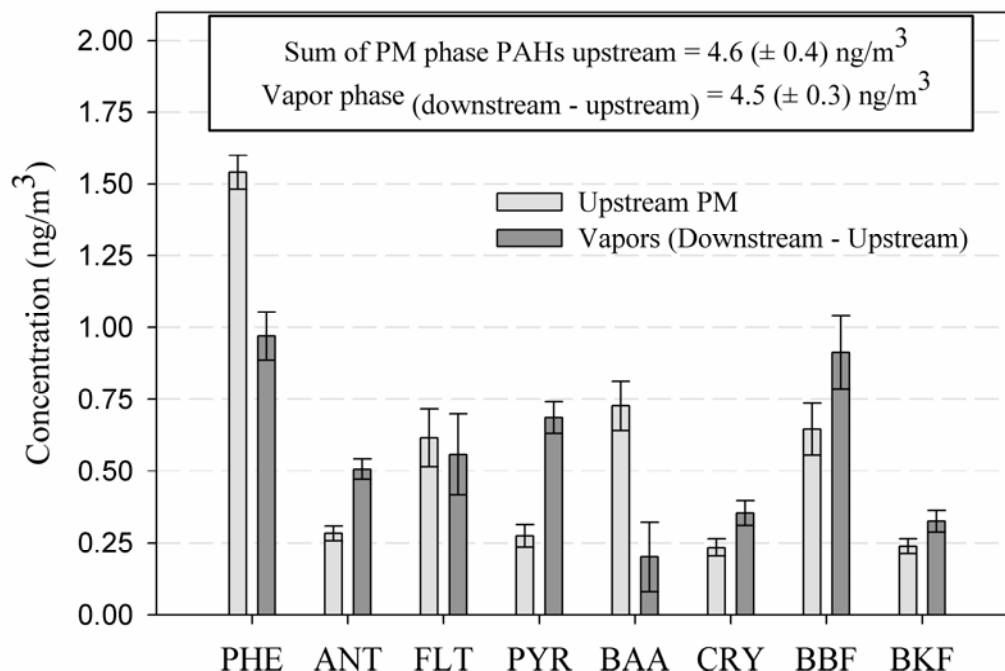


**Figure 3.9b** – Comparison of the upstream particle phase PAH concentrations ( $\pm$  standard error, SE) and the recovered vapor phase PAH concentrations ( $\pm$  SE), calculated by subtracting the upstream vapor phase concentration from the downstream vapor phase concentration of PAH species. The sum of particle phase concentrations of medium and high molecular weight PAHs entering the system was  $4.6 \pm 0.4 \text{ ng/m}^3$ , whereas their downstream minus upstream vapor concentrations were  $4.5 \pm 0.3 \text{ ng/m}^3$ .

It should be noted that in our field experiments discussed above, filter sampling was used to collect species in particulate phase, while XAD resin was used for vapor collection. These two methodologies represent the most commonly used approaches for organic PM and vapor sampling and chemical analysis. It was therefore assumed that the particulate and vapor phase PAH upstream of the VHF are properly captured by the filter and XAD samplers, respectively, and that the quartz filter in the heater captures only the non-volatile PM, without any gas phase adsorption, while the downstream XAD sampler collects only the vapor phase PAHs, including the volatile fraction that evaporates from their particle phase. However neither of these methodologies is artifact-free, and the interpretation of the results

and the degree of the agreement between upstream and downstream PAH concentrations will thus need to be viewed with caution and treated with the appropriate caveats introduced by the lack of an ideal method for the collection and analysis of semi-volatile species. For example, we already see evidence of gas phase PAH adsorption on the quartz heater filter for PAH entirely partitioned in the vapor phase (Figure 9a).

Nonetheless, the good overall agreement between the PAH concentrations measured upstream and downstream of the VHF and the reasonable overall PM recovery on the downstream XAD trap suggests that this system can be an attractive methodology for separating the particle and vapor phases of semi-volatile species and provide them for in-vivo exposure studies.

### 3.4 Summary and conclusions

We have developed and evaluated experimentally a sampling system designed to provide concentrated semi-volatile particles and vapors for in-vivo exposure studies. Ambient particles are initially concentrated using the VACES and then drawn through a heater to remove semi-volatile species from the PM phase. The quartz filter downstream of the heater removes non-volatile particles while allowing semi-volatile vapors, initially bound to the PM phase, to pass through. The air stream is then cooled down to ambient temperatures without the occurrence of nucleation. Laboratory tests using ammonium sulfate, adipic acid and glutaric acid identified an optimum volatilization temperature setting (120°C), which maximizes the removal of semi-volatile vapors from the particulate phase, while avoiding nucleation of these species after cooling. Field experiments, in which the PM and vapor phase concentrations of selected polycyclic aromatic hydrocarbons (PAHs) were measured before and after the VHF system, showed in general very good recovery of the measured semi-volatile species in vapor phase. These results indicate that the modified VACES-



heater-filter (VHF) system could provide separately concentrated PM (including their semi-volatile compounds), non-volatile PM (denuded of their semi-volatile species by replacing the filter with active carbon cartridge in the denuder, using the original Dekati thermodenuder set-up) and PM-bound semi-volatile species purely in their vapor phase for inhalation exposure studies. This technology makes it possible to conduct toxicity and inhalation exposure studies separately to the PM and vapor phases of semi-volatile organic pollutants in the urban atmosphere, and investigate the degree to which health effects attributable to these pollutants are affected by their phase. Given the dynamic behavior of these species in the atmosphere in terms of their partitioning between the PM and vapor phases, such investigations will become increasingly important.

### 3.5 Acknowledgments

This research has been supported by the Southern California Particle Center (SCPC), funded by EPA under STAR program through award number - 2145 G GB139, and by the California Air Resources Board (award number- 2009-2091). The research described herein has not been subjected to the agency's required peer and policy review and therefore does not necessarily reflect the views of the agency, and no official endorsement should be inferred. Mention of trade names or commercial products does not constitute an endorsement or recommendation for use. The authors would like to thank the USC Aerosol Lab members, Vishal Verma, Ka Lam Cheung, Winnie Kam and Nancy Daher for their help for some of the laboratory and field experiments.

## **Chapter 4 - Spatial and Temporal Variability of Coarse (PM<sub>10-2.5</sub>) Particulate Matter Concentrations in the Los Angeles Area**

### **4.1 Abstract**

Recent epidemiological and toxicological studies suggest that coarse particulate matter (CPM, particles smaller than 10 and larger than 2.5  $\mu\text{m}$  in diameter, PM<sub>10-2.5</sub>) concentrations may be associated with adverse health outcomes at levels similar to or larger than those associated with PM<sub>2.5</sub> concentrations. CPM may consist of several, mechanically-generated, potentially toxic components, including re-suspended road dust, industrial materials, brake linings, tire residues, trace metals, and bio-aerosols. In an effort to better understand and quantify the linkage between sources, composition and the toxicity of coarse PM, 10 sampling sites were set-up in the Los Angeles area. Sites within this diverse monitoring network were selected to encompass urban, rural, coastal, inland, near-freeway, community-based, upwind pollutant “source” and downwind pollutant “receptor” sites to fully characterize the range of conditions encountered in Southern California. At each location, a 24-hour time-integrated coarse PM sample was collected once per week for one year in order to assess the seasonal and spatial patterns in coarse PM concentrations. Annual geometric mean CPM mass concentrations varied from  $< 5.0 \mu\text{g}/\text{m}^3$  to approximately  $12 \mu\text{g}/\text{m}^3$  across the ten sites with individual weekly values ranging from ca. 1 to  $> 35 \mu\text{g}/\text{m}^3$ . Concentrations were 2 – 4 times higher in the summer than the winter, with the largest effect observed inland. CPM correlations between sites in close proximity to each other tended to be high ( $r^2 > 0.80$ ), but were poor between urban center and inland sites. The pollutant source sites in Long Beach as well as the desert site in Lancaster were distinctly different from the other sites in western, central and eastern Los Angeles. CPM correlations with PM<sub>2.5</sub> observations at the same site were poor overall, but good in the winter across the monitoring network.

The coefficients of divergence (COD) were also calculated across all site pairs to quantify CPM mass concentration spatial heterogeneity. The CODs (most median values > 0.2 calculated monthly) suggest modest heterogeneity overall, but the CODs calculated between the urban core site pairs were homogeneous. These observations suggest that differences in CPM sources and sinks within an urban region must be considered when calculating exposures.

Keywords: Particulate matter; Coarse particles; PM<sub>10</sub>; PM<sub>2.5</sub>; Resuspension

## 4.2 Introduction

National particulate matter (PM) standards have evolved over the years as PM<sub>10</sub> (particles smaller than 10 µm in diameter) replaced TSP (Total Suspended Particulate) in 1987 and PM<sub>2.5</sub> (particles smaller than 2.5 µm in diameter) was added in 1997. The standards changed as numerous epidemiological and toxicological studies linked elevated airborne PM mass concentration of size fractions ranging from ultrafine-to fine -to coarse, to a variety of adverse health outcomes including both respiratory and cardiac diseases (Becker et al. 2005; Hornberg et al. 1998; Kleinman et al. 2003; Li et al. 2003; Lipsett et al. 2006; Monn and Becker 1999; Oberdorster 2001; Pekkanen et al. 1997; Villeneuve et al. 2003; Xia et al. 2004; Yeatts et al. 2007). PM<sub>10</sub> consists of both fine (PM<sub>2.5</sub>) and coarse (PM<sub>10-2.5</sub> - smaller than 10 µm in diameter but larger than 2.5 µm, CPM) fractions of airborne particulate matter and therefore control of both PM<sub>2.5</sub> and CPM concentrations is required to meet PM<sub>10</sub> standards. These two PM size fractions can have substantially different sources and sinks. Therefore, the two fractions can be composed of varying chemical species contributing to potentially different health outcomes. Fine particles are known to primarily originate from combustion processes and from gas-to-particle conversion processes in the atmosphere. Coarse particles, on the other hand, arise predominantly from mechanical processes

including -- but not limited to -- brake lining abrasion, tire wear, windblown soil and dust, sea salt and bioaerosols such as pollen and fungal spores (Almeida et al. 2005; Chow et al. 1994; Edgerton et al. 2009; Harrison et al. 1997; Hinds 1999).

Abundant ambient  $PM_{2.5}$  mass concentration data are available world-wide through long-term regulatory monitoring networks and special studies (Motallebi et al. 2003b; Pinto et al. 2004). However, CPM mass concentration data are only available on a much more limited scale and hence significantly less is quantitatively known about spatial and seasonal characteristics of coarse particles.

Although data are limited, a review of PM studies showed that CPM mass concentration correlations among sites in some urban areas were lower than for accompanying  $PM_{2.5}$  (Wilson et al. 2005), although  $PM_{10}$  and  $PM_{2.5}$  concentrations themselves can be well-correlated in the Los Angeles area (Motallebi et al. 2003b; Turner and Allen 2008; Wilson et al. 2005). In rural areas the contribution of windblown dust to overall CPM mass concentrations dominated, while in urban areas the particles associated with motor vehicle operation are more important. Consequently, in urban areas traffic volume, traffic speed and distance from the road can strongly influence the overall CPM mass concentrations (Harrison et al. 2004; Lianou et al. 2007). Local meteorology is clearly also important.

In many epidemiological studies, central monitoring site data are used as a surrogate for population exposure to pollutants. Since CPM concentrations may vary widely in a given region (Wilson et al. 2005), this traditional method may not represent true population exposure (Brunekreef and Forsberg 2005; Monn 2001; Wilson et al. 2005) and could result in exposure misclassification. Therefore, it is important to study ambient CPM concentrations using a dense network of sites in multiple locations in order to understand the relationship between coarse PM mass concentrations, sources, sinks and their spatial and

temporal variability. Here the first results from a network of 10 CPM sampling sites in distinctly different regions of the Los Angeles area, encompassing rural-agricultural, urban and industrial sites are reported. We focus on the temporal and spatial variation of 24-hour time-integrated daily mean coarse particle mass concentrations obtained weekly for an entire year. A companion paper reports the spatial and temporal variability of near-continuous hourly CPM mass concentrations at a subset of these sites (Moore et al. 2009a). These studies – in conjunction with a later evaluation of the chemical composition and toxicological properties of the CPM (currently underway) will improve our understanding of the relationship between CPM concentrations and exposure. This will help the regulatory community develop improved strategies to protect the public from the adverse effects of CPM.

## 4.2. Methodology

### 4.2.1 Site Selection and Meteorology

The site selection criteria were designed to include and represent the diversity of CPM sources and sinks in greater Los Angeles. Consequently, the 10 sites (figure 1) selected include near-freeway, community (e.g. non-freeway), semi-rural, and desert sites (see Table 1). The sites may have more than one of these attributes and it is important to recognize that all sites are in reasonable proximity to roadways and thus have some potential to be impacted by motor vehicle traffic. It is useful to separate the sites geographically into Riverside County; Long Beach; eastern, central, and western Los Angeles and Lancaster.

Both Riverside county sites – GRA and VBR – are located about 80 km inland from downtown Los Angeles in the pollutant “receptor” area of the inland Los Angeles Basin (LAB). Both are located in residential areas of a semi-rural nature. However, GRA is

immediately to the North of CA-60 and may be strongly impacted by freeway traffic, while VBR is not as close to CA-60, although it is adjacent to significant surface roadways.

By contrast, the Long Beach site – HUD – is located in a mixed residential/commercial neighborhood approximately 2 km inland from the Ports of Los Angeles and Long Beach. The site is immediately to the east of the Terminal Island Freeway (SR-103) and 1.2 km west of the I-710. Both of these freeways have a high fraction and volume of heavy duty diesel vehicles in Port service. The Long Beach site is in a pollutant “source” region of the LAB.

Both of the eastern Los Angeles sites (HMS and FRE) are in close proximity to major freeways (see Table 1). The centrally-located University of Southern California (USC) site is a typical urban site in downtown Los Angeles, within 130 meters of I-110. Numerous studies have been conducted at this site (Moore et al. 2007; Ning et al. 2007; Sardar et al. 2005a). The CCL site is slightly west of the USC site and is located in South Central LA in a residential community adjacent to surface streets with significant motor vehicle traffic. The two western Los Angeles sites – GRD and LDS – can be classified as coastal sites, although LDS is immediately to the southwest of the I-405 freeway. The desert site – LAN – is in the Antelope Valley, north of the LAB. This site – in the city of Lancaster – is desert-dominated, although the area around the site is increasingly suburban. The LAN site is over 2 km from the nearest freeway, although it is near locally-significant surface arterial roadways.

Continuous meteorological data are not available at all sites. Briefly, meteorological conditions in the Los Angeles air basin are generally stable with light winds throughout the year, with some diurnal and season variations (ARB, 1992; NOAA, 1999). The diurnal temperature change is muted and the annual mean daily high is 25°C and the low is 15°C (NOAA, 1999). In the inland regions (e.g. Riverside) and in the mountains (e.g. LAN), the

temperature variability is higher than at the coast. The surface wind field throughout the year is characterized by calm or near calm winds predominantly from the N/NE overnight and into the early morning. During the morning, an onshore or sea breeze wind develops (predominantly from the SW in the coastal areas and W inland) and, while remaining relatively light, wind speeds peak in the afternoon. In the early evening, the wind speed starts to fall and the onshore breeze starts to shift to the overnight return flow. This pattern is relatively robust throughout the year, although the fall and winter are associated with more calm periods overnight, and weaker wind speeds during the day (Moore et al 2009a). During the fall and winter, this stable pattern can be disrupted by the occasional warm, dry off-shore wind events known locally as “Santa Ana” winds. Santa Ana conditions present typically strong winds from the N/NE throughout the air basin (ARB, 1992). The limited meteorological data available for this study are consistent with this description (data are presented in the companion paper, (Moore et al. 2009b)).

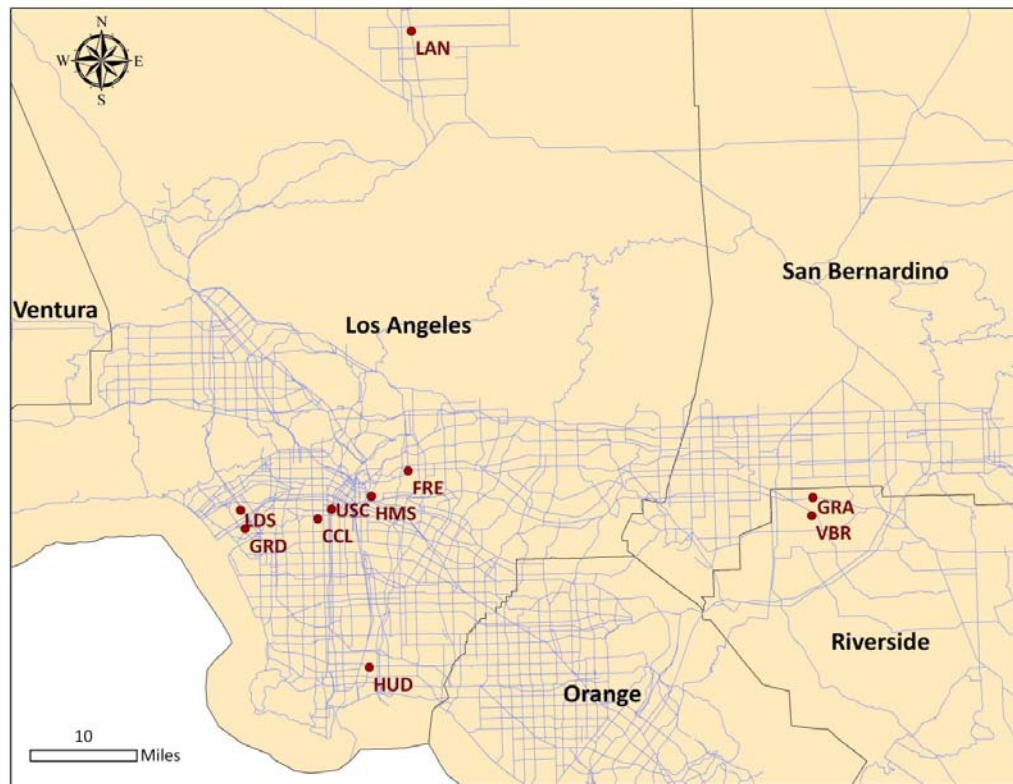


**Figure 4.1** - Map of 10 monitoring locations used in this study.



**Table 4.1.** Site information including sampling area, the designation code, description, geographic co-ordinates, site elevation, sampling period and data recovery

Area	Site designation	Site description	Additional notes	Latitude	Longitude	Inlet Elevation(m)*	Data recovery (%)
East Los Angeles	FRE	Urban, near-freeway	~ 50 m N of I-10	34° 04' 11" N	118° 09' 02" W	5	100%
	HMS	Urban, near-freeway	~ 800 m E of I-10, ~ 800 m N and E of I-5 curve	34° 02' 09" N	118° 12' 41" W	12	98%
Los Angeles	USC	Urban, near-freeway	Typical urban site in downtown LA, ~150 m W of I-110	34° 01' 09" N	118° 16' 38" W	4.8	88%
	CCL	Urban, community	~ 1.5 km E of I-110 and ~ 3.0 km S of I-10	34° 00' 23" N	118° 17' 59" W	6	98%
West Los Angeles	LDS	Urban, near-freeway	~ 100 m W of I-405, ~1.25 km S of I-10	34° 01' 12" N	118° 25' 33" W	6	94%
	GRD	Urban, community	~1.5 km W of I-405	33° 59' 40" N	118° 25' 07" W	6	90%
Long Beach	HUD	Urban, source, near-freeway	Located in the port of LA area, ~100 m E of Terminal Island Fwy, and 1.2 km W of I-710	33° 48' 09" N	118° 13' 12" W	4	98%
Riverside County	GRA	Semi-rural, receptor, near-freeway	semi-rural receptor site in the inland valley, ~100 N of CA-60	34° 01' 14" N	117° 29' 21" W	6	88%
	VBR	Semi-rural, receptor	semi-rural receptor site; ~ 3.0 km S of CA-60	33° 59' 45" N	117° 29' 31" W	4	92%
Lancaster	LAN	Desert	Typical desert site away from urban sources, 2.0 km of W of CA-14	34° 40' 09" N	118° 07' 51" W	5.5	88%

\*height relative to the ground.

#### 4.2.2 Sampling Period and Frequency

Sampling was conducted weekly at the 10 sites from April 2008-March 2009 to capture seasonal trends. Once per week, a 24-hour time-integrated CPM sample (described below) was collected at each site. Data recovery at each site was excellent (Table 1) and was over 88% overall. For logistical reasons, the regular weekly CPM samples were obtained from 12:00 AM PST to 12:00 PM PST on weekdays. All completed CPM samples were removed from the samplers within 24 hours and returned to USC for weighing.

#### 4.2.3 Sampling Equipment and Sample Screening

##### 4.2.3.1 Coarse Particulate Matter samplers

At each site dual Personal Cascade Impactor Samplers (Sioutas™ PCIS, SKC Inc., Eighty Four, PA, USA), were used to collect particles greater than 2.5  $\mu\text{m}$ , 2.5  $\mu\text{m}$ -0.25  $\mu\text{m}$  and less than 0.25  $\mu\text{m}$  at 9 liters per minute (LPM) downstream of an inlet designed to achieve the  $\text{PM}_{10}$  cutpoint (Misra et al. 2002; Singh et al. 2003). The  $\text{PM}_{10}$  inlet used for the two PCIS is described by (Misra et al. 2003). Teflon (25 and 37 mm, Zefluor™, 0.5  $\mu\text{m}$  pore size, Pall Corp, East Hills, NY) substrates were used and all PCIS-derived mass concentration data reported here are based upon the Teflon measurements.

At LAN, evidence suggested substantial particle bounce occurred between stages in the PCIS consistent with the very low RH observed at this site (discussed in the companion paper, (Moore et al. 2009b)) (Rao and Whitby 1977; Winkler 1973). Therefore at LAN, the CPM mass concentrations were reported using concurrent data collected by the USC Coarse Particle Concentrator (Kim et al. 2001; Misra et al. 2001). The Coarse Particle Concentrator is composed of a virtual impactor upstream of a stainless steel filter holder. In this application, the virtual impactor is operated at a total flow rate of ca. 50 LPM and a minor

flow rate of ca. 2 LPM. Operated downstream of an inlet designed to achieve the  $PM_{10}$  cutpoint (similar to the inlet used for PCIS), particles between ca. 2.4 – 10  $\mu m$  are relatively concentrated by a factor of approximately 25 and collected on the downstream Teflon filter (47 mm, Teflo™, 2.0  $\mu m$  pore size, Pall Corp, East Hills, NY). These units are described in greater detail by (Misra et al. 2001) and are now commercially available (Continuous Particulate TEOM Monitor, Series 1405, Thermo Fisher Scientific Inc. Waltham, MA).

The CPM mass concentrations measured by the USC Coarse Particle Concentrator and the PCIS coarse fraction were compared for validation at all the sites. With the exception of the LAN site, at which the USC Coarse Particle Concentrator measured on average about 50% higher CPM concentrations, the agreement between CPM mass concentration measurements made by both methods was typically within 20% or less (the average USC Coarse Particle Concentrator –to- PCIS CPM concentration was  $1.15 (\pm 0.11)$ , as shown in Figure S-4 of the Supplement). All mass concentration data reported here are from the PCIS with the exception of the LAN data.

All filter substrates were weighed before and after sampling to determine the collected CPM mass. The filters were equilibrated for 24 hours in a room with controlled relative humidity ( $30\% \pm 5\%$ ) and temperature ( $21^{\circ}C \pm 2^{\circ}C$ ) before weighing using a microbalance (Model MT 5, Mettler-Toledo Inc., Highstown, NJ). Consecutive mass measurements within 3  $\mu g$  were considered “stable”. In the field, sampler flow rates were checked before and after sample collection. Samples with flow rates that varied more than 5% from the nominal value were discarded.

### 4.3. Results and Discussion

#### 4.3.1 Temporal and Spatial variations

As described earlier, it is convenient to group the sampling sites into geographic groups – three clusters for West (LDS and GRD), Central (USC and CCL) and East Los Angeles (FRE and HMS), and Riverside County (GRA and VBR). The Lancaster (LAN) and Long Beach (HUD) sites are assessed separately. Table 2 shows a summary of CPM mass concentration data and statistics for the study, including geometric and arithmetic means and standard deviations at each site.

The annual geometric mean concentrations observed across all 10 sites are very similar with the exception of LAN which is about half (ca.  $5 \mu\text{g}/\text{m}^3$ ) of the rest of the values (ca.  $10 \mu\text{g}/\text{m}^3$ ). CPM concentrations at LAN were consistently lower than at the other sites and seasonal variation at this site is muted. In contrast, summer CPM mass concentrations were 2 – 4 times greater than the winter concentrations at most sites. CPM mass concentrations at the HUD site were the exception where concentrations in the summer were typically lower than in the winter. HUD is directly affected by port activities and high heavy duty truck traffic, neither of have a substantial seasonal variation (Moore et al 2009); however elevated concentrations in winter might be due to lower atmospheric mixing height. The two Riverside sites had the largest change from winter to summer CPM mass concentrations (Table 2). CPM concentrations at the USC were consistent with prior studies ( $14.6$  to  $24.0 \mu\text{g}/\text{m}^3$ ) (Sardar et al. 2005a).

**Table 4.2.** Summary of statistics for the coarse particles mass concentrations ( $\mu\text{g}/\text{m}^3$ ) at each sampling site.

Area	Site designation	Annual GM <sup>a</sup>	Annual average <sup>b</sup>	SD <sup>c</sup>	Winter average <sup>d</sup>	SD	Summer average <sup>e</sup>	SD	Max	Min
East Los Angeles	FRE	8.8	9.8	4.5	5.7	2.0	12.4	3.9	22.4	2.9
	HMS	9.8	10.9	4.6	6.7	3.1	12.9	4.3	23.3	3.1
Los Angeles	USC	11.2	12.4	5.0	9.2	5.8	14.0	4.3	22.7	3.2
	CCL	9.4	10.3	4.2	7.1	3.3	12.2	4.4	20.9	3.0
West Los Angeles	LDS	8.5	9.6	4.0	6.5	2.6	11.6	3.5	17.3	0.6
	GRD	9.2	10.1	4.0	6.3	2.6	11.4	3.0	18.1	2.9
Long Beach	HUD	12.1	13.4	6.0	13.8	8.6	11.2	4.0	29.7	3.7
Riverside County	GRA	10.0	13.2	7.9	5.4	2.9	20.9	5.6	35.7	1.0
	VBR	10.3	13.7	7.9	6.0	5.3	16.4	5.6	30.5	0.4
Lancaster	LAN	4.3	5.2	3.2	3.1	2.5	5.2	2.5	13.7	1.2

<sup>a</sup> Geometric mean. <sup>b</sup> Arithmetic mean. <sup>c</sup> Standard deviation.

<sup>d</sup> winter = December-February. <sup>e</sup> Summer = June-August

Figure 2 shows the seasonal variations of monthly average CPM concentrations by cluster/site. As described above, a characteristic seasonal variation can be observed at most sites with relatively elevated CPM concentrations observed in the warmer seasons peaking in August and September. This is consistent with the earlier California study that showed the CPM fraction dominates total  $\text{PM}_{10}$  concentrations during the summer in California (Motallebi et al. 2003a). Higher summertime CPM concentrations can be attributed to elevated wind speed that enhances wind induced re-suspended CPM concentrations. Wind speeds are higher in the summer, in general (see section 2.0 and the companion paper – (Moore et al. 2009b)). Harrison and colleagues also showed a similar seasonal pattern in Birmingham, UK with lower concentrations during winter which was attributed to increased precipitation and higher relative humidity (Harrison et al. 2001). A somewhat similar pattern – if reduced in magnitude – was observed at Lancaster, but a very different one is observed in Long Beach. In Long Beach, peak cargo traffic typically occurs in the fall of

each year (Moore et al 2009a). Higher port activity coupled with the lower mixing height in the fall (discussed above) may produce these higher Long Beach CPM concentrations.

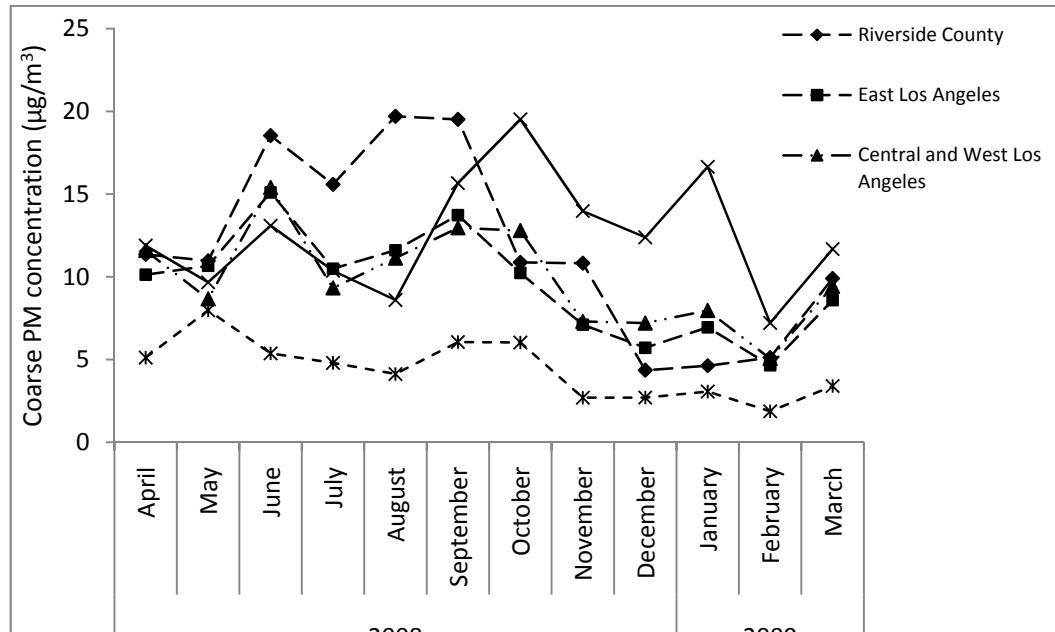


**Figure 4.2** – Average monthly coarse PM concentrations in three site clusters and Long Beach and Lancaster sites.

Temporal variations in  $PM_{2.5}$  concentrations are shown in figure 3 (Lancaster is not shown due to the lack of available data). The  $PM_{2.5}$  concentrations vary less seasonally compared to CPM mass concentrations. This has been observed previously in the Los Angeles area (Pinto et al. 2004; Wilson et al. 2005). The primary direct source for  $PM_{2.5}$  – motor-vehicle emissions – in the LAB is not directly affected by seasons. In contrast, secondary atmospheric formation of fine particles through photochemical processes is higher during the summer (relatively higher concentrations are observed from May – October). Stronger source strength in the summer however is counterbalanced by the lower mixing height in winter months thus dampening seasonal variability. The Long Beach site, as previously described, is located in a pollutant “source” region of Los Angeles and shows different seasonal trends for both  $PM_{2.5}$  and CPM mass concentrations. Similarly to the CPM

concentrations, high winter  $PM_{2.5}$  concentrations may be due to pollutant build-up due to decreased atmospheric ventilation. The ratio of  $PM_{2.5}$  to  $PM_{10}$  at these sites varied modestly throughout the year (approximately 0.6) with little discernible seasonal trend. CPM mass concentrations show more variability and are generally lower than  $PM_{2.5}$  mass concentrations across the monitoring network, which is consistent with the more heterogeneous sources and stronger atmospheric removal processes associated with CPM.

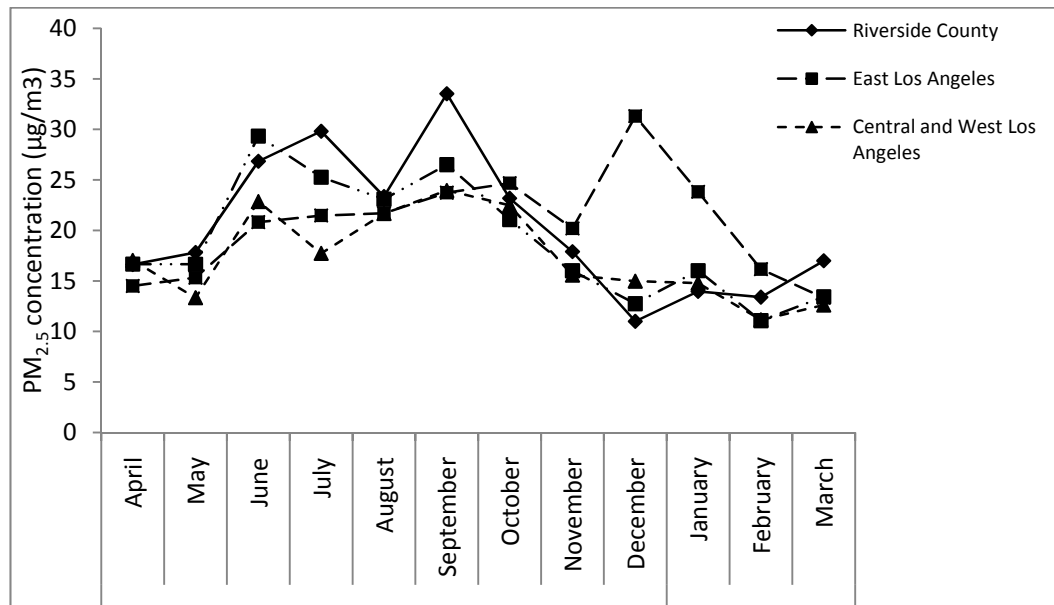


**Figure 4.3** - monthly  $PM_{2.5}$  concentrations in three site clusters and Long Beach sites.

CPM concentration correlations between different sites/clusters yield interesting observations about the temporal variability of mass concentrations between sites. Figure 4 shows the site-by-site correlation contour plot. Strong correlations are observed between the urban sites in Los Angeles, particularly among sites in western and central Los Angeles.

The two coastal sites – LDS and GRD – showed very good correlation ( $r^2 = 0.80$ , figure 4) throughout the year. Moving inland, both USC and CCL sites, located in central Los Angeles, show strong correlations with other urban sites located in Los Angeles, whereas their correlations with east Los Angeles sites become relatively lower (figure 4). Even over

the relatively small distances between the central and eastern Los Angeles sites – subject to very similar sources—differences in source strength and intensity can limit predictability. Correlations between the Los Angeles cluster of sites and sites in Riverside County were generally poor (figure 4).

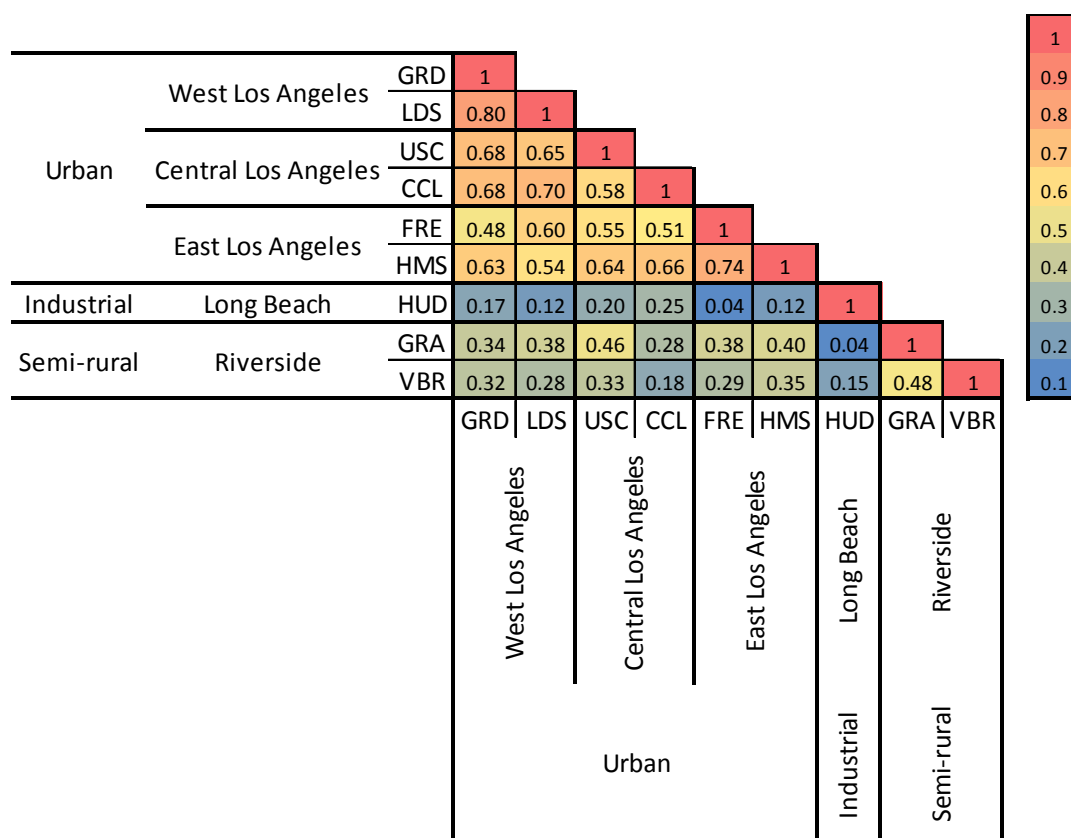


**Figure 4.4** - Site-by-site correlation contour plot of CPM mass concentrations.

Although the VBR and GRA sites are less than 3 km apart, the relatively weak correlation between the two Riverside County sites ( $r^2 = 0.46$ ) suggest different sources of coarse particles or source strengths at these locations. As discussed previously, GRA is located close to the CA-60 freeway and may be disproportionately affected by resuspended CPM from vehicular traffic. In contrast, VBR is located 3 kilometers south (i.e mostly upwind) of



the CA-60 and may also be affected by windblown dust (from agricultural fields, (Sardar et al. 2005a)).

CPM correlations in Long Beach are different than observed elsewhere. Very little correlation is seen between HUD and the other sites (Figure 4). This is a “source” region for pollutants in Los Angeles, as discussed previously, and it has been observed elsewhere that a higher particle resuspension rates are associated with HDDVs compared to light duty vehicles, (Charron and Harrison 2005). Heavy duty vehicles also have higher brake-wear emission rates than light duty vehicles due to stronger abrasion processes. Both of these factors together can result in higher emission rates of coarse particles (Garg et al. 2000). There may also be a different intensity and proximity to industrial CPM sources near the Long Beach site.

#### 4.3.2 Comparison of PM<sub>2.5</sub> and CPM concentrations and relationships

Selected comparisons between annual, winter and summer CPM and PM<sub>2.5</sub> concentrations are shown in figures 5 - 8 (similar figures for additional sites are included in the supplement). Across all of the sites shown, winter-time correlations (up to  $r^2 = 0.80$ ) are much higher than the summer correlations (most  $r^2$  values are less than 0.10). Only at FRE – and at LAN where no data are available – is the winter correlations relatively poor ( $r^2 = 0.36$ ). The moderate annual correlation is driven by the high correlation coefficients observed in the winter. In Riverside (figure 5), the poor summertime correlation suggests how the relative importance of homogeneous (e.g. atmospheric processing of PM<sub>2.5</sub>) and heterogeneous (e.g. wind-driven coarse PM) to atmospheric PM concentrations can vary throughout the year. The lack of correlation in the summer may be driven by the strong impact of atmospheric photochemistry on PM<sub>2.5</sub> emissions, while not affecting CPM concentrations. The relatively good correlation in the winter (e.g. in Riverside at GRA and

VBR,  $r^2 = 0.73$  and  $0.77$ , respectively) may be due to reduced photochemistry coupled with the lower boundary layer and more calm conditions, thus enhancing the contribution of traffic sources to both PM fractions.

A similar trend was observed in the urban sites located in Los Angeles County (figures 6 and 7). While  $PM_{2.5}$  and CPM mass concentrations show a strong correlation in winter, significantly weaker correlations are seen in summer months. The  $r^2$  correlation coefficients in summer range from 0.01 to 0.30 which indicate very low or no correlation between  $PM_{2.5}$  and  $PM_{10}$ , while in winter  $r^2$  values observed were higher than 0.66 (with exception of “FRE”,  $r^2 = 0.36$ ). The urban sites are in close proximity to relatively strong vehicular sources of primary  $PM_{2.5}$  and CPM. The lower summer correlations at the sites in closer proximity of major roads (“LDS”, “CCL” and “HMS”) and relatively higher winter time correlations at these sites emphasize the more dominant role of vehicle traffic on particle concentrations in this urban area. The differences in winter and summer correlations can be seen in the Long Beach site as well. We attribute these differences to the higher influence of wind-induced resuspension of CPM in summer compared to the resuspension of road dust by traffic in wintertime. Chemical composition data, currently under way, will provide more insight into the factors driving these differences.

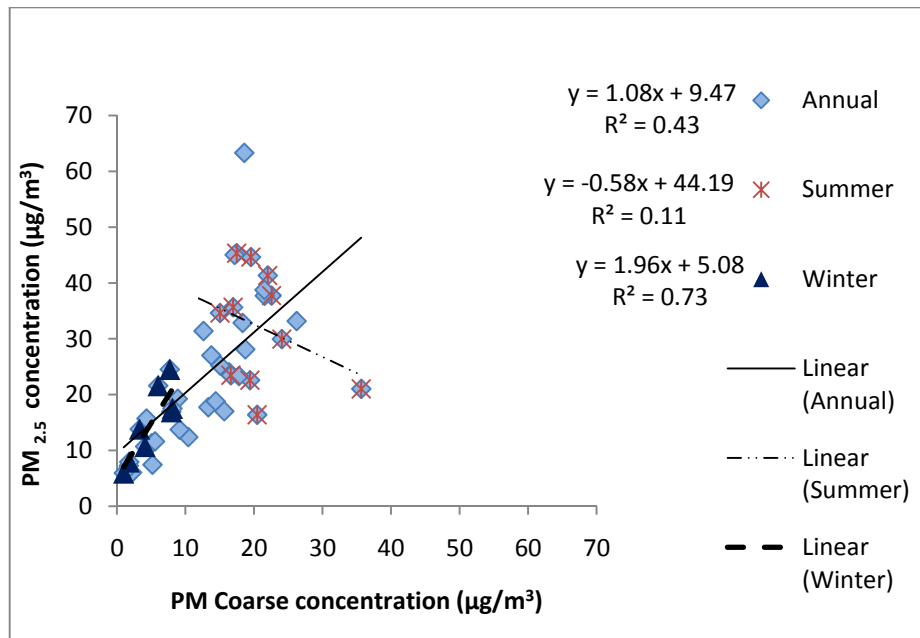


**Figure 4.5** – Annual and seasonal correlations between PM<sub>2.5</sub> and CPM in Riverside County cluster GRA. Data shown are from April 2008 – March 2009.

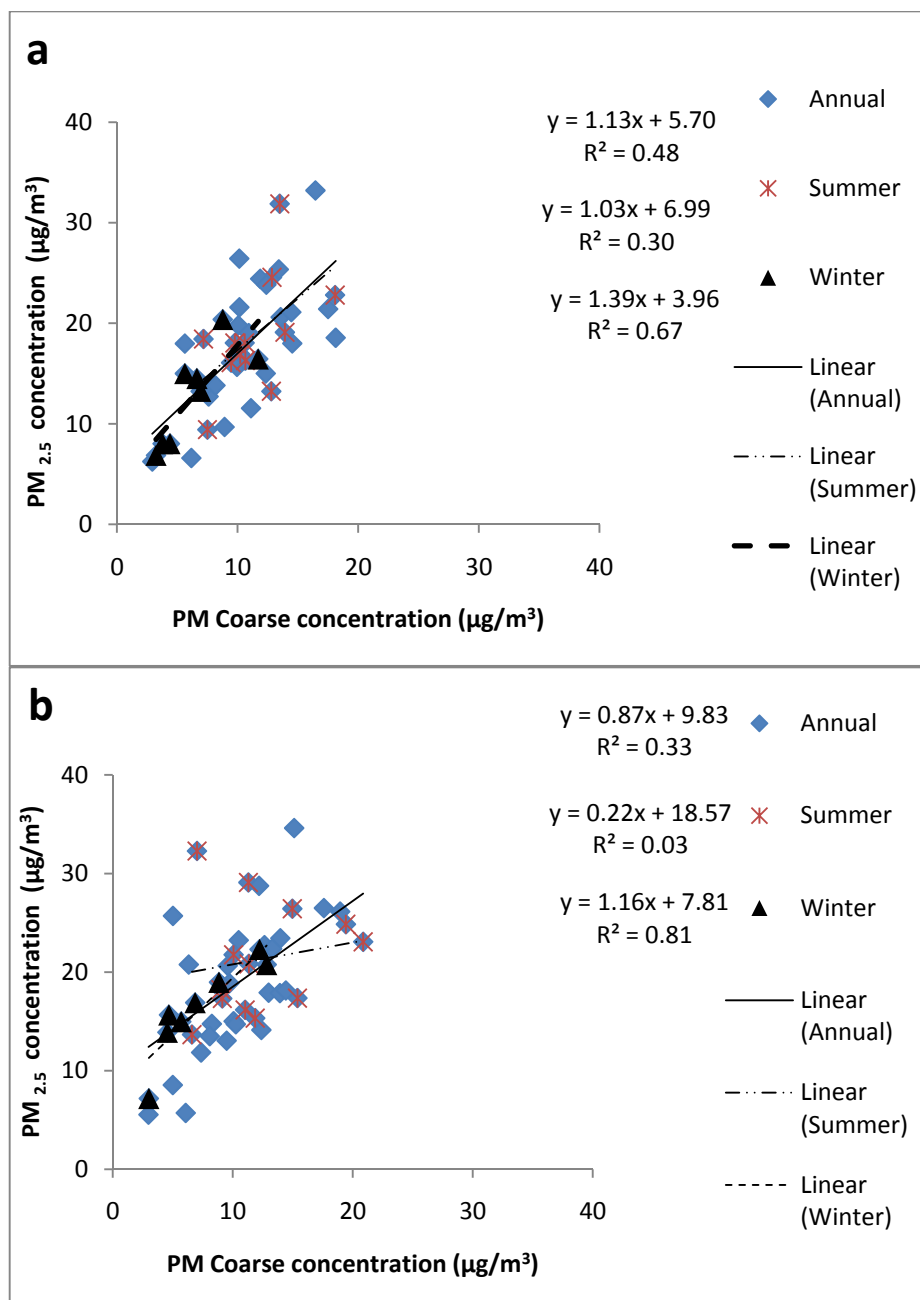


**Figure 4.6** - Annual and seasonal correlations between PM<sub>2.5</sub> and CPM in Los Angeles and West Los Angeles clusters (a) GRD, (b) CCL. Data from April 2008 – March 2009.

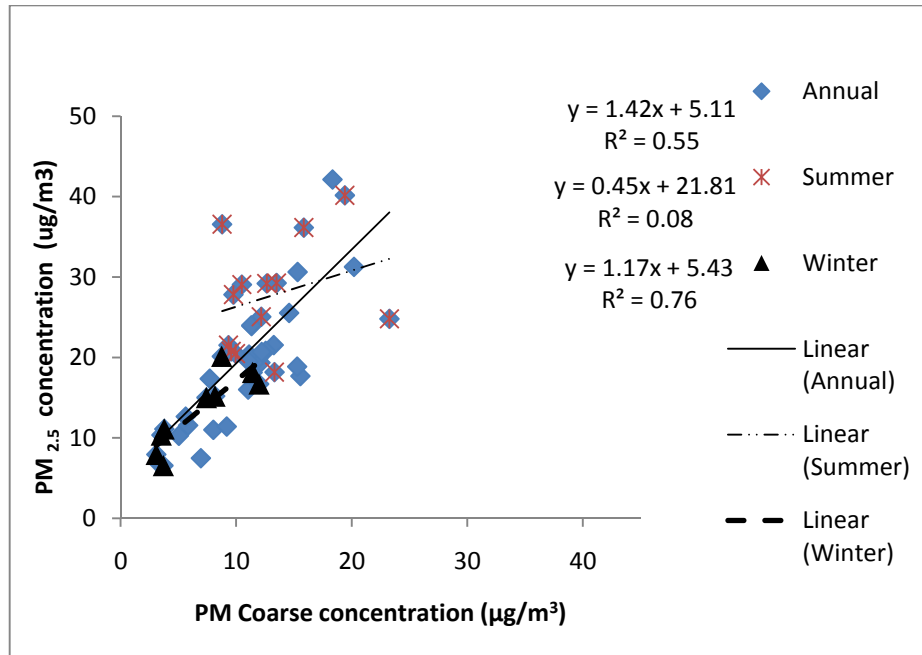


**Figure 4.7** - Annual and seasonal correlations between PM<sub>2.5</sub> and CPM in East Los Angeles cluster HMS. Data from April 2008 – March 2009.

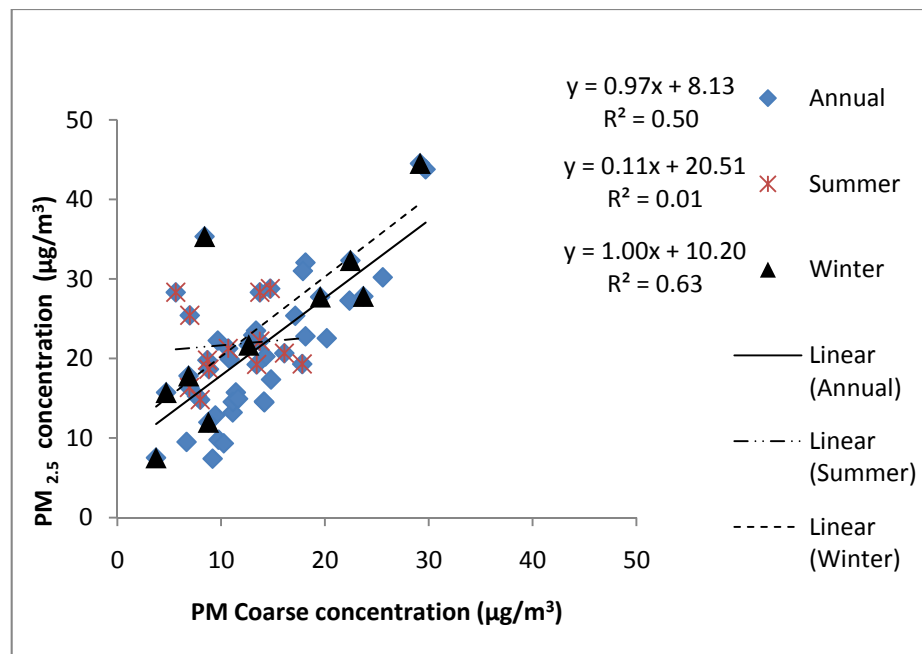


**Figure 4.8** - Annual and seasonal correlations between PM<sub>2.5</sub> and CPM in Long Beach site.

#### 4.3.3 Coefficients of Divergence (COD) calculations for CPM mass concentrations

In a review on intraurban variability of PM mass concentrations, Wilson and colleagues suggest using coefficient of divergence (COD) in conjunction with correlation coefficients and PM concentration data to better characterize intraurban variability (Wilson et al. 2005). High/low temporal correlation and high/low spatial homogeneity do not necessarily correspond (Turner and Allen 2008) so evaluating both parameters are warranted. The COD is defined as:

$$COD_{jk} = \sqrt{\frac{1}{n} \sum_{i=1}^n \left( \frac{x_{ij} - x_{ik}}{x_{ij} + x_{ik}} \right)^2}$$

where  $x_{ij}$  is the  $i$ -th concentration measured at site  $j$  for a given sampling period,  $j$  and  $k$  are two different sites, and  $n$  is the number of observations (Krudysz et al. 2009). COD values vary between 0 and 1, with 0 values indicating similar concentrations at both sites and 1 indicating different concentrations. The monthly CODs were calculated across all site pairs (with the exception of LAN) for all of the study weekly data (Figure 9). LAN was not included in the COD calculations as PCIS data were not available, although we would expect including LAN to increase the range of the COD values calculated as concentrations are relatively low there compared to the other sites, consistent with the results reported in an earlier study of PM<sub>2.5</sub> mass concentrations (Pinto et al 2004). The median COD values ranged from 0.15 to 0.33 suggesting a homogeneous-to modestly heterogeneous distribution of CPM for the chosen sites. The range between the 1<sup>st</sup> and 3<sup>rd</sup> quartiles was approximately 0.2. The median COD values during the summer and winter seasons were 0.21 and 0.30, respectively, although it is difficult to discern month-to-month trends in the data (figure 9). Focusing on the urban sites only (figure 10) the average median COD value is 0.13, ranging

from 0.10 to 0.18, which indicates little spatial variability. This suggests that exposures to CPM in the urban core sites may be well-estimated using a central monitoring site at least for 24 hr -based concentrations. With the exception of April and May, the COD values seem to have insignificant variation by season (average COD values of 0.14 and 0.15 during the summer and winter, respectively). In general, the high maximum COD values were associated with site pairs including sites from different areas in which the paired coarse PM concentration data exhibit the largest difference. These sites were also less correlated, which signifies the necessity of multiple monitoring sites in order to assess the spatial variability in CPM concentrations in a broader metropolitan area. On the other hand, minimum COD values, implying spatial homogeneity, were associated with site pairs located in similar areas, affected by similar sources where correlation was also excellent. These sources appear to vary similarly in time across the sites. Across the sites reported here, spatial homogeneity (e.g. low COD values) does not need to be associated with high temporal correlation (e.g. high  $r^2$  values) as has been observed before (Turner and Allen 2008). The CPM COD values reported here are lower than those reported recently in Helsinki and Athens ( $0.5 \pm 0.1$  and  $0.6 \pm 0.1$ ), and consistent with two other European cities (Amsterdam ( $0.07 \pm 0.01$ ) and Birmingham ( $0.2 \pm 0.1$ )) (Lianou et al. 2007).

There are important caveats to the results reported here. While the CPM mass concentration data can usefully be interpreted within the framework used to determine the location of the sites (e.g. near-freeway vs. community, etc.), we acknowledge that it is not possible to quantitatively apportion the observed CPM concentrations between different sources. This is the first of several papers reporting the results from the comprehensive study of CPM in the Los Angeles area. Further, the time-integrated samples reported here may well average over significant diurnal differences in concentrations that may be relevant to acute exposures (see Moore et al 2009b). As the chemical composition and toxicological data become

available, it will be useful to interpret those data within the context of the material reported herein.

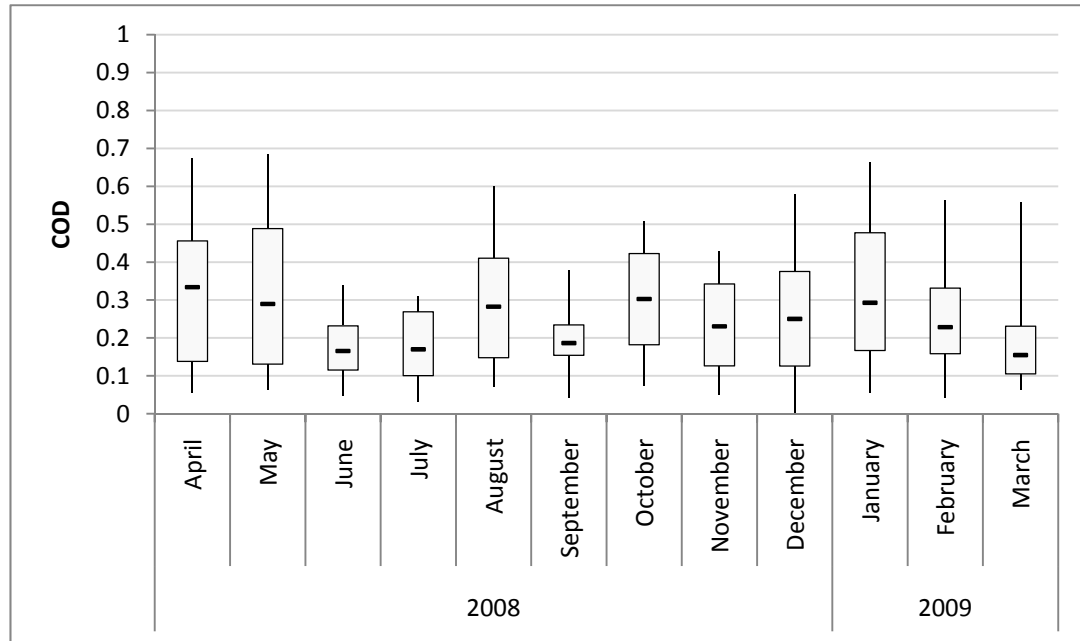


**Figure 4.9** - Coefficients of Divergence for Coarse PM concentrations calculated across all sites pairs (with the exception of the Lancaster site) by month for the entire study (April 2008 – March 2009). Whisker-box plot shows minimum, 1<sup>st</sup> quartile, median, 3<sup>rd</sup> quartile and maximum values.

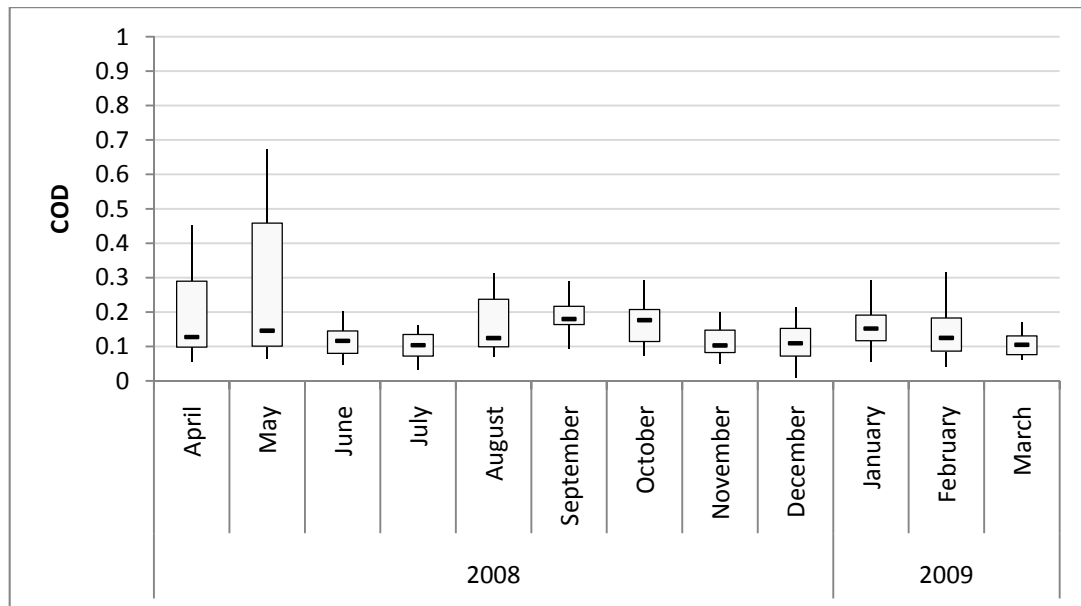


**Figure 4.10** - Coefficients of Divergence for coarse PM concentrations calculated across all urban site pairs (USC, CCL, FRE, HMS, GRD and LDS) by month for the entire study (April 2008 – March 2009). Whisker-box plot as described previously.



#### 4.4. Conclusions and Summary

This study focuses on ambient coarse PM mass concentrations, and the relationships between CPM and PM<sub>2.5</sub> mass concentrations at 10 distinctly different locations in the Los Angeles region. The significant differences in concentrations and seasonal patterns showing the similarities and differences between coarse particle concentrations illustrate the influence of local sources on observations. The CPM mass concentrations observed are consistent with those reported previously in the Los Angeles area.

High correlations were observed between PM<sub>2.5</sub> and CPM near major roads, where the dominant source of coarse particles is traffic induced resuspended particulate matter. A different behavior is observed in more rural areas, where windblown dust is a significant contributor to overall coarse particle concentrations, although even relatively rural sites in the Los Angeles are impacted by motor vehicle-related coarse PM concentrations as well. Correlation of CPM and PM<sub>2.5</sub> concentrations are much higher during winter than summer. For the year of sampling, the average median COD of 0.24 complements the paired correlation coefficients showing modest heterogeneity of CPM in Los Angeles basin. We acknowledge that using 24-hour time-integrated samples may obscure a potentially (and likely) higher variability observed during specific time periods of the day (discussed at length in the companion paper).

This research will help to better understand the sources and behavior of coarse particles in a primarily urban and motor-vehicle dominated environment. There is clear evidence supporting the strong impact of road traffic activity on ambient coarse particle concentrations. While the chemical and toxicological analyses of these samples (currently underway) will provide insight into the specific sources of coarse PM, our observations nonetheless highlight the degree of variability even in 24-hour time-integrated mass

concentrations, which suggests that further work specifically targeting coarse PM emission sources is warranted.

#### 4.5 Acknowledgements

This work was supported by the US Environmental Protection Agency (STAR award #RD833743) and MESA Air grant #RD831697. The authors would like to thank the contribution of USC Aerosol Lab (A. Polidori, M Arhami, Z Ning, N Hudda, KL Cheung), Suresh Thuraiatnam, Ed Avol, Antelope Valley Air Quality Management District, the South Coast Air Quality Management District, St. Cecilias Church, Granite Hill Elementary School, Fremont Elementary School, LAUSD and Hollenbeck Middle School, St. Gerards Church and Church of Jesus Christ of Latter-Day Saints. This manuscript has not been subjected to the EPA's peer and policy review and therefore does not necessarily reflect the view of EPA agency.

## **Chapter 5 - Seasonal and Spatial Coarse Particle Elemental Concentrations in the Los Angeles Area**

### **5.1 Abstract**

The concentrations of trace metals and elements in the coarse fraction of atmospheric particulate matter (CPM, particles smaller than 10 and larger than 2.5  $\mu\text{m}$  in diameter,  $\text{PM}_{10-2.5}$ ) and their spatial and temporal trends were investigated in the greater Los Angeles area. Ten distinct sampling sites were chosen to encompass a variety of CPM sources, including urban, rural, coastal, inland, and near-freeway sites. 24-hr time-integrated CPM samples were collected at each location once a week, for an entire year, from April 2008 to March 2009, to characterize drivers of the seasonal and spatial patterns of the CPM trace metal content. Metals were quantified using sector-field inductively-coupled plasma mass spectrometry (SF-ICP-MS).

Trace metals in CPM displayed distinct seasonal and temporal variations, and a principal component analysis (PCA) was performed to aid identification of the CPM sources underlying these variations. The probable sources of each principal component were identified using elemental tracers. Major sources of CPM metals and elements identified were crustal and mineral matter, abrasive vehicular emissions, industrial, sea spray and catalytic converters, explaining more than 80% of the total variance of CPM metal content. Mineral and crustal elements, most notably Fe, Ca, Al, Mg, K, Ti and Mn, were the main contributor to overall CPM mass, accounting for over 33% of total variance, followed by abrasive vehicular markers such as Cu, Ba and Sb, accounting for over 16% of the variance, with an increasing contribution in the urban sites. Temporal and spatial variations in each identified class of CPM sources were also investigated.

*Keywords:* Coarse particulate matter, trace metals, principal component analysis, resuspended dust, chemical characterization, Los Angeles.

## 5.2 Introduction

An extensive literature has demonstrated associations between exposure to inhalable particulate matter (PM), both PM<sub>2.5</sub> and PM<sub>10</sub>, and a variety of acute and chronic health outcomes, including both respiratory and cardiac diseases (Becker et al. 2005; Hornberg et al. 1998; Kleinman et al. 2003; Lipsett et al. 2006; Monn and Becker 1999; Villeneuve et al. 2003; Yeatts et al. 2007). Studies suggest that PM size is an important factor influencing aerosol toxicity; however it is still unclear whether toxic PM properties are concentrated in a particular size range. Current PM emission regulations, which focus on mass emissions of PM<sub>2.5</sub> and PM<sub>10</sub>, have several caveats. PM<sub>10</sub> includes particles in both the PM<sub>2.5</sub> range as well as coarse PM (CPM – particles between 2.5 µm and 10 µm in aerodynamic diameter), and these size fractions can have substantially different sources, thus different chemical composition and as a result may lead to potentially different health outcomes (Pakbin et al. 2010). Most PM<sub>2.5</sub> particles are produced by combustion processes, whereas airborne coarse particles are generally products of fugitive soil and dust. Non-tailpipe emissions from traffic-induced resuspension of road dust can be as significant as primary exhaust emissions (Harrison et al. 2001). Moreover, an increasing number of studies have reported associations between adverse health effects and specific PM chemical classes or species, rather than total PM mass (Claiborn et al. 2002; Tsai et al. 2000). Among these compounds, trace element and metal species have been linked to various health impacts (Gavett and Koren 2001; Luttinger and Wilson 2003). A number of studies suggest that the biochemical activity of certain metals and trace elements can contribute to the toxic properties of particles (Lighty et al. 2000; Smith and Aust 1997). Among the trace metal species, only As, Be, Cd, Co, Cr,

Hg, Mn, Ni, Pb, Sb and Se are listed by the US Environmental Protection Agency (EPA) as air toxics; however various studies have linked many other trace metals to adverse health outcomes.

Non-exhaust roadway PM emissions are the result of resuspension of road dust, deposited from multiple sources, such as windblown soil, abrasion of road surface, wear of tires and brake linings, and from dry deposition of ambient PM, including those directly emitted from vehicular exhaust (Thorpe and Harrison 2008). While road dust is primarily composed of mineral material (most commonly Al, Ca, K, Ti, etc.), it is also enriched in heavy metals and metalloids (Amato et al. 2009). Wear of brake lining and tire wear contribute greatly to the high metal content of particles, especially those in the coarse PM mode. Ba, Cu and Zn are commonly used in brake linings as friction agents, while Mo, Sb and Sn and sulfides are added as lubricants (Chan and Stachowiak 2004; Garg et al. 2000; Iijima et al. 2007). Vehicle exhaust catalytic converters are the main emission source of platinum group elements (PGEs; Rh, Pd, Pt) in the urban atmosphere, resulting from the mechanical stress on catalytic converters. Other elements such as Ce, La, Mo and Ni are also commonly employed in catalytic converters (Colombo et al. 2008; Gandhi et al. 2003; Morcelli et al. 2005). Furthermore, analysis of PM elemental composition, in addition to the evaluation of its impact on human health, can be used in the identification of specific emission sources (Canepari et al. 2009; Querol et al. 2007).

The goal of this study was to provide a database of the trace element and metal content of coarse PM in the greater Los Angeles area. Coarse PM samples were collected at 10 sites in distinctly different regions of the greater Los Angeles area, encompassing urban, rural-agricultural, industrial, coastal, and background desert sites, and affected by a variety of PM sources. Sampling was conducted once a week for an entire year, to cover the seasonal

variations at all the sites. Concentrations of 49 trace elements were quantified by sector-field inductively coupled plasma mass spectrometry (SF-ICP-MS) and principal component analysis was employed to help identify their emission sources.

### 5.3 Methodology

#### 5.3.1 Sample collection

Ambient coarse PM samples were collected once a week from April 2008 to March 2009 at 10 sites in the greater Los Angeles area to capture the spatial and temporal variations in CPM constituents. Time-integrated 24-hour samples were obtained from 12:00 AM PST to 11:59 PM PST on a weekday. Samples were collected using Personal Cascade Impactor Samplers (Sioutas™ PCIS, SKC Inc., Eighty Four, PA, USA), at an air flow rate of 9 liters per minute (LPM). Particles larger than 2.5µm are impacted on Zefluor (25mm, Zefluor™, 0.5 µm pore size, Pall Corp., East Hills, NY, USA) after passage through a commercially available inlet designed to achieve the PM<sub>10</sub> cutpoint (Misra et al. 2003; Misra et al. 2002; Singh et al. 2003). All the filter substrates were weighed before and after sampling, in the laboratory under controlled conditions, to determine the collected CPM mass. All filters were conditioned for 24 hours in a room with controlled temperature (21°C ± 2°C) and relative humidity (30% ± 5%) before being weighed using a microbalance (Model MT5, Mettler-Toledo Inc., Highstown, NJ, USA). Additional details of the sample collection protocols may be found in (Pakbin et al. 2010).

#### 5.3.2 Site selection

Sampling sites were chosen to encompass the diversity of CPM sources and sinks in the greater Los Angeles area. The 10 selected sites (Figure 4.1) include urban sites near-freeways, residential sites located some distance from freeways, semi-rural, and desert sites.

Table 4.1 summarizes relevant information about each site, including sampling region, designation code, description, geographic co-ordinates and data recovery. Sites are categorized geographically into Eastern, Central and Western Los Angeles; Riverside County; Long Beach; and Lancaster. A detailed description of each site has been reported previously by (Pakbin et al. 2010). In brief, sampling sites located in the urban regions of Los Angeles were segregated into three regions; eastern, central and western Los Angeles. Eastern Los Angeles sites – HMS and FRE – and the centrally located USC and CCL sites were in close proximity to a network of major freeways, east and south of Downtown Los Angeles respectively, while the western Los Angeles sites – LDS and GRD – can be classified as coastal sites, although both sites were also close to major roadways.

Riverside sites – GRA and VBR - were located 80 km inland from downtown Los Angeles, in residential areas with a semi-rural nature. Both sites were adjacent to major roadways; however GRA was located immediately (300 m) north of the CA-60 freeway and therefore it may be impacted to a greater extent by freeway traffic. The Long Beach site – HUD – was located immediately to the east of the Terminal Island Freeway (SR-103) and close to the I-710 freeway, both of which have a high fraction and volume of heavy duty diesel vehicle traffic. HUD was also directly affected by the ports of Los Angeles and Long Beach activities. In contrast, the desert site (LAN) was in desert dominated Antelope Valley, north of the Los Angeles Basin (LAB), and over 2 km away from nearest freeway, although in the proximity of locally significant surface arterial roadways. More detail on each site and the general meteorology of the various regions is described in (Pakbin et al. 2010).

#### 5.4 Analytical methods

The elemental composition of the coarse particulate matter samples was determined by high resolution sector-field inductively coupled plasma mass spectrometry (SF-ICP-MS) after

dissolution of the filter-borne PM using a microwave-aided mixed-acid digestion (Herner et al. 2006; Lough et al. 2005). A mixture of 1.0 mL of 16 N HNO<sub>3</sub> (Optima grade, Fisher Scientific), 0.2 mL of 28 N HF (Ultex grade, J.T. Baker) and 0.35 mL of 12 N HCl (Optimaade, Fisher Scientific) was used for PM dissolution in Teflon bombs with a programmable microwave digestion unit (ETHOS, Milestone). The procedure is described in detail by (Herner et al. 2006). Digestates were diluted to 15 mL with high purity water (18 MΩ cm<sup>-1</sup>) and stored in low-density polyethylene (LDPE) bottles, pre-cleaned in 2.4 N HCl for 48 h, 3.2 N HNO<sub>3</sub> for 48 h and rinsed with milli-Q (Millipore, Bedford, MA).

The digestates were analyzed for 49 elements by SF-ICPMS (Thermo-Finnigan Element 2), of which 42 were selected, based on signal-to-noise metrics, for inclusion in the data analysis. The analytical uncertainties were determined by sum-of-squares propagation of the uncertainty of the SF-ICP-MS measurement (standard deviation of 3 replicate measurements), the uncertainty of the method blank (standard deviation of 4-5 batch specific blanks), and an estimate of the uncertainty in the digestion method and the standard deviation of replicate analyses of NIST Standard Reference Materials (SRMs). Six solid samples of three SRMs were digested and analyzed with every batch of 25 samples. Subsequently, the total uncertainty of each measurement was determined by propagation of the analytical component (above) with the uncertainty of the field blanks. The elemental data were considered detectable if the sample value was greater than twice the estimated total uncertainty. The method detection limits (MDLs) for the quantified species are presented in Table S1.



## 5.5 Results and Discussion

### 5.5.1 Temporal and spatial variations in CPM mass concentrations

A summary of CPM mass concentration data, including geometric and arithmetic means and standard deviations are presented for each site in Table 4.1. A detailed description of temporal and spatial variations in CPM mass from this study was reported previously by (Pakbin et al. 2010). Briefly, the annual geometric mean concentrations observed across all 10 sites were in similar range ( $\text{ca. } 10 \pm 2 \mu\text{g/m}^3$ ) with the exception of LAN which had a significantly lower concentration ( $\text{ca. } 5 \mu\text{g/m}^3$ ). At most sites, summer CPM concentrations were about 2 – 4 times higher than winter concentrations, with the exception of the HUD site, heavily influenced by port activities in Long Beach and high heavy duty truck traffic, which had summer concentrations slightly lower than winter. The rural sites in Riverside showed the highest seasonal variations. The generally higher summer CPM concentrations were attributed to higher contributions of windblown soils and dusts to overall PM concentrations due to increased southwesterly winds (Moore et al. 2010; Pakbin et al. 2010; Sardar et al. 2005b). More stable atmospheric conditions in winter, coupled with relatively lower mixing heights, result in reduced contribution of windblown dust, thus increasing the relative contribution of vehicular traffic induced emissions, such as those from abraded brake lining and tire wear.

Most trace metal concentrations lie within the range of  $0.01 - 10 \text{ ng/m}^3$ , with only Na ( $554.5 \pm 293.8 \text{ ng/m}^3$ ), Fe ( $312.6 \pm 99.0 \text{ ng/m}^3$ ), Ca ( $209.7 \pm 67.2 \text{ ng/m}^3$ ), Al ( $209.6 \pm 73.1 \text{ ng/m}^3$ ), Mg ( $119.0 \pm 41.5 \text{ ng/m}^3$ ), S ( $110.4 \pm 43.8 \text{ ng/m}^3$ ), K ( $91.4 \pm 31.1 \text{ ng/m}^3$ ), Ti ( $19.7 \pm 5.8 \text{ ng/m}^3$ ), Ba ( $15.5 \pm 5.5 \text{ ng/m}^3$ ) and Cu ( $13.5 \pm 4.3 \text{ ng/m}^3$ ) exceeding  $10 \text{ ng/m}^3$ . Concentrations generally rise in proximity of roadways, reaching values up to 10 times higher than at the rural desert site in Lancaster. The inter-correlation of selected trace

elements and metals are presented in Figure 1(a-d), in a matrix comprised of Pearson coefficients. The elements selected for presentation were chosen based upon the source apportionment analysis and data interpretation presented in the subsequent sections.

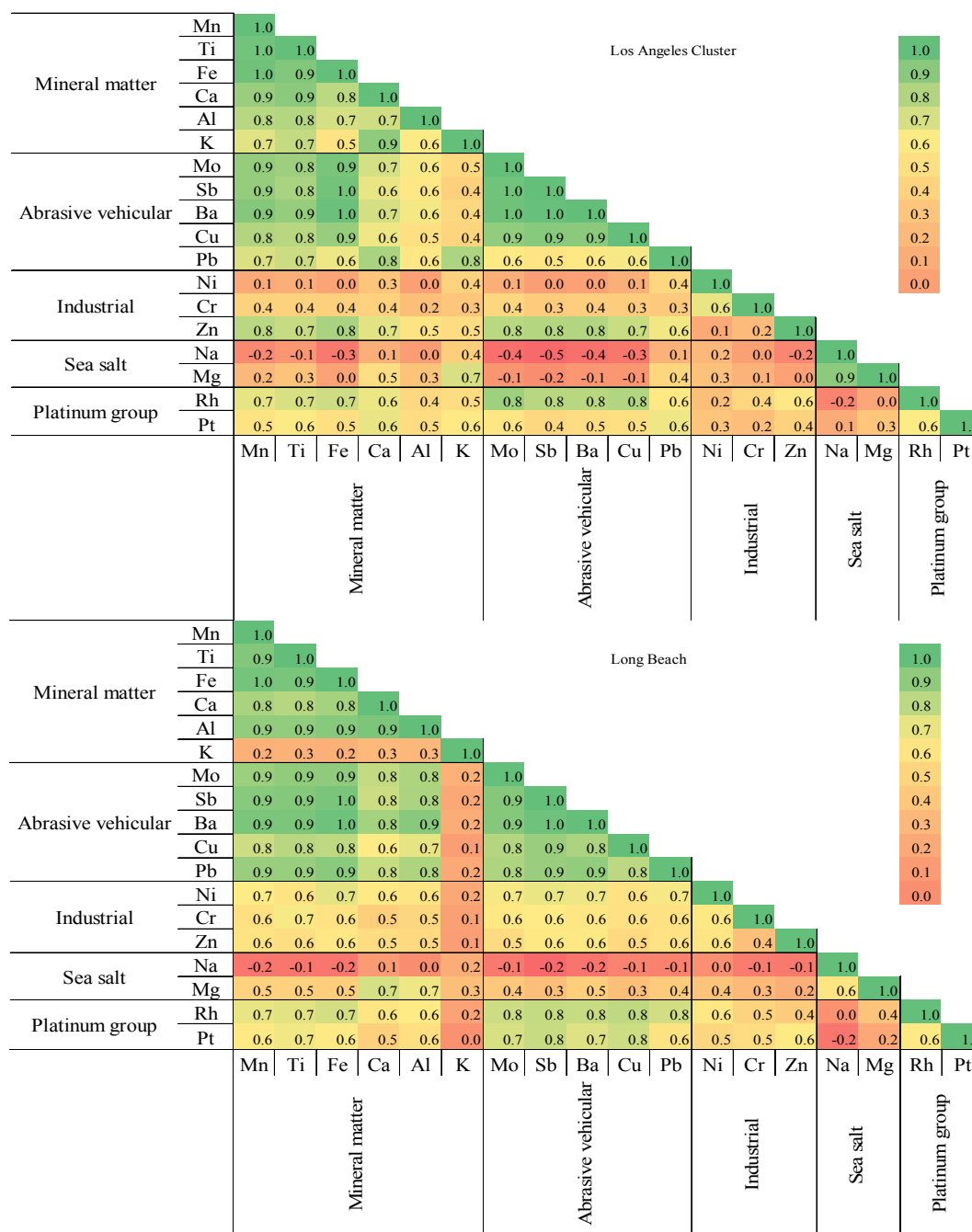


**Figure 5.1 (a – b)** - Pearson coefficient matrix for selected trace metals in each site cluster; a) Los Angeles cluster, b) Long Beach.

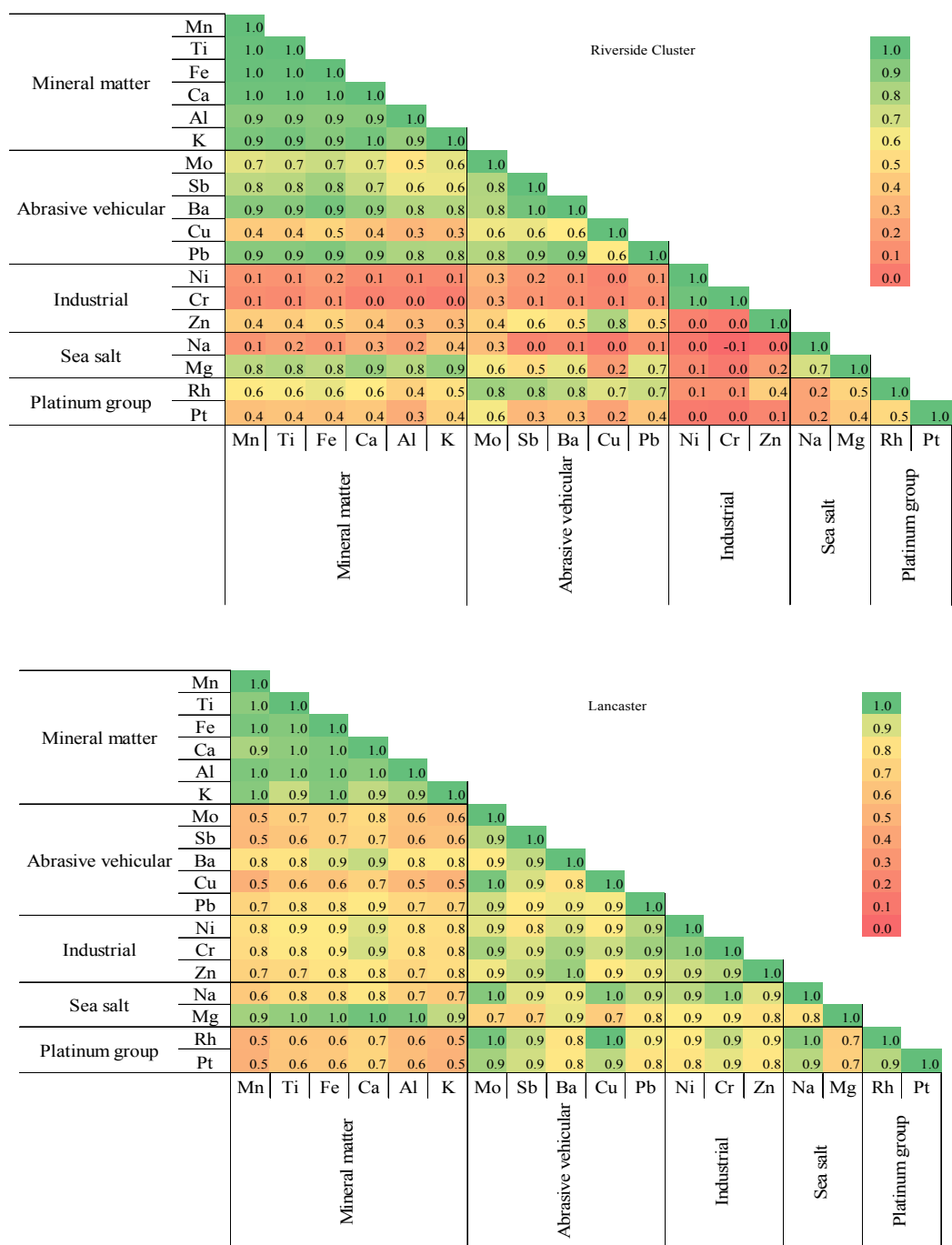


**Figure 5.1 (c – d)** - Pearson coefficient matrix for selected trace metals in each site cluster; c) Riverside cluster, and d) Lancaster.

### 5.5.2 Principal Component Analysis (PCA)

To qualitatively identify the potential sources of trace metals species in CPM, principal component analysis (PCA) was employed. PCA was chosen as the receptor model, because the application of chemical mass balance (CMB) requires detailed quantitative knowledge of the emission source profiles, currently unavailable for many of the trace element and metal species quantified in this study, whereas for PCA, qualitative knowledge of the sources is sufficient. Moreover, the source profiles may not be consistent among the different sites due to physico-chemical changes of the urban aerosols with transport from source to receptor areas of the basin, which may result in differences in particle size distributions for key coarse PM sources. Using PCA the elements were clustered in terms of their temporal and spatial variations, suggesting common sources. PCA was applied to a matrix comprised of chemically fractionated CPM data, including only species that had signal to noise ratios (S/N) above unity in more than 80% of the samples (42 species from the total 49 species analyzed by SF-ICP-MS). Values below the criterion threshold ( $S/N < 1$ ) were replaced by a value chosen randomly between zero and the method detection limit (MDL) of that specific element for the statistical analysis, in order to avoid false correlations between variables with multiple below detection limit values.

In PCA, the algorithm attempts to explain the variance in a multivariate dataset with the minimum possible number of factors. If the variables are correlated with each other, a large portion of variance in the dataset can be explained with a small number of factors.

The primary PCA was applied to a pooled data set from all the sampling sites with the exception of the Lancaster site. The Lancaster site was heavily influenced by wind-induced soil emissions from the surrounding deserts, thereby making it a unique “desert-like” site compared to the rest, and therefore PCA was performed separately for that site. The

VARIMAX rotated factor matrix for the coarse PM metal data from all sites (except Lancaster) is presented in Table 1 along with the factor loadings, associated eigenvalues and variance, while the PCA results for Lancaster are presented in Table S2. VARIMAX rotation was used to redistribute the variance to give a more interpretable structure to the factors (Henry 1987). In the Tables, PCA factors are sorted in descending order of the corresponding eigenvalues. Eight components with eigenvalues greater than unity after the VARIMAX rotation were retained in the PCA, accounting for over 80% of the total variance, with roughly 34% accounted for by the first component. The elements were considered to identify source categories when their factor loadings were larger than 0.5. Identifications of probable sources of each principal component were based primarily on the source profiles and the presence of marker species. These identifications should not be considered definitive, as there could be some blending between factors.

**Table 5.1.** Principal component loadings (VARIMAX normalized) of selected trace element and metal species in airborne coarse particulate matter.

	Principal Component							
	PC1	PC2	PC3	PC4	PC5	PC6	PC7	PC8
Mn	<b>0.93</b>	0.06	-0.11	0.01	-0.02	-0.09	0.04	-0.07
Nd	<b>0.93</b>	-0.19	-0.06	0.12	-0.04	-0.03	-0.01	0.12
Yb	<b>0.92</b>	-0.25	-0.08	-0.02	0.01	0.00	-0.02	0.01
Ti	<b>0.92</b>	0.14	-0.13	0.00	-0.05	-0.07	0.00	-0.05
Dy	<b>0.91</b>	-0.34	-0.10	0.03	-0.03	-0.02	0.02	0.02
Ho	<b>0.90</b>	-0.32	-0.06	-0.10	-0.03	0.01	0.03	0.01
Pr	<b>0.89</b>	-0.09	-0.03	0.16	-0.08	-0.03	-0.05	0.18
Y	<b>0.89</b>	-0.21	-0.07	0.15	-0.06	0.01	0.00	0.00
Sr	<b>0.88</b>	0.10	-0.09	0.17	0.09	0.12	-0.02	-0.08
Lu	<b>0.86</b>	-0.20	-0.01	-0.21	-0.04	0.10	-0.03	0.06
Sm	<b>0.86</b>	-0.32	0.15	0.07	-0.06	-0.11	-0.19	0.14
Fe	<b>0.84</b>	0.44	-0.16	-0.01	-0.05	-0.03	-0.07	-0.08
Rb	<b>0.84</b>	-0.37	-0.18	0.13	0.00	-0.11	0.10	-0.06
Cs	<b>0.84</b>	-0.40	-0.06	-0.02	0.07	0.06	0.12	-0.02
Ca	<b>0.83</b>	-0.18	-0.01	0.14	0.15	0.21	0.07	0.06
Nb	<b>0.79</b>	0.11	0.18	-0.38	0.12	0.14	0.09	0.14
Eu	<b>0.78</b>	0.16	-0.14	0.11	0.01	0.01	-0.06	0.10
Sc	<u>0.63</u>	-0.31	0.30	-0.53	-0.02	0.23	0.00	0.08
Co	<u>0.62</u>	0.09	0.35	-0.11	0.23	-0.25	-0.15	-0.30
As	<u>0.59</u>	0.08	-0.19	0.12	0.16	-0.08	0.05	-0.23
Li	<u>0.59</u>	-0.27	-0.18	0.26	0.04	-0.06	0.05	-0.14
Th	<u>0.59</u>	-0.26	0.34	-0.57	-0.01	0.25	0.02	0.07
Al	<u>0.57</u>	-0.18	-0.10	0.16	0.04	0.01	0.01	-0.08
K	<u>0.51</u>	-0.28	-0.01	0.15	0.13	-0.01	0.13	-0.21
V	0.40	-0.20	0.40	0.25	0.01	-0.31	-0.34	-0.08
Mo	0.49	<b>0.79</b>	-0.11	-0.04	0.08	0.00	-0.13	-0.04
Sb	<u>0.51</u>	<b>0.78</b>	-0.20	-0.07	-0.08	0.05	-0.12	-0.06
Ba	<u>0.64</u>	<u>0.69</u>	-0.17	-0.03	-0.09	0.02	-0.12	-0.06
Cu	0.48	<u>0.68</u>	-0.07	-0.02	-0.11	0.12	-0.08	-0.11
Rh	0.36	<u>0.66</u>	-0.03	-0.09	0.04	0.29	-0.16	0.03
Pb	0.44	<u>0.51</u>	-0.04	0.10	-0.05	-0.05	-0.06	0.12
S	-0.10	0.12	<u>0.60</u>	<u>0.54</u>	-0.04	0.10	-0.16	-0.10
W	0.23	-0.03	<u>0.59</u>	-0.38	0.15	-0.07	-0.31	-0.29
Zn	0.48	0.30	<u>0.54</u>	-0.24	-0.36	0.06	0.19	-0.04
La	0.23	0.00	0.46	0.38	-0.09	-0.25	-0.43	0.38
Ni	0.10	0.29	0.24	0.00	<u>0.67</u>	-0.31	0.34	0.11
Cr	0.23	0.37	0.18	-0.03	<u>0.64</u>	-0.28	0.30	-0.03
Mg	0.30	-0.17	0.09	0.39	0.36	<u>0.67</u>	-0.02	-0.02
Na	-0.45	0.08	0.28	0.34	0.26	<u>0.58</u>	-0.05	-0.11
Cd	0.28	0.28	0.42	0.24	-0.41	-0.02	<u>0.56</u>	-0.08
Ce	0.42	0.27	0.37	0.29	-0.37	-0.01	0.44	0.07
Pt	0.16	0.29	0.03	0.01	0.24	0.03	0.04	<u>0.69</u>
Eigenvalue	14.12	6.73	3.48	2.22	2.09	1.99	1.79	1.22
% of Variance	33.62	16.03	8.28	5.28	4.97	4.73	4.27	2.91

Loadings higher than 0.7 are shown in bold with dark gray background, and loadings between 0.5 and 0.7 are underlined with gray background.

PCA was also applied to the data pooled by different site cluster (i.e. Los Angeles, Long Beach, Riverside and Lancaster). Due to space limitations, the results of PCA for each site cluster are not presented herein, but were used in the interpretation of the results, and are presented in the supplement (Table S2 – S5). In general, PCA yielded consistent patterns across different site clusters, with relatively similar source profiles in sampling sites located in Los Angeles, Long Beach and Riverside; while in Lancaster, most trace element and metal species had predictably high factor loadings in the soil-driven first principal component, accounting for 33.2% of total variance, emphasizing the dominant influence of soil emissions at this site (Table S2).

With this approach, the main sources and the most representative variables were quantitatively identified. The first principal component (PC1) appears to represent soil dust, with a strong contribution from the major crustal metals such as Mn, Ti, Fe, Ca, Li, Al, K, and many of the soil source dominated rare earth elements (Nd, Yb, Dy, Ho, Pr, Sr, Lu, etc.). PC2 has strong factor loadings for species that are considered tracers of abrasive vehicular emissions (e.g., tire and break wear), most notably Mo, Sb, Ba, Cu, Rh and Pb, and Fe (the latter with a relatively lower factor loading).

The interpretation of PC3 is not as clear, partly because of the distribution of some of the PC3 factor loadings between PC3 and other components. For example, Zn factor loadings are of similar magnitude in both PC1 and PC3 (and to a lower extent in PC2), while S also exhibits relatively high factor loadings in PC4. These species, in particular W, had much higher factor loadings when PCA was applied to data from Long Beach (Table S3), and may represent nearby industrial sources. PC4 represents a sulfur source, as the only element with factor loading higher than 0.5 is S, accounting for 5.3% of total variance.

PC5 has the highest loadings for Ni and Cr. These two metal species are often associated with plating industries and abrasive vehicular emissions, and had much higher factor loadings in the Long Beach site. PC6 contains most of the variability for Na and Mg, evidently representing sea salt aerosol spray transported from the Pacific Ocean. High factor loadings of Cd and Ce in PC7 may represent plastic dust, resulting from degradation of plastic materials. Both Cd and Ce are commonly used as dyeing agents in plastic production. The last principal component has high factor loadings for Pt, with considerably higher loadings in Los Angeles site cluster, likely resulting from vehicular catalytic converter wear.

### 5.5.3 Crustal material

The contribution of mineral dust and other crustal materials to total CPM mass was identified mainly by the presence of elements such as Mn, Ti, Fe, Ca, Li, Al and K, which are typical tracers of mineral materials (Moreno et al. 2006; Perrino et al. 2009; Watson et al. 1994). The first principal component accounted for 33.6% of total variance. The average concentrations of total crustal elements in CPM varied both temporally and spatially. The most abundant crustal elements found in CPM were Fe (median  $312.6 \pm 99.0 \text{ ng/m}^3$  across all the sites), Ca ( $209.7 \pm 67.2 \text{ ng/m}^3$ ), Al ( $209.6 \pm 73.1 \text{ ng/m}^3$ ), Mg ( $119.0 \pm 41.5 \text{ ng/m}^3$ ), K ( $91.4 \pm 31.1 \text{ ng/m}^3$ ), Ti ( $19.7 \pm 5.8 \text{ ng/m}^3$ ), Mn ( $4.4 \pm 1.4 \text{ ng/m}^3$ ) and Sr ( $2.5 \pm 3.1 \text{ ng/m}^3$ ). The sum of the elemental concentrations of these eight elements accounted for on average 56.7% of the total CPM metal content of the 49 measured elements (sum of the elemental concentrations of all analyzed elements) across all the sampling sites. The annual variations in concentrations of selected mineral material tracers across all sites are shown in Figure 2. The highest concentrations of Al, K, Ca and Ti were observed in the Riverside sites, followed closely by HUD in Long Beach, and the Los Angeles sites, while concentrations of these species in Lancaster were much lower than those in other sampling sites. However, the normalized per PM mass concentrations of Fe, Al, K, Sr and Ti were highest in Lancaster,



followed by the Riverside site cluster, indicating a higher contribution of crustal elements to the overall CPM mass in more rural sites. While the absolute metal concentrations ( $\text{ng}/\text{m}^3$ ) represent total exposure to these species, the relative (per PM mass) metal concentrations ( $\text{ng}$  of metal/ $\text{mg}$  of CPM) provide insight into different source contributions at different geographic regions. This observation is consistent with the source apportionment analysis based on temporal and seasonal variations in CPM mass concentrations, discussed in details by (Pakbin et al. 2010), showing higher contribution of windblown soil and dust in more rural areas. (Moore et al. 2010) showed that CPM concentrations in the Lancaster site accounted for the majority of  $\text{PM}_{10}$  concentrations, because of the predominant contribution of windblown dust to overall PM concentrations.

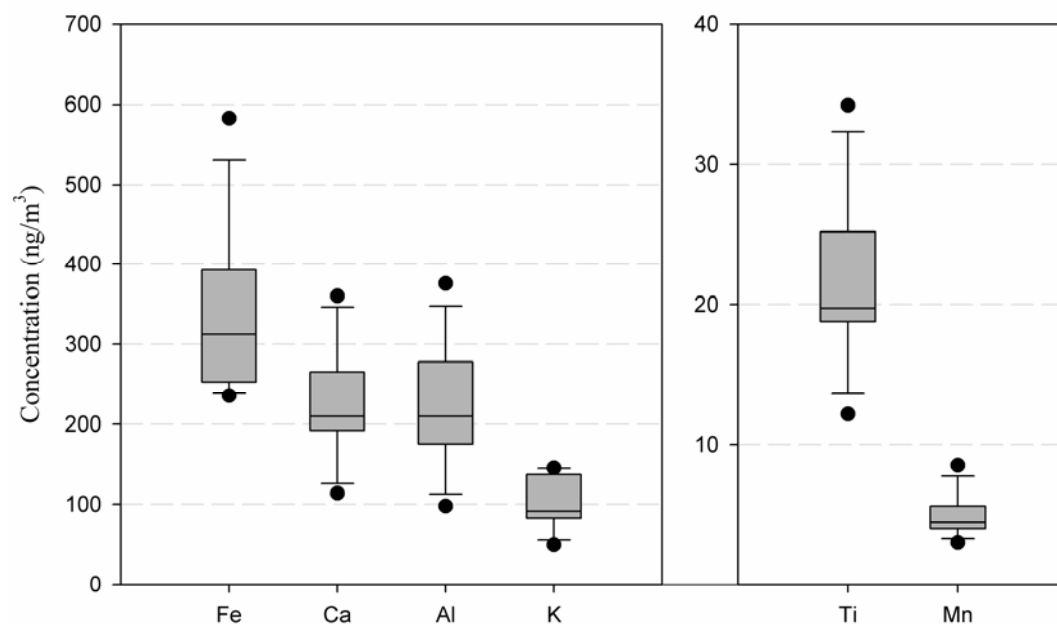


**Figure 5.2** - Annual variations of crustal material tracers across all sampling sites.

Patterns of temporal variation in ambient concentrations of the crustal elements differed among site clusters. Urban sites in Los Angeles and the Long Beach site showed higher concentrations of crustal metals (e.g. Al, Ca, K, Ti, Fe, Sr and Mg) during winter, despite higher overall CPM mass concentrations in summer (Pakbin et al. 2010); crustal metal concentrations peaked in October, with continued elevated concentrations evident through January/February. The concentrations of selected crustal tracers during summer remained lower and with less temporal variation. In contrast, the rural sites in Riverside and Lancaster exhibited higher crustal metal contributions during summer, coupled with higher CPM mass concentrations in the same time period, suggesting higher overall contribution of windblown dust to total CPM mass in rural areas (Figure 3a – 3d), while in the urban sites the contribution of traffic-induced resuspended road dust is dominating, leading to higher elemental concentrations in the more stable atmospheric conditions.

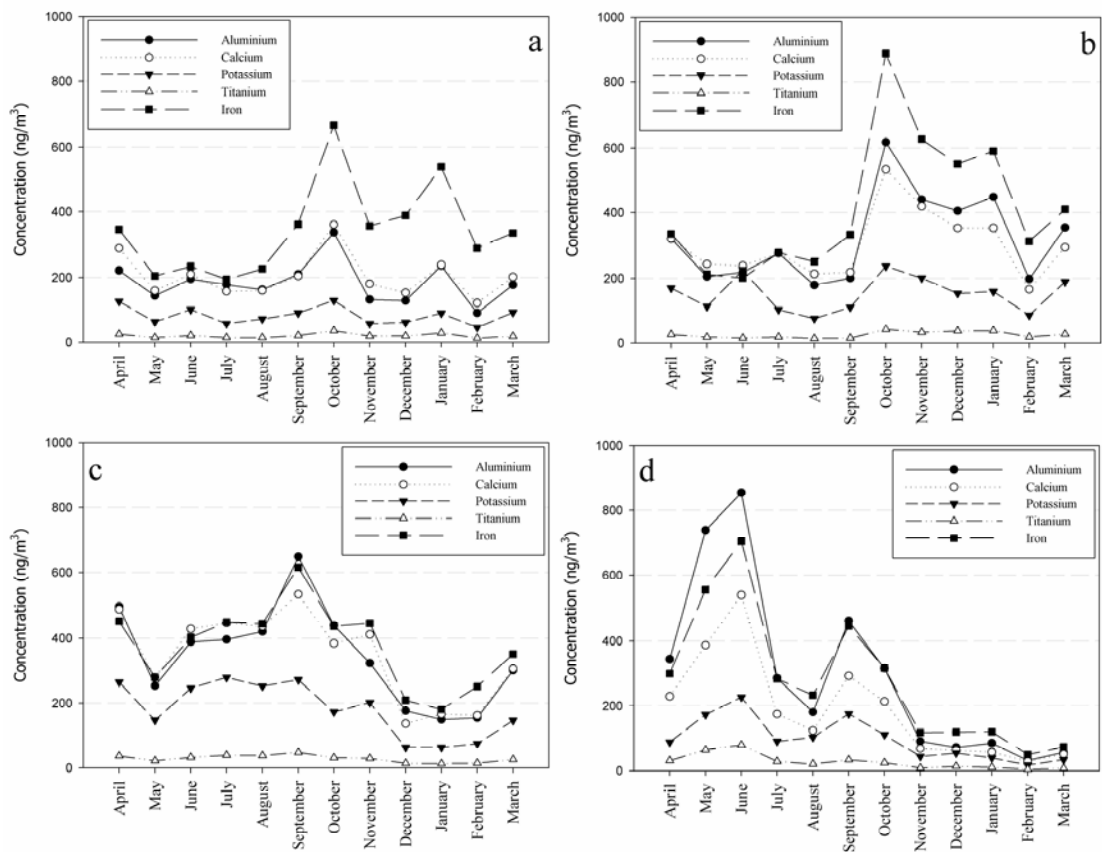


**Figure 5.3(a – d)** - Temporal variation of selected mineral dust tracers in different sampling site clusters; a) Los Angeles cluster, b) Long Beach, c) Riverside cluster, and d) Lancaster.

#### 5.5.4 Abrasive vehicular emissions

The second principal component (PC2) was identified as abrasive vehicular emissions, comprising trace elements such as Mo, Sb, Ba, Cu, Rh, Pb and Fe. Among them, antimony and barium are known as tracers of brake wear (Dietl et al. 1997; Lough et al. 2005). It should be noted that Fe had a higher factor loading in PC1 (0.84 compared to 0.44 in PC2, Table 3), suggesting both geologic and anthropogenic sources, also reported by (Lough et al. 2005). Brake wear emissions contain significant amounts of Ba, Sb, Fe, Cu and Zn (Garg et al. 2000) consistent with their use in brake linings; for example Cu, Mo, Sb and Sn are high-

temperature lubricants, present in most brake linings, while barium and zinc sulfates are commonly used as friction modifiers (Chan and Stachowiak 2004; Garg et al. 2000; Iijima et al. 2007; Sanders et al. 2003; Sternbeck et al. 2002).

Lead (Pb) may be emitted from several sources, including brake wear and resuspension of road dust (Cadle et al. 1997; Garg et al. 2000; Young et al. 2002). (Root 2000) demonstrated that the lead wheel weights, widely used to balance motor vehicle wheels, which are dropped from vehicle wheels, can be rapidly abraded and pulverized by traffic, thereby enriching the lead content of roadway dust. High correlations between Pb concentrations and other abrasive vehicular emission markers demonstrate that they probably have similar sources (Figure 2a – 2d). While Zn had its highest factor loading in PC3 (0.54), it also had relatively high factor loadings in PC1 and PC2 (Table 3). Zinc is used in the form of zinc dithiophosphate in lubricating oils for gasoline vehicles as an antiwear and antioxidant additive, which may contribute to zinc emissions in CPM (Cadle et al. 1997), whilst (Councell et al. 2004; Fauser et al. 1999) identified zinc as a tracer for particles from tire wear.

The most abundant elements in PC2 were Fe, Ba and Cu with average concentration of  $312.6 \pm 99.0 \text{ ng/m}^3$ ,  $15.5 \pm 5.5 \text{ ng/m}^3$  and  $13.5 \pm 4.3 \text{ ng/m}^3$ , respectively. The average CPM concentrations of Zn, Sb, Pb, Mo and Rh were  $5.7 \pm 2.2 \text{ ng/m}^3$ ,  $1.6 \pm 0.6 \text{ ng/m}^3$ ,  $1.0 \pm 0.3 \text{ ng/m}^3$ ,  $0.4 \pm 0.2 \text{ ng/m}^3$  and  $1.13 \pm 0.31 \text{ pg/m}^3$ . Most of elements identified in PC2 had their highest measured concentrations at Los Angeles sites, followed by Long Beach, Riverside and Lancaster site clusters, a trend that parallels vehicular traffic volume and reinforces a likely dominant vehicular source for these elements. Cu, Sb, Ba and Pb concentrations were highest at the Los Angeles site cluster ( $16.8 \pm 6.9 \text{ ng/m}^3$ ,  $2.1 \pm 1.3 \text{ ng/m}^3$ ,  $19.2 \pm 9.6 \text{ ng/m}^3$  and  $1.3 \pm 0.5 \text{ ng/m}^3$ , respectively), while Fe and Zn concentrations were higher in Long

Beach ( $374.2 \pm 207.7 \text{ ng/m}^3$  and  $9.9 \pm 5.9 \text{ ng/m}^3$ , respectively), probably due to additional contribution from non-abrasive vehicular emissions in Long Beach (e.g. local industrial sources such as oil refineries). The annual variations in ambient concentrations of selected brake wear markers across all the sites are presented in Figure 4. The elemental concentrations of these metal species were highest during fall/winter at all the sites with exception of the Lancaster site, with the highest deviations observed in the urban sites of Los Angeles between seasons, most likely due to relatively more stable atmospheric conditions.

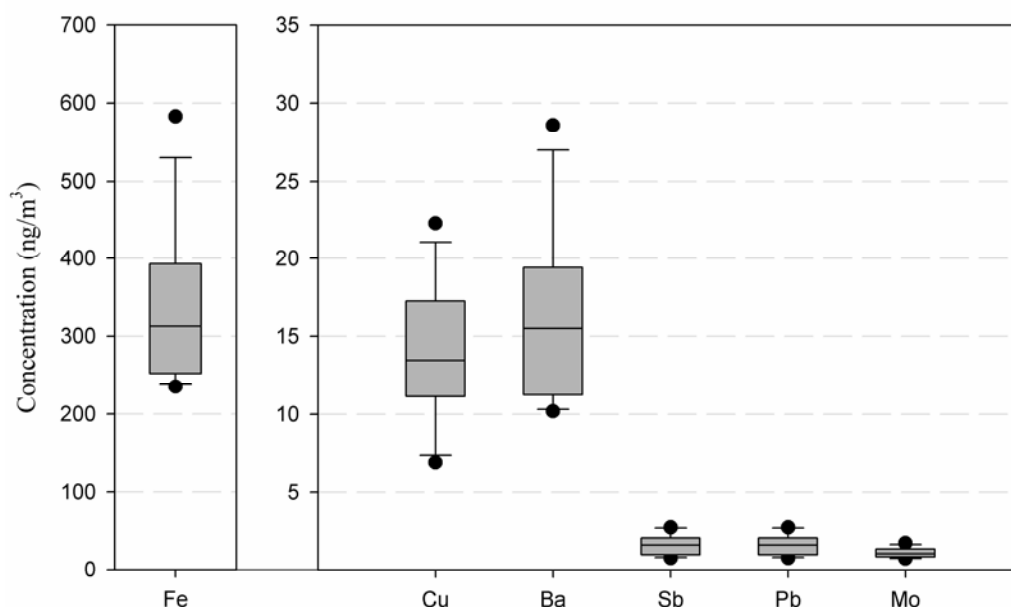


**Figure 5.4** - Annual variation of abrasive vehicular tracers across all sampling sites.

A number of studies have reported the Cu/Sb ratio as a characteristic index of brake wear, however, different values in the range of 4 to 12 were reported in different urban environments (Canepari et al. 2008; Furuta et al. 2005; Gomez et al. 2005; Sternbeck et al. 2002; Weckwerth 2001). Although this ratio can be dependent on the composition of the brake lining used in the studied area, our data show very little variation in the Cu/Sb ratio

among all the site clusters - with the exception of Lancaster, the Cu/Sb ratio was on average ( $8.3 \pm 0.8$ ). The Cu/Sb ratio in Lancaster was much higher (27.3), possibly because Cu may have other sources than abraded brake wear in this area. At the Lancaster site, Cu has a high factor loading in PC1 (Table S2) (along with crustal materials) and also exhibits good correlations with soil tracers (Figure 2d), further confirming this hypothesis. The Cu/Sb ratio in Long Beach (9.2) was relatively higher than Los Angeles (7.6) and Riverside (7.9), probably due to higher brake wear emissions resulting from stronger abrasion processes of heavy duty vehicles in the I-710 freeway near the sampling site.

#### 5.5.5 Other sources of CPM-bound metals and trace elements

The highest elemental factor loadings in the third principal component corresponds to S, W, Zn, La, and V (Table 3). La, V, W and Zn have various industrial sources, most notably industrial catalytic converters, while sulfur is also associated to industrial emissions, in particular emissions from oil refineries and also emissions from ships. La, V, S and Zn have even higher factor loadings (Table S3) and higher average concentrations in PC3 in Long Beach, both indicative of their industrial origins in this region in proximity to multiple oil refineries. PC4 represents sulfur sources, with sulfur the only element with factor loading higher than 0.5, along with lower factor loadings of La, Mg and Na, all of which distributed between multiple principal components. Sulfur may be in the form of ammonium sulfate and its presence in coarse PM may reflect a “tail” in the upper size distribution range of ammonium sulfate, which is mostly in the PM<sub>2.5</sub> size range (Cheung et al. 2010; Seinfeld and Pandis 2006).

The fifth principal component has high factor loadings for the two trace metals Ni and Cr, both often identified as markers of industrial emissions. (Singh et al. 2002) attributed Ni and Cr to emissions from power plants and refineries in Long Beach, whereas (Querol et al.

2007) identified Ni and V as markers of petrochemical emissions in Spanish cities, while As, Cd, Cr, Cs, Cu, Mn, Mo, Ni, Zn were markers of different forms of metallurgy. When PCA was applied to the Long Beach data, one of the main factors (PC2) was characterized by high loadings of Cu, Cd, Cr, Mo, and Ni, along with some of the abrasive vehicular tracers (Fe, Sb, Ba, Pb) and platinum group (Pt and Rh) (Table S3), suggesting that the emissions of these elements are most likely related to the activities of the ports of Long Beach and Los Angeles as well as the heavy duty diesel truck traffic associated with these ports and their transport activities.

Marine aerosols play an important role in the overall PM composition in Los Angeles, due to the geographic orientation of the city, its proximity to the Pacific Ocean, and the prevailing westerly wind patterns. The elements with highest loading on the sixth principal component (PC6) were Na and Mg, and this component was identified as sea spray aerosols. The PCA estimated that the marine contribution explains 4.7% of the total variance (Table 3). Na concentrations notably decreased from the coastal to the inland sites (Figure 6), with highest concentrations observed in Long Beach ( $681.5 \pm 253.4 \text{ ng/m}^3$ ), followed by Los Angeles sites ( $570.2 \pm 361.8 \text{ ng/m}^3$ ), the Riverside sites ( $356.7 \pm 284.5 \text{ ng/m}^3$ ) and Lancaster ( $124.1 \pm 122.7 \text{ ng/m}^3$ ). Within the Los Angeles site cluster, the western Los Angeles sites had higher average concentrations of both Na and Mg ( $716.6 \pm 423.7 \text{ ng/m}^3$ ). Figure 5 shows the annual variation in concentrations of Na across all site clusters. The spatial variation in Mg concentrations is negligible compared to Na, with relatively higher concentrations observed in Riverside compared to Los Angeles. Mg is also a tracer of mineral dust as well as sea spray, which explains the relatively high factor loadings in both PC1 (associated to mineral dust) and PC6 (associated with sea spray). PC7 has the highest factor loadings for Cd and Ce, two trace metals commonly used in dyeing process of plastics, which may be enriched and accumulated in soil and road dust over time. The spatial variations of these two species

were quite low across the sampling sites, with the exception of relatively higher concentrations of Cd in Lancaster.

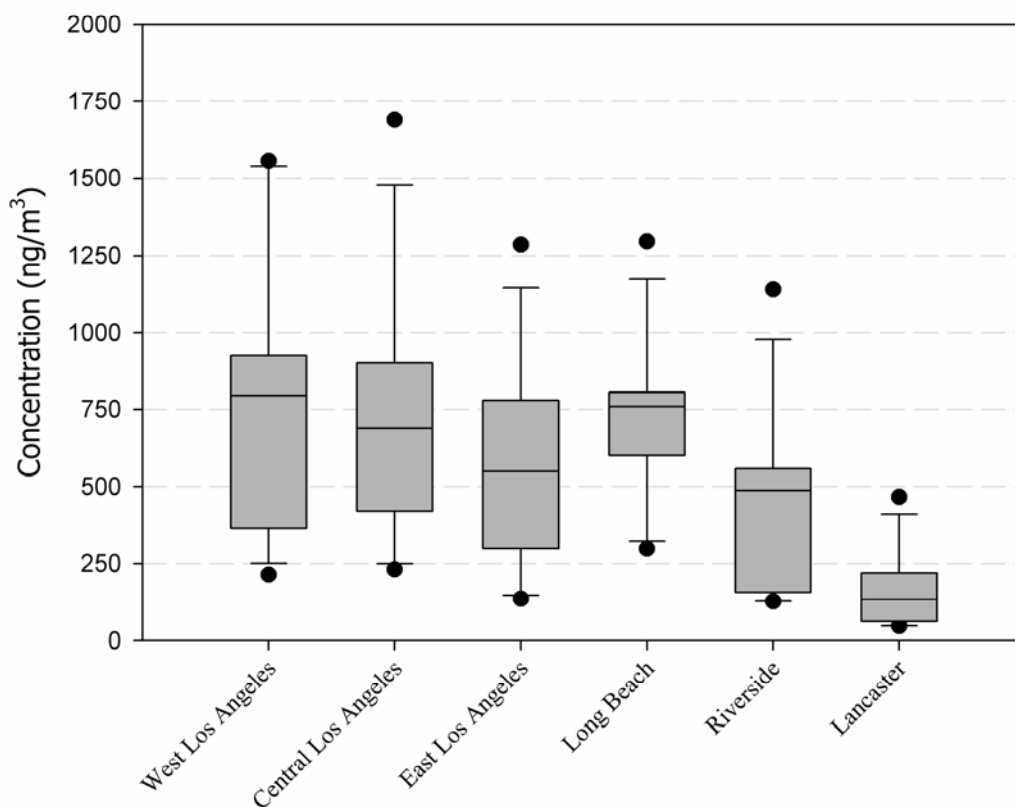


**Figure 5.5** – Annual variation of sodium, a sea salt tracer, across all sampling sites.

Platinum group elements (PGEs), particularly Pt, Pd and Rh, are widely used in automobile catalytic converters. A number of studies have linked airborne PGE concentrations to emissions resulting from chemical, physical and thermal stresses due to mechanical abrasion and high temperatures (Gomez et al. 2002; Rauch et al. 2001; Wiseman and Zereini 2009; Zereini et al. 2001), while other studies showed an increase in PGE levels in urban soils and dusts (Whiteley and Murray 2003; Zereini et al. 1997; Zereini et al. 2007). The average annual CPM concentration of Pt and Rh were  $2.27 (\pm 0.74) \text{ pg/m}^3$  and  $1.13 (\pm 0.31) \text{ pg/m}^3$ ,



respectively, while Pd concentrations were below detection limits. Pt and Rh concentrations were highest in the Los Angeles site cluster, followed by Long Beach and rural sites, with lowest concentrations observed in Lancaster. These concentrations are lower than those reported by (Rauch et al. 2005) in Boston, USA ( $9.4 \text{ pg/m}^3$  and  $2.2 \text{ pg/m}^3$  for Pt and Rh, respectively). In the principal component analysis, platinum had high factor loadings in PC8, while the highest factor loading of Rh was observed in PC2. When PCA was applied to the data from the sites in each cluster separately, both Pt and Rh were in PC2 in Long Beach, along with abrasive vehicular and industrial markers (Table S3). This may be the result of higher emissions of catalytic converter debris from heavy duty vehicles and/or higher industrial activity in the area of Long Beach.

Among the metal species discussed, some are reported by the US Environmental Protection Agency (EPA) as hazardous air pollutants. These elements are antimony, beryllium, arsenic, cadmium, chromium, cobalt, lead, manganese, mercury, nickel and selenium; among which mercury was not detectable by ICP-MS methodology while, beryllium and selenium concentrations were below the detection limit in more than 80% of collected samples and therefore not reported. The average concentrations of these elements across all the sites were Sb ( $1.58 \pm 0.64 \text{ ng/m}^3$ ), As ( $0.079 \pm 0.022 \text{ ng/m}^3$ ), Cd ( $0.016 \pm 0.005 \text{ ng/m}^3$ ), Cr ( $1.06 \pm 0.41 \text{ ng/m}^3$ ), Co ( $0.11 \pm 0.03 \text{ ng/m}^3$ ), Pb ( $1.03 \pm 0.29 \text{ ng/m}^3$ ), Mn ( $4.36 \pm 1.43 \text{ ng/m}^3$ ) and Ni ( $0.64 \pm 0.16 \text{ ng/m}^3$ ). The variations in CPM concentrations of these elements are presented in Figure 6 (a – d). Sb, Co and Zn had the highest concentrations in Long Beach, while Cr and Mn had relatively higher concentrations in Los Angeles and Riverside.

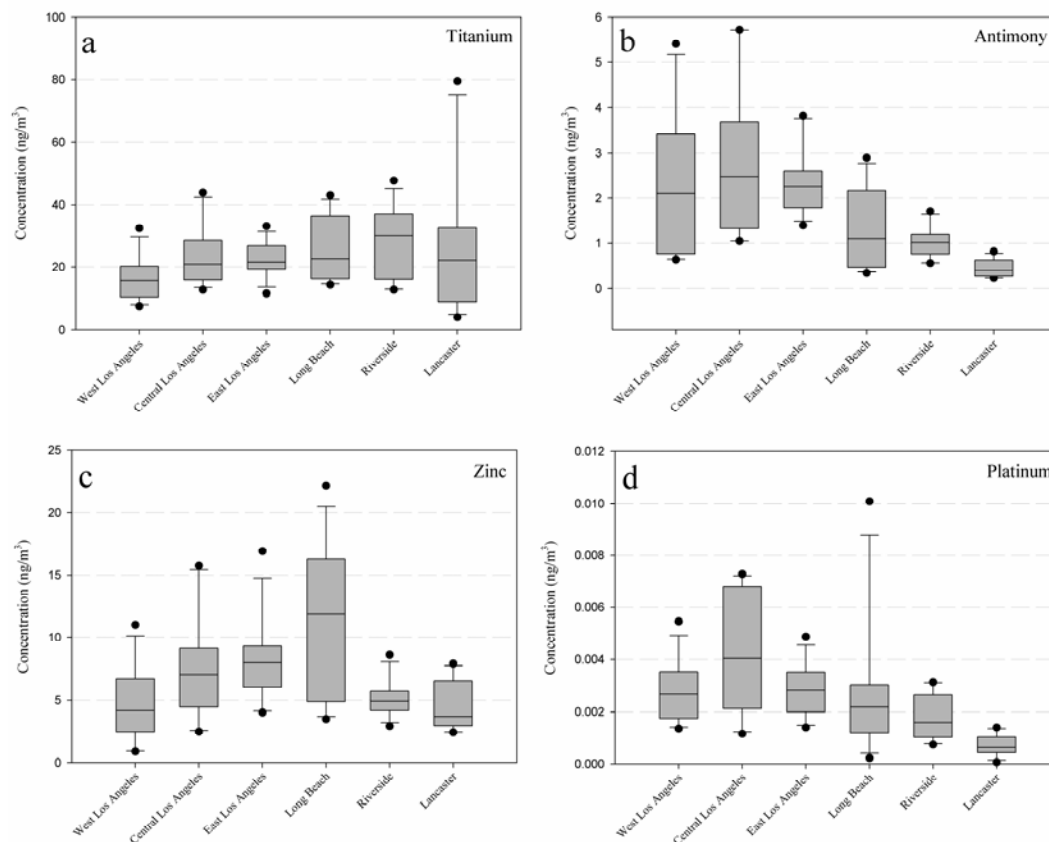


**Figure 5.6 (a – d)** - Annual variation of selected metal species from the identified sources using principal component analysis across all sampling sites (Annual variation of sea salt tracer, sodium, is presented in figure 5.4).

## 5.6 Summary and Conclusions

Samples of CPM from a year-long measurement campaign at 10 sites in the greater Los Angeles area, subject to various aerosol/pollution sources, were quantified for their element content. Principal component analysis (PCA) was applied in order to help identify CPM sources in the study area. The PCA revealed a suite of identifiable CPM sources that were consistent with data available in the literature, but also identified additional elemental markers for some of these CPM sources that are reported here for the first time. In general, trace metals associated with airborne mineral dust dominated the overall CPM mass (mainly

Al, Ca, Fe, K, Mg, Ti), while abrasive vehicular emission tracers (Fe, Ba, Cu) also contributed significantly. Other identified CPM sources were industrial emissions, sea salt spray and catalytic converter emissions. Each of these classes of CPM trace element and metal markers had their distinct temporal and spatial variations. Figure 8 shows the temporal variation of selected trace elements from each identified source, across all site clusters. Elements in the same class had generally similar spatial variation patterns across the sites.

So far only 11 metal species have been listed in EPA as airborne toxics, while many more may induce hazardous outcomes in human health. Heavy metals accumulate in road dust as a result of atmospheric deposition and can subsequently become airborne by wind or traffic induced turbulence. The accumulation of heavy metals is more rapid in dry locations, such as the greater Los Angeles area, with about only 30 cm of annual precipitation on average (National Oceanic and Atmospheric Administration, NOAA). These species can also pollute urban water runoffs and/or bioaccumulate in plants. In this study we provided detailed description of the temporal and spatial variations of the CPM metal content in the greater Los Angeles area, and linked trace element and metal species to their potential sources, and identified additional potential markers for rural and urban CPM sources. We believe that this information will help the US EPA as well as state regulatory agencies to develop and implement cost-effective strategies to protect the public from exposure to toxic compounds of coarse particulate matter.

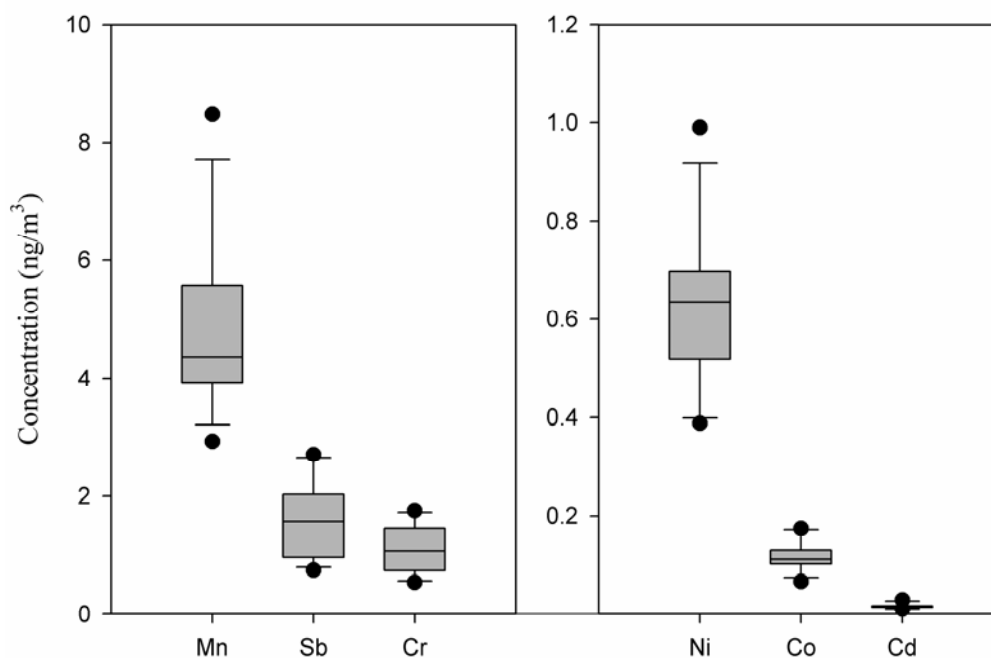


**Figure 5.7** - Annual variation of trace metals listed as air pollutants by US Environmental Protection Agency.

## 5.7 Acknowledgements

This research was supported by the US Environmental Protection Agency (EPA) under STAR grant #RD833743 and MESA Air grant #RD831697. We acknowledge the assistance of the Antelope Valley Air Quality Management District, the South Coast Air Quality Management District, and the USC Aerosol Laboratory group current and previous members, Dr. A. Polidori, Dr. K.F. Moore, Dr. M. Arhami, V. Verma, N. Hudda, K.L. Cheung, for their participation in this project. This manuscript has not been subjected to the EPA's peer and policy review and therefore does not necessarily reflect the view of EPA agency.

## **Chapter 6 - Future Research**

### **6.1 Conclusions**

Numerous epidemiological studies have associated the adverse respiratory and cardiovascular effects to atmospheric particulate matter (PM) exposure (Pope et al. 2002; Samet et al. 2000; USEPA 2004). Particle size is known as the most important parameter for characterizing the properties of particulate matter and researchers have focused on different size ranges (e.g. ultrafine, fine and coarse PM) in order to assess their association with human health. There is ample literature providing evidence of adverse effects for all mentioned particle size ranges (Nel 2005; Oberdorster et al. 2004), however the biological mechanisms responsible for the toxicity of PM are still uncertain. Due to the lack of data about how different PM components act in a complex mixture, it is not possible to precisely quantify the contributions from the main sources and components to the effects on human health. Thus, PM in health impact assessments is usually regarded as a uniform pollutant, regardless of the contribution from different sources, and assuming the same effect on mortality. This is probably not a correct assumption, but is a pragmatic compromise while waiting for sufficient knowledge that will allow the use of indicators other than particle mass. As a result linking the toxicity of PM with several of its chemical components has been the focus of considerable research over the past decade. Several studies have attempted to link the PM toxicity to organic- and elemental- carbon content (OC-EC) (Mar et al. 2000; Metzger et al. 2004), trace metals (Saldiva et al. 2002; Wellenius et al. 2003) and polycyclic aromatic hydrocarbons (PAH) (Dejmek et al. 2000). These chemical and toxicological studies should be focused on all particle size fractions, since particles falling into ultrafine, fine and coarse size fractions can have substantially different sources and as a result can be composed of varying chemical species which subsequently contribute to different health

outcomes. The associations between health endpoints with the hundreds of potentially toxic chemical species and PM characteristics may be daunting and not cost efficient. Therefore it is desirable to focus on the casualty of the few critical chemical components that current science supports as potentially the most harmful to human health. Such information will allow for more effective regulatory control strategies, more targeted air quality standards, and as a result, reductions in population exposure to the most harmful types of airborne PM.

One of the PM chemical classes known for their toxic potency are semi-volatile organic carbon compounds. These SVOC species are in dynamic equilibrium with their vapor phase in the atmosphere, and when in gas phase promote the formation of secondary organic aerosols (SOA) by photo-oxidation (Robinson et al. 2007). Numerous studies have linked the exposure to SVOC to adverse health effects (Arif and Shah 2007; Baltensperger et al. 2008; Boeglin et al. 2006; Delfino et al. 2009; Ntziachristos et al. 2007a; Rumchev et al. 2004), however the importance of the specific phase of the SVOC on toxicity remains an open area of research. Some recent studies have underscored the significance of vapor phase SVOC species in exposure (Eiguren-Fernandez et al. 2010; Elder et al. 2007) which emphasizes the need for health and risk assessment studies to include both particles and vapors when assessing the overall toxic potency of ambient aerosols. Traditionally thermodenuders have been used to remove semi-volatile species from the particle phase by heating, and subsequently removing them from the non-volatile fraction by adsorption, providing only non-volatile PM for chemical and toxicological studies. The toxic properties of the non-volatile fraction is compared to the toxicity response of the mixed aerosol, comprising of both semi-volatile (and volatile) and non-volatile species, to assess the toxicity properties of the semi-volatile species (Verma et al. 2011). This approach, while widely acceptable in the aerosol science community, may induce additional uncertainty due to the indirect comparison. In the present study, the thermodenuder was modified by

replacing the adsorption section with a newly designed filter holder, and tested in tandem with the VACES in order to separate semi-volatile species from the particle phase, and provide them in *vapor phase* for inhalation exposure studies. This technology makes it possible to conduct toxicity and inhalation exposure studies separately to the PM and vapor phases of semi-volatile organic pollutants in the urban atmosphere, and investigate the degree to which health effects attributable to these pollutants are affected by their phase. Given the dynamic behavior of these species in the atmosphere in terms of their partitioning between the PM and vapor phases, such investigations will become increasingly important.

Smaller particles (e.g. ultrafine and fine) are known to primarily originate from combustion processes and also gas-to-particle conversion processes in the atmosphere. In an urban environment, vehicles have become the major source of particulate matter via fuel combustion (Gertler et al. 2000), therefore most of chemical and toxicological research on aerosols have been focused on fine and ultrafine size fractions. Coarse particles, on the other hand, arise predominantly from mechanical processes including -- but not limited to -- brake lining abrasion, tire wear, windblown soil and dust, sea salt and bioaerosols such as pollen and fungal spores (Almeida et al. 2005; Chow et al. 1994; Edgerton et al. 2009; Harrison et al. 1997; Hinds 1999). Literature on chemical and toxicological properties of CPM is only available on a much more limited scale and hence significantly less is known quantitatively about the physical, chemical and toxicological characteristics of coarse particles.

In the present study the seasonal and spatial variations in ambient coarse PM mass concentrations at 10 distinct locations in Los Angeles air basin are discussed. Furthermore, the relationship between CPM and PM<sub>2.5</sub> mass concentrations is studied. High correlations between CPM and PM<sub>2.5</sub> were observed near major roads and freeways, depicting that the dominant source of coarse particles at these locations is traffic induced resuspended

particulate matter. The two particle size fractions are significantly less correlated in rural areas. Although the relatively rural sites selected in this study are impacted by vehicle-related coarse particle concentrations as well, windblown soil and dust contribute greatly to overall coarse PM mass at these locations.

Temporal relationship between CPM and PM<sub>2.5</sub> revealed much higher correlations between the two in winter than summer. Low correlations in the summer may be driven by the strong impact of atmospheric photochemistry on PM<sub>2.5</sub> emissions (while not affecting CPM concentrations), whereas relatively good correlations in the winter may be due to reduced photochemistry coupled with the lower boundary layer and more calm conditions, thus enhancing the contribution of traffic sources to both PM fractions. Moreover the coefficient of divergence between all the site pairs in the study depicts modest heterogeneity of CPM in Los Angeles Basin which may be due to the effect of local sources to CPM concentrations and suggests that a network of monitoring sites would be needed to accurately monitor the CPM concentrations in an urban area such as Los Angeles, as the traditional and widely used central monitoring sites for fine PM measurements may not represent true population exposure to more locally affected CPM.

In order to improve our understanding of the relationship between CPM concentrations and exposure, the chemical composition and toxicological properties of the CPM should be evaluated. Of particular interest is the concentrations of the selected metal species known to be potentially toxic from previous inhalation and in vitro studies (Becker et al. 2005; Samet et al. 2000; Vogl and Elstner 1989). Some of the trace elements and metals are also unique markers for various PM emission sources. The CPM samples were analyzed by means of Inductively Coupled Plasma-Mass Spectroscopy (ICP-MS) to determine the particle concentrations of the trace elements and metals. These species are known to be tracers of



abrasive vehicular emissions, in particular through brake lining and tire wear. Principal component analysis (PCA) was employed in order to identify CPM sources of the analyzed species, revealing a suite of identifiable CPM sources that were consistent with data available in the literature, but also identifying additional elemental markers for some of these CPM sources that are reported here for the first time. In general, trace metals associated with airborne mineral dust dominated the overall CPM mass (mainly Al, Ca, Fe, K, Mg, Ti), while abrasive vehicular emission tracers (Fe, Ba, Cu) also contributed significantly. Other identified CPM sources include industrial emissions, sea salt spray and catalytic converter emissions.

Heavy metals accumulate in road dust as a result of atmospheric deposition and can subsequently become airborne by wind or traffic induced turbulence. These species can also pollute urban water runoffs and/or bio-accumulate in plants. In this study we provided detailed description of the temporal and spatial variations of the CPM metal content in the greater Los Angeles area, and linked trace element and metal species to their potential sources, and identified additional potential markers for rural and urban CPM sources, which can help the regulatory agencies to develop and implement cost-effective strategies to protect the public from exposure to toxic compounds of CPM. Furthermore, filters will be analyzed for elemental carbon (EC), organic carbon (OC) and subsequently analyzed by means of ion chromatography (IC) for sulfate, nitrate, sodium, potassium and ammonium ions. The toxicity properties of the CPM would be evaluated to refine the relationship between coarse PM composition and toxicity. CPM toxicity is evaluated by means of molecular assays (e.g. dithiothreitol (DTT) and dihydroxy benzoic acids (DHBA)) and biological assay (redox assays). The proposed research will result in much needed and currently unavailable information on the relationships between coarse PM sources, spatial and seasonal characteristics, and toxicity. This study can help US EPA in their efforts to

design and support a national monitoring network for CPM. The wide range of sampling sites spanning both rural and urban locations will help to examine the hypothesis that chemical composition related to different CPM sources impacts severity of CPM toxicity. The ultimate goal of this study is to help US EPA to establish the linkage between sources, composition and toxicity of CPM and provide scientific basis to develop cost-effective strategies to protect the public from the toxic sources of CPM.

## 6.2 Discussion and Future Recommendations

The current particulate matter emission standards are based on PM mass only. Based on the new findings in PM toxicity research, linking hazardous health effects with PM chemical components however, such single metric as the standard for regulation is not sufficient in order to protect public health. The prevailing scientific opinion contends that PM mass is a surrogate measure of other physical and chemical properties of PM that are the actual causes of the observed health effects. New advanced vehicle emission control technologies have emerged to meet the mass based emission standards. These after-treatment technologies are effective in reducing solid, non-labile PM emissions by means of filtration. However the reduction in particle mass emissions is accompanied by substantial increase of particle number emissions from retrofitted vehicles due to formation of nucleation mode particles from organic vapors in the exhaust upon atmospheric dilution. These smaller particles may pose a greater threat to public health, because they deposit deeper in the respiratory system due to their size, and their chemical composition appears to be intrinsically more toxic than the non-labile PM. Moreover, these semi-volatile species undergo many atmospheric processes such as nucleation, condensation, coagulation and secondary photochemical reactions, which significantly change particle size distribution and number concentration. In addition, the semi-volatile PM fraction is one of the key determinants of PM toxicity as they

are highly correlated with PM redox activity which indicates its ability to induce oxidative stress. These are some of the properties of semi-volatile species that highlight the difficulties and uncertainties in establishing meaningful standards for both vehicular emissions and ambient air quality standards based on particle mass concentration only. A better understanding of the linkages between PM chemistry and toxicity should be developed in order to adopt better regulatory strategies to protect public health. Moreover, efforts should be made to reduce the vehicular emissions of semi-volatile species, which penetrate the current tail-pipe emission control devices and subsequently undergo gas-to-particle conversion with the cooling of the exhaust to form semi-volatile particles. New regulations focusing on these species will motivate the engine manufacturing community to develop advance engine designs to reduce the gas-phase precursors formed during the combustion process.

The higher number concentration of particles emitted from the vehicles retrofitted with after-treatment devices may suggest that the particle surface area or particle number is a better metric than mass for future regulatory strategy. However, there are serious drawbacks associated with such standards, as most of the potentially more harmful volatile species remain unregulated. Moreover, while different PM chemical components act in a complex mixture, such standard regards all these components as a uniform pollutant, regardless of their chemical characterization or potential health effects. A more direct approach focusing on the major players in inducing hazardous health effects may be more effective and more cost efficient.

In the latest step in its review of the National Ambient Air Quality Standards (NAAQS), the U.S. Environmental Protection Agency (EPA) established the foundation for unprecedented regulation of coarse PM by reducing the CPM mass based standard. However, it would be

virtually impossible to comply with such standard as most of the CPM emissions are from hard to control sources, such as windblown dust. These non-exhaust PM emissions are the result of windblown soil and resuspension of road dust, deposited from multiple sources, such as wear of tires and brake linings. As a result EPA has retained the existing 24-hour  $\text{PM}_{10}$  standard of  $150 \mu\text{g}/\text{m}^3$  since 1997. For example a more stringent standard may affect the agricultural industries as the standard would not be met because of everyday activities, forcing states to impose extreme dust-control requirements on businesses across the board.

In summary, based on the emerging studies focused on the physicochemical and toxicological characteristics of urban aerosols, the current mass-based PM emission regulations and the ambient air quality standards have to be revised. Mass concentration, as the only metric for the current regulations is not sufficient and new metrics such as particle number concentration, chemical composition and PM volatility can be considered as supplementary metrics in future regulations. Focusing on the critical PM chemical components that current scientific knowledge supports as potentially hazardous to human health may be the most effective and cost-efficient approach.

## Bibliography

- Allen, J. O., Mayo, P. R., Hughes, L. S., Salmon, L. G. and Cass, G. R. (2001). Emissions of size-segregated aerosols from on-road vehicles in the Caldecott Tunnel. *Environ Sci Technol* 35:4189-4197.
- Almeida, S. M., Pio, C. A., Freitas, M. C., Reis, M. A. and Trancoso, M. A. (2005). Source apportionment of fine and coarse particulate matter in a sub-urban area at the Western European Coast. *Atmos Environ* 39:3127-3138.
- Amato, F., Pandolfi, M., Escrig, A., Querol, X., Alastuey, A., Pey, J., Perez, N. and Hopke, P. K. (2009). Quantifying road dust resuspension in urban environment by Multilinear Engine: A comparison with PMF2. *Atmos Environ* 43:2770-2780.
- Arif, A. A. and Shah, S. M. (2007). Association between personal exposure to volatile organic compounds and asthma among US adult population. *Int Arch Occ Env Hea* 80:711-719.
- Ayala, A., Kado, N. Y., Okamoto, R. A., Holmen, B. A., Kuzmicky, P. A., Kobayashi, R., Stiglitz, K. E. and (2002). Diesel and heavy –duty transit bus emissions over multiple driving schedules: Regulated pollutants and project Overview. *SAE paper 2002-01-1722*.
- Baltensperger, U., Dommen, J., Alfarra, R., Duplissy, J., Gaeggeler, K., Metzger, A., Facchini, M. C., Decesari, S., Finessi, E., Reinnig, C., Schott, M., Warnke, J., Hoffmann, T., Klatzer, B., Puxbaum, H., Geiser, M., Savi, M., Lang, D., Kalberer, M. and Geiser, T. (2008). Combined determination of the chemical composition and of health effects of secondary organic aerosols: The POLYSOA project. *J Aerosol Med Pulm D* 21:145-154.
- Baron, P. A. and Willeke, K. (2001). *Aerosol measurement : principles, techniques, and applications*. Wiley, New York.
- Baron, P. A. and Willeke, K. (1992). *Aerosol measurement; principles, techniques, and application*. Wiley Interscience Publication, New York.
- Becker, S., Dailey, L. A., Soukup, J. M., Grambow, S. C., Devlin, R. B. and Huang, Y. C. T. (2005). Seasonal variations in air pollution particle-induced inflammatory mediator release and oxidative stress. *Environ Health Persp* 113:1032-1038.
- Biswas, S., Hu, S. H., Verma, V., Herner, J. D., Robertson, W. H., Ayala, A. and Sioutas, C. (2008). Physical properties of particulate matter (PM) from late model heavy-duty diesel vehicles operating with advanced PM and NOx emission control technologies. *Atmos Environ* 42:5622-5634.
- Biswas, S., Verma, V., Schauer, J. J., Cassee, F. R., Cho, A. K. and Sioutas, C. (2009). Oxidative Potential of Semi-Volatile and Non Volatile Particulate Matter (PM) from Heavy-Duty Vehicles Retrofitted with Emission Control Technologies. *Environ Sci Technol* 43:3905-3912.

Boeglin, M. L., Wessels, D. and Henshel, D. (2006). An investigation of the relationship between air emissions of volatile organic compounds and the incidence of cancer in Indiana counties. *Environ Res* 100:242-254.

Brunekreef, B. and Forsberg, B. (2005). Epidemiological evidence of effects of coarse airborne particles on health. *Eur Respir J* 26:309-318.

Burtscher, H., Baltensperger, U., Bukowiecki, N., Cohn, P., Hüglin, C., Mohr, M., Matter, U., Nyeki, S., Schmatloch, V., Streit, N. and Weingartner, E. (2001). Separation of volatile and non-volatile aerosol fractions by thermodesorption: instrumental development and applications. *J Aerosol Sci* 32:427-442.

Cadle, S. H., Mulawa, P. A., Ball, J., Donase, C., Weibel, A., Sagebiel, J. C., Knapp, K. T. and Snow, R. (1997). Particulate emission rates from in use high emitting vehicles recruited in Orange County, California. *Environ Sci Technol* 31:3405-3412.

Canepari, S., Perrino, C., Olivieri, F. and Astolfi, M. L. (2008). Characterisation of the traffic sources of PM through size-segregated sampling, sequential leaching and ICP analysis. *Atmos Environ* 42:8161-8175.

Canepari, S., Pietrodangelo, A., Perrino, C., Astolfi, M. L. and Marzo, M. L. (2009). Enhancement of source traceability of atmospheric PM by elemental chemical fractionation. *Atmos Environ* 43:4754-4765.

CARB (1998). Proposed identification of diesel exhaust as a toxic air contaminant. *Appendix III. Part A: Exposure assessment*.

Cassee, F. R., Boere, A. J. F., Fokkens, P. H. B., Leseman, D. L. A. C., Sioutas, C., Kooter, I. M. and Dormans, J. A. M. A. (2005). Inhalation of concentrated particulate matter produces pulmonary inflammation and systemic biological effects in compromised rats. *J Toxicol Env Heal A* 68:773-796.

Chan, D. and Stachowiak, G. W. (2004). Review of automotive brake friction materials. *P I Mech Eng D-J Aut* 218:953-966.

Charron, A. and Harrison, R. M. (2005). Fine (PM<sub>2.5</sub>) and coarse (PM<sub>2.5-10</sub>) particulate matter on a heavily trafficked London highway: Sources and processes. *Environ Sci Technol* 39:7768-7776.

Cheung, K. L., Daher, N., Kam, W., Shafer, M., Ning, Z., Schauer, J. J. and Sioutas, C. (2010). Spatial and Temporal Variation of Chemical Composition and Mass Closure of Ambient Coarse Particulate Matter (PM<sub>10-2.5</sub>) in the Los Angeles Area. *Submitted to Atmospheric Environment*.

Chow, J. C., Watson, J. G., Fujita, E. M., Lu, Z. Q., Lawson, D. R. and Ashbaugh, L. L. (1994). Temporal and Spatial Variations of Pm(2.5) and Pm(10) Aerosol in the Southern California Air-Quality Study. *Atmos Environ* 28:2061-2080.

Claiborn, C. S., Larson, T. and Sheppard, L. (2002). Testing the metals hypothesis in Spokane, Washington. *Environ Health Persp* 110:547-552.

Clarke, A. D. (1991). A Thermo Optic Technique for Insitu Analysis of Size-Resolved Aerosol Physicochemistry. *Atmos Environ a-Gen* 25:635-644.

Colombo, C., Monhemius, A. J. and Plant, J. A. (2008). Platinum, palladium and rhodium release from vehicle exhaust catalysts and road dust exposed to simulated lung fluids. *Ecotox Environ Safe* 71:722-730.

Councell, T. B., Duckenfield, K. U., Landa, E. R. and Callender, E. (2004). Tire-wear particles as a source of zinc to the environment. *Environ Sci Technol* 38:4206-4214.

Cruz, C. N. and Pandis, S. N. (1999). Condensation of organic vapors on an externally mixed aerosol population. *Aerosol Sci Tech* 31:392-407.

Dejmek, J., Solansky, I., Benes, I., Lenicek, J. and Sram, R. J. (2000). The impact of polycyclic aromatic hydrocarbons and fine particles on pregnancy outcome. *Environ Health Persp* 108:1159-1164.

Delfino, R. J., Brummel, S., Wu, J., Stern, H., Ostro, B., Lipsett, M., Winer, A., Street, D. H., Zhang, L., Tjoa, T. and Gillen, D. L. (2009). The relationship of respiratory and cardiovascular hospital admissions to the southern California wildfires of 2003. *Occup Environ Med* 66:189-197.

Dietl, C., Reifenhauer, W. and Peichl, L. (1997). Association of antimony with traffic - occurrence in airborne dust, deposition and accumulation in standardized grass cultures. *Sci Total Environ* 205:235-244.

Dockery, D. W., Pope, C. A., Xu, X. P., Spengler, J. D., Ware, J. H., Fay, M. E., Ferris, B. G. and Speizer, F. E. (1993). An Association between Air-Pollution and Mortality in 6 United-States Cities. *New Engl J Med* 329:1753-1759.

Edgerton, E. S., Casuccio, G. S., Saylor, R. D., Lersch, T. L., Hartsell, B. E., Jansen, J. J. and Hansen, D. A. (2009). Measurements of OC and EC in Coarse Particulate Matter in the Southeastern United States. *J Air Waste Manage* 59:78-90.

Eiguren-Fernandez, A., Miguel, A. H., Froines, J. R., Thurairatnam, S. and Avol, E. L. (2004). Seasonal and spatial variation of polycyclic aromatic hydrocarbons in vapor-phase and PM 2.5 in Southern California urban and rural communities. *Aerosol Sci Tech* 38:447-455.

Eiguren-Fernandez, A., Miguel, A. H., Jaques, P. A. and Sioutas, C. (2003). Evaluation of a denuder-MOUDI-PUF sampling system to measure the size distribution of semi-volatile polycyclic aromatic hydrocarbons in the atmosphere. *Aerosol Sci Tech* 37:201-209.

Eiguren-Fernandez, A., Shinyashiki, M., Schmitz, D. A., DiStefano, E., Hinds, W., Kumagai, Y., Cho, A. K. and Froines, J. R. (2010). Redox and electrophilic properties of vapor- and particle-phase components of ambient aerosols. *Environ Res* 110:207-212.

Elder, A., Couderc, J. P., Gelein, R., Eberly, S., Cox, C., Xia, X. J., Zareba, W., Hopke, P., Watts, W., Kittelson, D., Frampton, M., Utell, M. and Oberdorster, G. (2007). Effects of on-

road highway aerosol exposures on autonomic responses in aged, spontaneously hypertensive rats. *Inhal Toxicol* 19:1-12.

EPA (2002). Prepared by the National Center for Environmental Assessment, Washington, DC, for the Office of Transportation and Air Quality; Health assessment document for diesel engine exhaust, EPA/600/8-90/057F; U.S. Environmental Protection Agency, National Technical Information Service: Springfield, VA, 2002; PB2002-107661.

Fauser, P., Tjell, J. C., Mosbaek, H. and Pilegaard, K. (1999). Quantification of tire-tread particles using extractable organic zinc as tracer. *Rubber Chem Technol* 72:969-977.

Fine, P. M., Chakrabarti, B., Krudysz, M., Schauer, J. J. and Sioutas, C. (2004). Diurnal variations of individual organic compound constituents of ultrafine and accumulation mode particulate matter in the Los Angeles basin. *Environ Sci Technol* 38:1296-1304.

Forsberg, B., Hansson, H. C., Johansson, C., Areskoug, H., Persson, K. and Jarvholm, B. (2005). Comparative health impact assessment of local and regional particulate air pollutants in Scandinavia. *Ambio* 34:11-19.

Furuta, N., Iijima, A., Kambe, A., Sakai, K. and Sato, K. (2005). Concentrations, enrichment and predominant sources of Sb and other trace elements in size classified airborne particulate matter collected in Tokyo from 1995 to 2004. *J Environ Monitor* 7:1155-1161.

Gandhi, H. S., Graham, G. W. and McCabe, R. W. (2003). Automotive exhaust catalysis. *J Catal* 216:433-442.

Garg, B. D., Cadle, S. H., Mulawa, P. A., Groblicki, P. J., Laroo, C. and Parr, G. A. (2000). Brake wear particulate matter emissions. *Environ Sci Technol* 34:4463-4469.

Gavett, S. H. and Koren, H. S. (2001). The role of particulate matter in exacerbation of atopic asthma. *Int Arch Allergy Imm* 124:109-112.

Gerlofs-Nijland, M. E., Rummelhard, M., Boere, A. J. F., Leseman, D. L. A. C., Duffin, R., Schins, R. P. F., Borm, P. J. A., Sillanpaa, M., Salonen, R. O. and Cassee, F. R. (2009). Particle Induced Toxicity in Relation to Transition Metal and Polycyclic Aromatic Hydrocarbon Contents. *Environ Sci Technol* 43:4729-4736.

Gertler, A. W., Gillies, J. A. and Pierson, W. R. (2000). An assessment of the mobile source contribution to PM<sub>10</sub> and PM<sub>2.5</sub> in the United States. *Water Air Soil Poll* 123:203-214.

Gomez, B., Palacios, M. A., Gomez, M., Sanchez, J. L., Morrison, G., Rauch, S., McLeod, C., Ma, R., Caroli, S., Alimonti, A., Petrucci, F., Bocca, B., Schramel, P., Zischka, M., Petterson, C. and Wass, U. (2002). Levels and risk assessment for humans and ecosystems of platinum-group elements in the airborne particles and road dust of some European cities. *Sci Total Environ* 299:1-19.

Gomez, D. R., Gine, M. F., Bellato, A. C. S. and Smichowski, P. (2005). Antimony: a traffic-related element in the atmosphere of Buenos Aires, Argentina. *J Environ Monitor* 7:1162-1168.



- Gordon, T., Nadziejko, C., Schlesinger, R. and Chen, L. C. (1998). Pulmonary and cardiovascular effects of acute exposure to concentrated ambient particulate matter in rats. *Toxicol Lett* 96-7:285-288.
- Grose, M., Sakurai, H., Savstrom, J., Stolzenburg, M. R., Watts, W. F., Morgan, C. G., Murray, I. P., Twigg, M. V., Kittelson, D. B. and McMurry, P. H. (2006). Chemical and physical properties of ultrafine diesel exhaust particles sampled downstream of a catalytic trap. *Environ Sci Technol* 40:5502-5507.
- Harrison, R. M., Deacon, A. R., Jones, M. R. and Appleby, R. S. (1997). Sources and processes affecting concentrations of PM<sub>10</sub> and PM<sub>2.5</sub> particulate matter in Birmingham (UK). *Atmos Environ* 31:4103-4117.
- Harrison, R. M., Jones, A. M. and Barrowcliffe, R. (2004). Field study of the influence of meteorological factors and traffic volumes upon suspended particle mass at urban roadside sites of differing geometries. *Atmos Environ* 38:6361-6369.
- Harrison, R. M., Yin, J. X., Mark, D., Stedman, J., Appleby, R. S., Booker, J. and Moorcroft, S. (2001). Studies of the coarse particle (2.5-10  $\mu$  m) component in UK urban atmospheres. *Atmos Environ* 35:3667-3679.
- Harvey, R. D. (1985). *Polycyclic Hydrocarbons and Carcinogenesis*. American Chemical Society, Washington, DC.
- Heck, R. M. and Farrauto, R. J. (1995). *Catalytic Air Pollution Control: Commercial Technology*. John Wiley & Sons, New York.
- Henry, R. C. (1987). Current Factor-Analysis Receptor Models Are Ill-Posed. *Atmos Environ* 21:1815-1820.
- Herner, J. D., Green, P. G. and Kleeman, M. J. (2006). Measuring the trace elemental composition of size-resolved airborne particles. *Environ Sci Technol* 40:1925-1933.
- Herner, J. H., Robertson, W. H., Ayala, A., Chang, O., Biswas, S., Sioutas, C. and (2007). Nucleation mode particle emissions from in-use heavy duty vehicles equipped with DPF and SCR retrofits. *American Association for Aerosol Research, 26th Annual Aerosol Conference, Sept 24 – 18, 200 Reno, NV*.
- Hewstone, R. K. (1994). *Sci. Total Environ.*:255.
- Hinds, W. C. (1999). *Aerosol Technology: Properties, Behavior, and Measurement of Airborne Particles*. Wiley.
- Hornberg, C., Maciuleviciute, L., Seemayer, N. H. and Kainka, E. (1998). Induction of sister chromatid exchanges (SCE) in human tracheal epithelial cells by the fractions PM-10 and PM-2.5 of airborne particulates. *Toxicol Lett* 96-7:215-220.
- Hu, S. H., Biswas, S., Verma, V., Schauer, J. J., Herner, J. D., Robertson, W. H., Ayala, A. and Sioutas, C. (2008). Chemical Speciation of PM Emissions from Heavy-Duty Diesel

Vehicles Equipped with Diesel Particulate Filter (DPF) and Selective Catalytic Reduction (SCR) Retrofits. *Submitted to Atmospheric Environment*.

Iijima, A., Sato, K., Yano, K., Tago, H., Kato, M., Kimura, H. and Furuta, N. (2007). Particle size and composition distribution analysis of automotive brake abrasion dusts for the evaluation of antimony sources of airborne particulate matter. *Atmos Environ* 41:4908-4919.

Khlystov, A., Zhang, Q., Jimenez, J. L., Stanier, C., Pandis, S. N., Canagaratna, M. R., Fine, P., Misra, C. and Sioutas, C. (2005). In situ concentration of semi-volatile aerosol using water-condensation technology. *J Aerosol Sci* 36:866-880.

Kim, S., Jaques, P. A., Chang, M. C., Barone, T., Xiong, C., Friedlander, S. K. and Sioutas, C. (2001). Versatile aerosol concentration enrichment system (VACES) for simultaneous in vivo and in vitro evaluation of toxic effects of ultrafine, fine and coarse ambient particles - Part II: Field evaluation. *J Aerosol Sci* 32:1299-1314.

Kittelson, D. B., Watts, W. F., Johnson, J. P., Rowntree, C., Payne, M., Goodier, S., Warrens, C., Preston, H., Zink, U., Ortiz, M., Goersmann, C., Twigg, M. V., Walker, A. P. and Caldow, R. (2006). On-road evaluation of two diesel exhaust after treatment devices. *J Aerosol Sci* 37:1140-1151.

Kleeman, M. J., Riddle, S. G., Robert, M. A. and Jakober, C. A. (2008). Lubricating oil and fuel contributions to particulate matter emissions from light-duty gasoline and heavy-duty diesel vehicles. *Environ Sci Technol* 42:235-242.

Kleinman, M. T., Sioutas, C., Chang, M. C., Boere, A. J. F. and Cassee, F. R. (2003). Ambient fine and coarse particle suppression of alveolar macrophage functions. *Toxicol Lett* 137:151-158.

Klemm, R. J., Lipfert, F. W., Wyzga, R. E. and Gust, C. (2004). Daily mortality and air pollution in Atlanta: Two years of data from ARIES. *Inhal Toxicol* 16:131-141.

Krudysz, M., Moore, K., Geller, M., Sioutas, C. and Froines, J. (2009). Intra-community spatial variability of particulate matter size distributions in Southern California/Los Angeles. *Atmos Chem Phys* 9:1061-1075.

Kuhn, T., Biswas, S. and Sioutas, C. (2005). Diurnal and seasonal characteristics of particle volatility and chemical composition in the vicinity of a light-duty vehicle freeway. *Atmos Environ* 39:7154-7166.

Kumagai, Y., Arimoto, T., Shinyashiki, M., Shimojo, N., Nakai, Y., Yoshikawa, T. and Sagai, M. (1997). Generation of reactive oxygen species during interaction of diesel exhaust particle components with NADPH-cytochrome P450 reductase and involvement of the bioactivation in the DNA damage. *Free Radical Bio Med* 22:479-487.

Laden, F., Neas, L. M., Dockery, D. W. and Schwartz, J. (2000). Association of fine particulate matter from different sources with daily mortality in six US cities. *Environ Health Persp* 108:941-947.

- Li, N., Sioutas, C., Cho, A., Schmitz, D., Misra, C., Sempf, J., Wang, M. Y., Oberley, T., Froines, J. and Nel, A. (2003). Ultrafine particulate pollutants induce oxidative stress and mitochondrial damage. *Environ Health Persp* 111:455-460.
- Lianou, M., Chalbot, M. C., Kotronarou, A., Kavouras, I. G., Karakatsani, A., Katsouyanni, K., Puustinen, A., Hameri, K., Vallius, M., Pekkanen, J., Meddings, C., Harrison, R. M., Thomas, S., Ayres, J. G., ten Brink, H., Kos, G., Meliefste, K., de Hartog, J. J. and Hoek, G. (2007). Dependence of home outdoor particulate mass and number concentrations on residential and traffic features in urban areas. *J Air Waste Manage* 57:1507-1517.
- Lighty, J. S., Veranth, J. M. and Sarofim, A. F. (2000). Combustion aerosols: Factors governing their size and composition and implications to human health. *J Air Waste Manage* 50:1565-1618.
- Lipsett, M. J., Tsai, F. C., Roger, L., Woo, M. and Ostro, B. D. (2006). Coarse particles and heart rate variability among older adults with coronary artery disease in the Coachella Valley, California. *Environ Health Persp* 114:1215-1220.
- Liu, Z. G., Berg, D. R., Swor, T. A. and Schauer, J. J. (2008). Comparative analysis on the effects of diesel particulate filter and selective catalytic reduction systems on a wide spectrum of chemical species emissions. *Environ Sci Technol* 42:6080-6085.
- Lough, G. C., Schauer, J. J., Park, J. S., Shafer, M. M., Deminter, J. T. and Weinstein, J. P. (2005). Emissions of metals associated with motor vehicle roadways. *Environ Sci Technol* 39:826-836.
- Luttinger, D. and Wilson, L. (2003). A study of air pollutants and acute asthma exacerbations in urban areas: status report. *Environ Pollut* 123:399-402.
- Malm, W. C., Pitchford, M. L., McDade, C. and Ashbaugh, L. L. (2007). Coarse particle speciation at selected locations in the rural continental United States. *Atmos Environ* 41:2225-2239.
- Mar, T. F., Norris, G. A., Koenig, J. Q. and Larson, T. V. (2000). Associations between air pollution and mortality in Phoenix, 1995-1997. *Environ Health Persp* 108:347-353.
- Maricq, M. M. (2007). Chemical characterization of particulate emissions from diesel engines: A review. *J Aerosol Sci* 38:1079-1118.
- Marr, L. C., Kirchstetter, T. W., Harley, R. A., Miguel, A. H., Hering, S. V. and Hammond, S. K. (1999). Characterization of polycyclic aromatic hydrocarbons in motor vehicle fuels and exhaust emissions. *Environ Sci Technol* 33:3091-3099.
- Matter, U., Siegmann, H. C., Kasper, M. and Burtscher, H. (1999a). Distinction of volatile particles in exhaust of diesel engines with particulate traps. *J Aerosol Sci* 30:471-472.
- McGeehan, J. A., Yeh, S. M., Couch, M., Hinz, A. and Otterholm, B. (2005). On the road to 2010 emissions: field test results and analysis with DPF-SCR system and ultra-low-sulfur diesel fuel. *SAE Technical Paper* 2005-01-3716.

- Merrion, D. (2003). Heavy duty diesel emission regulations—past, present, and future. *Society of Automotive Engineers Technical Paper Series No. 2003-01-0040*.
- Metzger, K. B., Tolbert, P. E., Klein, M., Peel, J. L., Flanders, W. D., Todd, K., Mulholland, J. A., Ryan, P. B. and Frumkin, H. (2004). Ambient air pollution and cardiovascular emergency department visits. *Epidemiology* 15:46-56.
- Miguel, A. H., Kirchstetter, T. W., Harley, R. A. and Hering, S. V. (1998). On-road emissions of particulate polycyclic aromatic hydrocarbons and black carbon from gasoline and diesel vehicles. *Environ Sci Technol* 32:450-455.
- Misra, C., Geller, M. D., Shah, P., Sioutas, C. and Solomon, P. A. (2001). Development and evaluation of a continuous coarse (PM<sub>10</sub>-PM<sub>2.5</sub>) particle monitor. *J Air Waste Manage* 51:1309-1317.
- Misra, C., Geller, M. D., Sioutas, C. and Solomon, P. A. (2003). Development and evaluation of a PM<sub>10</sub> impactor-inlet for a continuous coarse particle monitor. *Aerosol Sci Tech* 37:271-281.
- Misra, C., Singh, M., Shen, S., Sioutas, C. and Hall, P. A. (2002). Development and evaluation of a personal cascade impactor sampler (PCIS). *J Aerosol Sci* 33:1027-1047.
- Monn, C. (2001). Exposure assessment of air pollutants: a review on spatial heterogeneity and indoor/outdoor/personal exposure to suspended particulate matter, nitrogen dioxide and ozone. *Atmos Environ* 35:1-32.
- Monn, C. and Becker, S. (1999). Cytotoxicity and induction of proinflammatory cytokines from human monocytes exposed to fine (PM<sub>2.5</sub>) and coarse particles (PM<sub>10-2.5</sub>) in outdoor and indoor air. *Toxicol Appl Pharm* 155:245-252.
- Moore, K., Krudysz, M., Pakbin, P., Hudda, N. and Sioutas, C. (2009a). Intra-Community Variability in Total Particle Number Concentrations in the San Pedro Harbor Area (Los Angeles, California). *Aerosol Sci Tech* 43:587-603.
- Moore, K., Verma, V., Minguillon, M. C. and Sioutas, C. (2009b). Inter- and Intra-community variability in continuous coarse particulate matter (PM<sub>10-2.5</sub>) concentrations in the Los Angeles area. *Aerosol Sci Tech*.
- Moore, K. F., Ning, Z., Ntziachristos, L., Schauer, J. J. and Sioutas, C. (2007). Daily variation in the properties of urban ultrafine aerosol - Part I: Physical characterization and volatility. *Atmos Environ* 41:8633-8646.
- Moore, K. F., Verma, V., Minguillon, M. C. and Sioutas, C. (2010). Inter- and Intra-Community Variability in Continuous Coarse Particulate Matter (PM<sub>10-2.5</sub>) Concentrations in the Los Angeles Area. *Aerosol Sci Tech* 44:526-540.
- Morcelli, C. P. R., Figueiredo, A. M. G., Sarkis, J. E. S., Enzweiler, J., Kakazu, M. and Sigolo, J. B. (2005). PGEs and other traffic-related elements in roadside soils from Sao Paulo, Brazil. *Sci Total Environ* 345:81-91.

- Moreno, T., Querol, X., Alastuey, A., Viana, M., Salvador, P., de la Campa, A. S., Artinano, B., de la Rosa, J. and Gibbons, W. (2006). Variations in atmospheric PM trace metal content in Spanish towns: Illustrating the chemical complexity of the inorganic urban aerosol cocktail. *Atmos Environ* 40:6791-6803.
- Motallebi, N., Taylor, C. A. and Croes, B. E. (2003a). Particulate matter in California: Part 2 - Spatial, temporal, and compositional patterns of PM<sub>2.5</sub>, PM<sub>10-2.5</sub>, and PM<sub>10</sub>. *J Air Waste Manage* 53:1517-1530.
- Motallebi, N., Taylor, C. A., Turkiewicz, K. and Croes, B. E. (2003b). Particulate matter in California: Part 1 - Intercomparison of several PM<sub>2.5</sub>, PM<sub>10-2.5</sub>, and PM<sub>10</sub> monitoring networks. *J Air Waste Manage* 53:1509-1516.
- Nel, A. (2005). Air pollution-related illness: effects of particles (vol 308, pg 804, 2005). *Science* 309:1326-1326.
- Ning, Z., Geller, M. D., Moore, K. F., Sheesley, R., Schauer, J. J. and Sioutas, C. (2007). Daily variation in chemical characteristics of urban ultrafine aerosols and inference of their sources. *Environ Sci Technol* 41:6000-6006.
- Ning, Z. and Sioutas, C. (2010). Atmospheric Processes Influencing Aerosols Generated by Combustion and the Inference of Their Impact on Public Exposure: A Review. *Aerosol Air Qual Res* 10:43-58.
- Ntziachristos, L., Froines, J., Cho, A. K. and Sioutas, C. (2007a). Relationship between redox activity and chemical speciation of size-fractionated particulate matter. *Particle and Fibre Toxicology* 4:5.
- Ntziachristos, L., Ning, Z., Geller, M. D. and Sioutas, C. (2007b). Particle concentration and characteristics near a major freeway with heavy-duty diesel traffic. *Environ Sci Technol* 41:2223-2230.
- Oberdorster, G. (2001). Pulmonary effects of inhaled ultrafine particles. *Int Arch Occ Env Hea* 74:1-8.
- Oberdorster, G., Sharp, Z., Atudorei, V., Elder, A., Gelein, R., Kreyling, W. and Cox, C. (2004). Translocation of inhaled ultrafine particles to the brain. *Inhal Toxicol* 16:437-445.
- Pakbin, P., Hudda, N., Cheung, K. L., Moore, K. F. and Sioutas, C. (2010). Spatial and Temporal Variability of Coarse (PM<sub>10-2.5</sub>) Particulate Matter Concentrations in the Los Angeles Area. *Aerosol Sci Tech* 44:514-525.
- Pekkanen, J., Timonen, K. L., Ruuskanen, J., Reponen, A. and Mirme, A. (1997). Effects of ultrafine and fine particles in urban air on peak expiratory flow among children with asthmatic symptoms. *Environ Res* 74:24-33.
- Penning, T. M., Buczynski, M. E., Hung, C. F., McCoull, K. D., Palackal, N. T. and Tsuruda, L. S. (1999). Dihydrodiol dehydrogenases and polycyclic aromatic hydrocarbon activation: Generation of reactive and redox active o-quinones. *Chem Res Toxicol* 12:1-18.

- Perrino, C., Canepari, S., Catrambone, M., Torre, S. D., Rantica, E. and Sargolini, T. (2009). Influence of natural events on the concentration and composition of atmospheric particulate matter. *Atmos Environ* 43:4766-4779.
- Peters, A. and Pope, C. A. (2002). Cardiopulmonary mortality and air pollution. *Lancet* 360:1184-1185.
- Pinto, J. P., Lefohn, A. S. and Shadwick, D. S. (2004). Spatial variability of PM<sub>2.5</sub> in urban areas in the United States. *J Air Waste Manage* 54:440-449.
- Polidori, A., Hu, S., Biswas, S., Delfino, R. J. and Sioutas, C. (2008). Real-time characterization of particle-bound polycyclic aromatic hydrocarbons in ambient aerosols and from motor-vehicle exhaust. *Atmos Chem Phys* 8:1277-1291.
- Pope, C. A., Burnett, R. T., Thun, M. J., Calle, E. E., Krewski, D., Ito, K. and Thurston, G. D. (2002). Lung cancer, cardiopulmonary mortality, and long-term exposure to fine particulate air pollution. *Jama-J Am Med Assoc* 287:1132-1141.
- Querol, X., Viana, M., Alastuey, A., Amato, F., Moreno, T., Castillo, S., Pey, J., de la Rosa, J., de la Campa, A. S., Artinano, B., Salvador, P., Dos Santos, S. G., Fernandez-Patier, R., Moreno-Grau, S., Negrál, L., Minguillón, M. C., Monfort, E., Gil, J. I., Inza, A., Ortega, L. A., Santamaria, J. M. and Zabalza, J. (2007). Source origin of trace elements in PM from regional background, urban and industrial sites of Spain. *Atmos Environ* 41:7219-7231.
- Rao, A. K. and Whitby, K. B. (1977). Non ideal collection characteristics of single stage and cascade impactors. *Journal of Industrial Hygiene Association* 38:174-179.
- Rauch, S., Hemond, H. F., Barbante, C., Owari, M., Morrison, G. M., Peucker-Ehrenbrink, B. and Wass, U. (2005). Importance of automobile exhaust catalyst emissions for the deposition of platinum, palladium, and rhodium in the Northern Hemisphere. *Environ Sci Technol* 39:8156-8162.
- Rauch, S., Lu, M. and Morrison, G. M. (2001). Heterogeneity of platinum group metals in airborne particles. *Environ Sci Technol* 35:595-599.
- Reed, G. A. (1988). *J. Environ. Sci. Health* C6, 223-259.
- Riddle, S. G., Robert, M. A., Jakober, C. A., Hannigan, M. P. and Kleeman, M. J. (2007). Size distribution of trace organic species emitted from heavy-duty diesel vehicles. *Environ Sci Technol* 41:1962-1969.
- Riddle, S. G., Robert, M. A., Jakober, C. A., Hannigan, M. P. and Kleeman, M. J. (2008). Size distribution of trace organic species emitted from heavy-duty diesel vehicles (vol 41, pg 1962, 2007). *Environ Sci Technol* 42:974-976.
- Robinson, A. L., Donahue, N. M., Shrivastava, M. K., Weitkamp, E. A., Sage, A. M., Grieshop, A. P., Lane, T. E., Pierce, J. R. and Pandis, S. N. (2007). Rethinking organic aerosols: Semivolatile emissions and photochemical aging. *Science* 315:1259-1262.

Rogge, W. F., Hildemann, L. M., Mazurek, M. A. and Cass, G. R. (1993). Sources of fine organic aerosol. 2. Noncatalyst and catalyst-equipped automobiles and heavy-duty diesel trucks. *Environ Sci Technol* 27:636-651.

Root, R. A. (2000). Lead loading of urban streets by motor vehicle wheel weights. *Environ Health Persp* 108:937-940.

Rumchev, K., Spickett, J., Bulsara, M., Phillips, M. and Stick, S. (2004). Association of domestic exposure to volatile organic compounds with asthma in young children. *Thorax* 59:746-751.

Saldiva, P. H. N., Clarke, R. W., Coull, B. A., Stearns, R. C., Lawrence, J., Murthy, G. G. K., Diaz, E., Koutrakis, P., Suh, H., Tsuda, A. and Godleski, J. J. (2002). Lung inflammation induced by concentrated ambient air particles is related to particle composition. *Am J Resp Crit Care* 165:1610-1617.

Samet, J. M., Dominici, F., Curriero, F. C., Coursac, I. and Zeger, S. L. (2000). Fine particulate air pollution and mortality in 20 US Cities, 1987-1994. *New Engl J Med* 343:1742-1749.

Sanders, P. G., Xu, N., Dalka, T. M. and Maricq, M. M. (2003). Airborne brake wear debris: Size distributions, composition, and a comparison of dynamometer and vehicle tests. *Environ Sci Technol* 37:4060-4069.

Sardar, S. B., Fine, P. M., Mayo, P. R. and Sioutas, C. (2005a). Size-fractionated measurements of ambient ultrafine particle chemical composition in Los Angeles using the NanoMOUDI. *Environ Sci Technol* 39:932-944.

Sardar, S. B., Fine, P. M. and Sioutas, C. (2005b). Seasonal and spatial variability of the size-resolved chemical composition of particulate matter (PM<sub>10</sub>) in the Los Angeles Basin. *J Geophys Res-Atmos* 110:-.

Schauer, J. J. (2003). Evaluation of elemental carbon as a marker for diesel particulate matter. *J Expo Anal Env Epid* 13:443-453.

Schauer, J. J., Kleeman, M. J., Cass, G. R. and Simoneit, B. R. T. (1999). Measurement of emissions from air pollution sources. 2. C-1 through C-30 organic compounds from medium duty diesel trucks. *Environ Sci Technol* 33:1578-1587.

Schauer, J. J., Kleeman, M. J., Cass, G. R. and Simoneit, B. R. T. (2002). Measurement of emissions from air pollution sources. 5. C1-C32 organic compounds from gasoline-powered motor vehicles. *Environmental Science and Technology* 36:1169-1180.

Schulz, H., Harder, V., Ibal-Mulli, A., Khandoga, A., Koenig, W., Krombach, F., Radykewicz, R., Stampfl, A., Thorand, B. and Peters, A. (2005). Cardiovascular effects of fine and ultrafine particles. *J Aerosol Med* 18:1-22.

Scott, W. D. and Cattell, F. C. R. (1979). Vapor-Pressure of Ammonium Sulfates. *Atmos Environ* 13:307-317.

- Seinfeld, J. H. and Pandis, S. N. (2006). *Atmospheric Chemistry and Physics - From Air Pollution to Climate Change*. John Wiley & Sons, Inc.
- Sempere, R. and Kawamura, K. (1994). Comparative Distributions of Dicarboxylic-Acids and Related Polar Compounds in Snow Rain and Aerosols from Urban Atmosphere. *Atmos Environ* 28:449-459.
- Singh, M., Jaques, P. A. and Sioutas, C. (2002). Size distribution and diurnal characteristics of particle-bound metals in source and receptor sites of the Los Angeles Basin. *Atmos Environ* 36:1675-1689.
- Singh, M., Misra, C. and Sioutas, C. (2003). Field evaluation of a personal cascade impactor sampler (PCIS). *Atmos Environ* 37:4781-4793.
- Smith, K. R. and Aust, A. E. (1997). Mobilization of iron from urban particulates leads to generation of reactive oxygen species in vitro and induction of ferritin synthesis in human lung epithelial cells. *Chem Res Toxicol* 10:828-834.
- Smith, K. R., Kim, S., Recendez, J. J., Teague, S. V., Menache, M. G., Grubbs, D. E., Sioutas, C. and Pinkerton, K. E. (2003). Airborne particles of the California central valley alter the lungs of healthy adult rats. *Environ Health Persp* 111:902-908.
- Solomon, G. M. and Balmes, J. R. (2003). *Health effects of diesel exhaust*. Clinics in Occupational and Environmental Medicine 3, 207-219.
- Squadrito, G. L., Cueto, R., Dellinger, B. and Pryor, W. A. (2001). Quinoid redox cycling as a mechanism for sustained free radical generation by inhaled airborne particulate matter. *Free Radical Bio Med* 31:1132-1138.
- Sternbeck, J., Sjodin, A. and Andreasson, K. (2002). Metal emissions from road traffic and the influence of resuspension - results from two tunnel studies. *Atmos Environ* 36:4735-4744.
- Thorpe, A. and Harrison, R. M. (2008). Sources and properties of non-exhaust particulate matter from road traffic: A review. *Sci Total Environ* 400:270-282.
- Tolbert, P., Klein, M., Metzger, K., Peel, J., Flanders, W. D., Todd, K., Mulholland, J., Ryan, P. B., Frumkin, H. and Team, A. S. (2001). Particulate pollution and cardiorespiratory emergency department visits in Atlanta, August 1998-August 2000 (ARIES/SOPHIA studies). *Epidemiology* 12:S54-S54.
- Tsai, F. C., Apte, M. G. and Daisey, J. M. (2000). An exploratory analysis of the relationship between mortality and the chemical composition of airborne particulate matter. *Inhal Toxicol* 12:121-135.
- Turner, J. R. and Allen, D. T. (2008). Transport of atmospheric fine particulate matter: Part 2 - Findings from recent field programs on the intraurban variability in fine particulate matter. *J Air Waste Manage* 58:196-215.



USEPA (2004). *Air Quality Criteria for Particulate Matter, US; Environmental Protection Agency*. Research Triangle Park.

Verma, V., Pakbin, P., Cheung, K. L., Cho, A. K., Schauer, J. J., Shafer, M. M., Kleinman, M. T. and Sioutas, C. (2011). Physicochemical and oxidative characteristics of semi-volatile components of quasi-ultrafine particles in an urban atmosphere. *Atmos Environ* 45:1025-1033.

Villeneuve, P. J., Burnett, R. T., Shi, Y. L., Krewski, D., Goldberg, M. S., Hertzman, C., Chen, Y. and Brook, J. (2003). A time-series study of air pollution, socioeconomic status, and mortality in Vancouver, Canada. *J Expo Anal Env Epid* 13:427-435.

Vogl, G. and Elstner, E. F. (1989). Diesel Soot Particles Catalyze the Production of Oxy-Radicals. *Toxicol Lett* 47:17-23.

Wang, J., Jia, C. R., Wong, C. K. and Wong, P. K. (2000). Characterization of polycyclic aromatic hydrocarbons created in lubricating oils. *Water Air Soil Poll* 120:381-396.

Ware, J. H., Spengler, J. D., Neas, L. M., Samet, J. M., Wagner, G. R., Coultas, D., Ozkaynak, H. and Schwab, M. (1993). Respiratory and Irritant Health-Effects of Ambient Volatile Organic-Compounds - the Kanawha County Health Study. *Am J Epidemiol* 137:1287-1301.

Watson, J. G., Chow, J. C., Lu, Z. Q., Fujita, E. M., Lowenthal, D. H., Lawson, D. R. and Ashbaugh, L. L. (1994). Chemical Mass-Balance Source Apportionment of Pm(10) during the Southern California Air-Quality Study. *Aerosol Sci Tech* 21:1-36.

Weckwerth, G. (2001). Verification of traffic emitted aerosol components in the ambient air of Cologne (Germany). *Atmos Environ* 35:5525-5536.

Wellenius, G. A., Coull, B. A., Godleski, J. J., Koutrakis, P., Okabe, K., Savage, S. T., Lawrence, J. E., Murthy, G. G. K. and Verrier, R. L. (2003). Inhalation of concentrated ambient air particles exacerbates myocardial ischemia in conscious dogs. *Environ Health Persp* 111:402-408.

Whiteley, J. D. and Murray, F. (2003). Anthropogenic platinum group element (Pt, Pd and Rh) concentrations in road dusts and roadside soils from Perth, Western Australia. *Sci Total Environ* 317:121-135.

Wilson, J. G., Kingham, S., Pearce, J. and Sturman, A. P. (2005). A review of intraurban variations in particulate air pollution: Implications for epidemiological research. *Atmos Environ* 39:6444-6462.

Winkler, P. (1973). Relative humidity and the adhesion of atmospheric particles to the plates of impactors. *Aerosol Science* 5:235 to 240.

Wiseman, C. L. S. and Zereini, F. (2009). Airborne particulate matter, platinum group elements and human health: A review of recent evidence. *Sci Total Environ* 407:2493-2500.

- Wong, P. K. and Wang, J. (2001). The accumulation of polycyclic aromatic hydrocarbons in lubricating oil over time - a comparison of supercritical fluid and liquid-liquid extraction methods. *Environ Pollut* 112:407-415.
- Wu, Z. J., Poulain, L., Wehner, B., Wiedensohler, A. and Herrmann, H. (2009). Characterization of the volatile fraction of laboratory-generated aerosol particles by thermodenuder-aerosol mass spectrometer coupling experiments. *J Aerosol Sci* 40:603-612.
- Xia, T., Korge, P., Weiss, J. N., Li, N., Venkatesen, M. I., Sioutas, C. and Nel, A. (2004). Quinones and aromatic chemical compounds in particulate matter induce mitochondrial dysfunction: Implications for ultrafine particle toxicity. *Environ Health Persp* 112:1347-1358.
- Yeatts, K., Svendsen, E., Creason, J., Alexis, N., Herbst, M., Scott, J., Kupper, L., Williams, R., Neas, L., Cascio, W., Devlin, R. B. and Peden, D. B. (2007). Coarse particulate matter (PM<sub>2.5-10</sub>) affects heart rate variability, blood lipids, and circulating eosinophils in adults with asthma. *Environ Health Persp* 115:709-714.
- Young, T. M., Heeraman, D. A., Sirin, G. and Ashbaugh, L. L. (2002). Resuspension of soil as a source of airborne lead near industrial facilities and highways. *Environ Sci Technol* 36:2484-2490.
- Zelikoff, J. T., Chen, L. C., Cohen, M. D., Fang, K. J., Gordon, T., Li, Y., Nadziejko, C. and Schlesinger, R. B. (2003). Effects of inhaled ambient particulate matter on pulmonary antimicrobial immune defense. *Inhal Toxicol* 15:131-150.
- Zereini, F., Skerstupp, B., Alt, F., Helmers, E. and Urban, H. (1997). Geochemical behaviour of platinum-group elements (PGE) in particulate emissions by automobile exhaust catalysts: experimental results and environmental investigations. *Sci Total Environ* 206:137-146.
- Zereini, F., Wiseman, C., Alt, F., Messerschmidt, J., Muller, J. and Urban, H. (2001). Platinum and rhodium concentrations in airborne particulate matter in Germany from 1988 to 1998. *Environ Sci Technol* 35:1996-2000.
- Zereini, F., Wiseman, C. and Puttmann, W. (2007). Changes in palladium, platinum, and rhodium concentrations, and their spatial distribution in soils along a major highway in Germany from 1994 to 2004. *Environ Sci Technol* 41:451-456.
- Zhang, J. F. and Morawska, L. (2002). Combustion sources of particles: 2. Emission factors and measurement methods. *Chemosphere* 49:1059-1074.
- Zhang, Q., Stanier, C. O., Canagaratna, M. R., Jayne, J. T., Worsnop, D. R., Pandis, S. N. and Jimenez, J. L. (2004). Insights into the chemistry of new particle formation and growth events in Pittsburgh based on aerosol mass spectrometry. *Environ Sci Technol* 38:4797-4809.
- Zielinska, B., Sagebiel, J., McDonald, J. D., Whitney, K. and Lawson, D. R. (2004). Emission rates and comparative chemical composition from selected in-use diesel and gasoline-fueled vehicles. *J Air Waste Manage* 54:1138-1150.